Development of a New Signaling Methodology for Anion Recognition

Xiaohong Hou

A dissertation submitted to
Kochi University of Technology
in partial fulfillment of the requirements
for the degree of

Doctor of Philosophy

Graduate School of Engineering
Kochi University of Technology
Kochi, Japan

March 2006

Development of a New Signaling Methodology for Anion Recognition **Xiaohong Hou**

Development of a New Signaling Methodology for Anion Recognition

Xiaohong Hou

A dissertation submitted to
Kochi University of Technology
in partial fulfillment of the requirements
for the degree of

Doctor of Philosophy

Graduate School of Engineering
Kochi University of Technology
Kochi, Japan

March 2006

Abstract

The thesis deals with studies on development of a new signaling methodology for anion recognition. Host **9** having a bicyclic guanidinium ion subunit as an anion binding site and host **10** being quite simple and commercially available 4-(*N*,*N*-dimethylamino)-benzoic acid, both of which possessing 4-(*N*,*N*-dimethylamino)benzoate (DMAB) group, are investigated to clarify the complexation behavior of them toward a variety of monovalent or divalent anions with trigonal planar, tetrahedral, dual-tetrahedral, or octahedral geometry by means of ^{1}H NMR, UV-vis, CD, and/or fluorescence spectroscopic studies. The versatility of the DMAB group as a signaling subunit and the availability of host **10** as a new class of chormogenic and fluorogenic host for anion recognition are discussed.

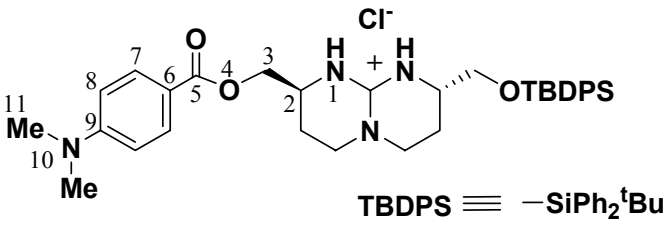

9

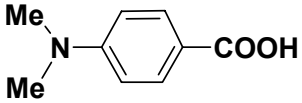

10

First, complexation behavior of host **9** with a variety of anions was studied by means of ^{1}H NMR, CD, and fluorescence spectroscopy. Divalent anions, SO_4^{2-}, HPO_4^{2-}, $H_2P_2O_7^{2-}$, and AMP^{2-}, as well as monovalent anions, ClO_4^-, NO_3^-, BF_4^-, HSO_4^-, PF_6^-, and $H_2PO_4^-$, were selected as tetrabutylammonium (TBA) salts, all of which are potentially able to bind to the guanidinium ion moiety.

^{1}H NMR spectral titration experiments were carried out in CD_3CN at 25 °C. The chemical shift changes of aromatic protons (H7 and H8) and *N*-methyl proton (H11) were monitored during the titrations. Host **9** showed stepwise 1:1 (host **9** : anion) and 2:1 complexation with divalent anions (SO_4^{2-}, HPO_4^{2-}, $H_2P_2O_7^{2-}$, and AMP^{2-}) and 1:1 complexation with monovalent anions (ClO_4^-, NO_3^-, BF_4^-, HSO_4^-, PF_6^-, and $H_2PO_4^-$). The binding constants between host **9** and the anions were determined in terms of non-linear least square curve fitting approach. Divalent anions showed much larger binding constants (SO_4^{2-}: log $K_{1:1}$ = 6.2, log $K_{2:1}$ = 4.7, HPO_4^{2-}: log $K_{1:1}$ = 6.2, log $K_{2:1}$ = 4.9, $H_2P_2O_7^{2-}$: log $K_{1:1}$ = 4.4, log $K_{2:1}$ = 1.8, AMP^{2-}: log $K_{1:1}$ > 7, log $K_{2:1}$ > 5) than the monovalent anions (log $K_{1:1}$ > 2), except for $H_2PO_4^-$ (log $K_{1:1}$ = 4.4). Therefore, the quantitative complexation information provided by the DMAB signaling subunit in ^{1}H NMR titrations demonstrated that host **9** had strong complexation ability and high selectivity toward divalent anions, SO_4^{2-}, HPO_4^{2-}, $H_2P_2O_7^{2-}$, and AMP^2 having a tetrahedral array of oxygen atoms over monovalent anions, ClO_4^-, NO_3^-, BF_4^-, HSO_4^-, and PF_6^-, except for H_2PO_4.

In CD titrations, the exciton chirality method was applied to investigate not only the complexation behavior of host **9** toward anions but also the absolute configuration of the 2:1 complexes generated by host **9** and divalent anions (SO_4^{2-}, HPO_4^{2-}, $H_2P_2O_7^{2-}$, and AMP^{2-}) in CH_3CN. CD titration profiles of host **9** by SO_4^{2-}, HPO_4^{2-}, and AMP^{2-} were so different from those by $H_2P_2O_7^{2-}$ and $H_2PO_4^-$, even all of which have strong or

relatively strong affinities to host **9**. That is to say, SO_4^{2-}, HPO_4^{2-} and AMP^{2-} exhibited typical negative first and positive second Cotton effect peaks, whereas $H_2P_2O_7^{2-}$ and $H_2PO_4^-$ showed simple CD intensity decreasing. In contrast, ClO_4^- having weak affinity to host **9** showed almost no CD intensity change. Moreover, in the 2:1 complex, there are two stereochemical possibilities in the complexation mode. One is that the two DMAB groups are placed counterclockwise from the front-to-back, whose chirality is negative. The other is that the two DMAB groups are placed clockwise, whose chirality is positive. The observed negative first and positive second Cotton effect peaks in the 2:1 complexes of host **9** with divalent anions (SO_4^{2-}, HPO_4^{2-}, and AMP^{2-}) clearly indicated that the spatial array of the two DMAB chromophores in the 2:1 complexes was negative (counterclockwise) rather than positive (clockwise). Thus, the combination of the DMAB signaling subunit and the chiral guanidinium binding site allowed us to understand the detailed complexation information and the absolute confirmation of the 2:1 complexes between host **9** and the divalent anions in CD titrations.

Fluorescence titration experiments were performed in CH_3CN. The DMAB signaling subunit in host **9** showed dual fluorescence emissions from LE (locally excited) and TICT (twisted intramolecular charge transfer) states. Quenching behavior of LE and TICT intensity of host **9** upon titrations by the divalent anions was remarkably different from those by the monovalent anions. The dual fluorescence behavior of host **9** upon complexation with SO_4^{2-}, HPO_4^{2-}, $H_2P_2O_7^{2-}$, and AMP^{2-}, all of which have strong or relatively strong binding affinities to host **9**, indicated the successive formations of 1:1 and 2:1 complexation, while host **9** exhibited 1:1 complexation with ClO_4^-, NO_3^-, BF_4^-, HSO_4^-, PF_6^-, and $H_2PO_4^-$, all of which have weak or relatively weak affinities to host **9**. These results are highly consonant with those

obtained in ^{1}H NMR titrations. On the other hand, the active participation of the lipophilic countercation such as TBA and/or the hydrophilic residue in AMP increased and/or decreased, respectively, the LE and TICT intensity in the 1:1 complexation via changing the microenvironmental polarity around the DMAB signaling subunit. Therefore, the unique dual fluorescence feature of the DMAB signaling subunit in host **9** upon complexation with a variety of anions demonstrated not only the quantitative binding information about stoichiometry but also the roles of lipophilic countercation such as TBA and/or the hydrophilic residue in AMP.

The investigation, therefore, clarifies the scope and limitations of the DMAB signaling subunit in host **9** on complexation with a variety of anion and finds out that the DMAB group is a versatile signaling subunit for anion sensing in terms of ^{1}H NMR, CD, and fluorescence spectroscopic studies.

Second, commercially available 4-(*N,N*-dimethylamino)benzoic acid (**10**) as a new class of chromogenic and fluorogenic host was directly applied for anion recognition. Divalent anions, HPO_4^{2-}, SO_4^{2-}, and $H_2P_2O_7^{2-}$ and monovalent anions, $H_2PO_4^-$, NO_3^-, BF_4^-, ClO_4^-, HSO_4^-, and PF_6^-, were selected as TBA salts. The scope and limitations as well as the versatility of the DMAB signaling subunit upon complexation with the anions were investigated by means of UV-vis and fluorescence spectroscopic studies.

UV-vis titrations were carried out in CH_3CN to know the complexation behavior of host **10** toward a variety of anions. The UV-vis titration profiles of host **10** with HPO_4^{2-} and SO_4^{2-} were obviously distinguished from those with the monovalent anions ($H_2PO_4^-$, HSO_4^-, ClO_4^-, BF_4^-, PF_6^-, and NO_3^-) and $H_2P_2O_7^{2-}$. The decreasing absorption monitored at 309 nm along with the increasing one monitored at 275 nm upon addition of HPO_4^{2-} and SO_4^{2-} were observed, while the absorption changes at the two

wavelengths were quite small upon addition of the monovalent anions and divalent anion, $H_2P_2O_7^{2-}$. Host **10** exhibited 2:1 complexation stoichiometry with HPO_4^{2-} and SO_4^{2-} and 1:1 complexation stoichiometry with monovalent anions ($H_2PO_4^-$, HSO_4^-, ClO_4^-, BF_4^-, PF_6^-, and NO_3^-) and $H_2P_2O_7^{2-}$. The binding constants of host **10** with divalent and monovalent anions were measured in terms of non-linear least square curve fitting approach. HPO_4^{2-} and SO_4^{2-} showed quite larger binding constants (log $K_2 > 10$) than the monovalent anions and $H_2P_2O_7^{2-}$ (log K_1 = 3.4-4.8). The combination of the basicity and negative charges of anions played a crucial role in affecting the affinity and selectivity of host **10** with anions. Therefore, the aromatic DMAB signaling subunit provided detailed complexation information such as complexation stoichiometry and binding constants in UV-vis titrations.

In fluorescence titrations, host **10** exhibited dual fluorescence of LE and TICT emissions in CH_3CN by excitation at 300 nm. The LE and TICT titration profiles of host **10** with HPO_4^{2-} and SO_4^{2-} were quite different from those with the monovalent anions and $H_2P_2O_7^{2-}$. In particular, the titration profiles of host **10** observed at TICT emission turned out to be quite similar to those obtained in UV-vis titrations. The complexation stoichiometry of host **10** with HPO_4^{2-} and SO_4^{2-}, namely, was turned out to be 2:1, while host **10** showed 1:1 complexation with $H_2PO_4^-$, HSO_4^-, ClO_4^-, BF_4^-, PF_6^-, NO_3^-, and $H_2P_2O_7^{2-}$. These results are consistent with those obtained in UV-vis titrations. In addition, the Stern-Volmer plots of host **10** at TICT emission showed sigmoidal and monotonic increasing profiles upon titrations with HPO_4^{2-} and SO_4^{2-}, respectively, while almost linear profiles with the monovalent anions and $H_2P_2O_7^{2-}$ were observed. Therefore, the dual fluorescence behavior and the Stern-Volmer plots also indicated that host **10** possessed strong affinities and high binding selectivity toward divalent anions (HPO_4^{2-} and SO_4^{2-}) over monovalent anions ($H_2PO_4^-$, HSO_4^-, ClO_4^-, BF_4^-, PF_6^-, and

NO_3^-) and $H_2P_2O_7^{2-}$.

The investigation demonstrates that simple and commercially available 4-(*N,N*-dimethylamino)benzoic acid (**10**) is capable of being a new class of anion host and the DMAB group is a versatile signaling subunit for anion sensing by means of UV-vis and fluorescence spectroscopic studies.

CONTENTS

Chapter 1.

General Introduction

Anion recognition chemistry is a rapidly developed discipline in the field of supramolecular chemistry. It started to grow in the late 1960s when C.H. Park and H. E. Simmonds of the du Pont de Nemours Company reported the complexation properties of a series of positively charged ammonium macrocyclic hosts termed katapinand (**1**) with halide.[1] It progressed sporadically throughout the 1970s and the early 1980s with the syntheses of cryptand hosts, which are analogous to the katapinands. Anion recognition chemistry, however, became an attractive topic just from the late 1980s. In the past more than twenty years, a huge number of supramolecular host systems for the selective complexation of anionic guests have been harvested.[2]

Why have sustained efforts been devoted to the realm of anion recognition chemistry? The reason is that anions are ubiquitous and play important roles in a wide range of chemical, biological, medical, and environmental fields.[3] For example, in the field of chemistry, anions have various roles, such as catalysts in accelerating some reactions, bases in neutralizing the acidic components in solution, and oxidizing agents

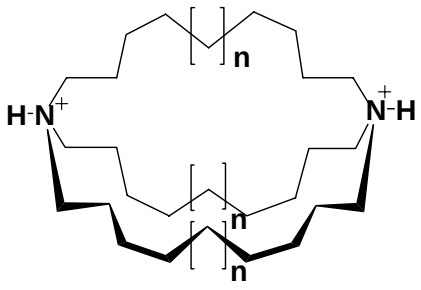

1 **n = 0: (1a)**
n = 1: (1b)
n = 2: (1c)

used in redox electrodes.[4] In biological field, almost 75 percent of enzyme substrates and cofactors are negatively charged. The majority of them are inorganic phosphate and phosphate residues in AMP, ADP, and especially in ATP, which is the energy source of life.[5] In medical field, the cystic fibrosis, a genetically inherited disease, is caused by the misregulation of chloride transfer channels which are controlled by extracellular chloride anion. However, there is no suitable chloride analysis method currently for medical examination.[4] In a routine blood analysis, the concentration level of phosphate in serum is determined for diagnosing the hyperphosphatemia and hypophosphatemia diseases.[6] In environmental field, the over use of fertilizers containing phosphate or nitrate has posed sever water pollution problems. Selective binding, extraction, and sensing of such anions are significantly important for the ecological balance and the health of human being.[7]

One of the most important investigations in anion recognition field is designing host molecules, which discriminate a target anion from others. For this purpose, the intrinsic properties of anions should be taken into account. First, anions, especially simple inorganic anions, have a wide range of shapes and geometries, such as spherical, linear, trigonal planner, tetrahedron, dual-tetrahedron, and octahedron (Figure 1-1). The host molecules have to be designed to organize a complementary binding site in their structures to match the geometry of the target anion.[1, 4] Second, anions are relatively larger than cations in their ionic size.[8] For instance, the radii of representative anions, $H_2PO_4^-$, SO_4^{2-}, and ClO_4^-, are 2.00 Å, 2.30 Å, and 2.50 Å, respectively, while the ionic radius of Na^+ is only 1.02 Å.[1] This feature requires that the sizes of the binding sites in the designed hosts should be considerably larger than those for cationic species so that the space in the host is enough to accomodate the anions. Third, anions have high free energies of solvation in comparison with cations, for example, the free energy of the

representative anions, $H_2PO_4^-$, SO_4^{2-}, and ClO_4^-, are -465 KJ•mol^{-1}, -1080 KJ•mol^{-1}, and -430 KJ•mol^{-1}, respectively, while that of Na^+ is -365 KJ•mol^{-1}.[1] In this sense, hosts have to compete more effectively with the surrounding medium in order to complex with the target anion. In addition, many anions are sensitive to the pH value of solvent environment. Since they would be protonated at low pH and lose their negative charges, the host molecules have to work efficiently within the relatively narrow pH window of their target anions.

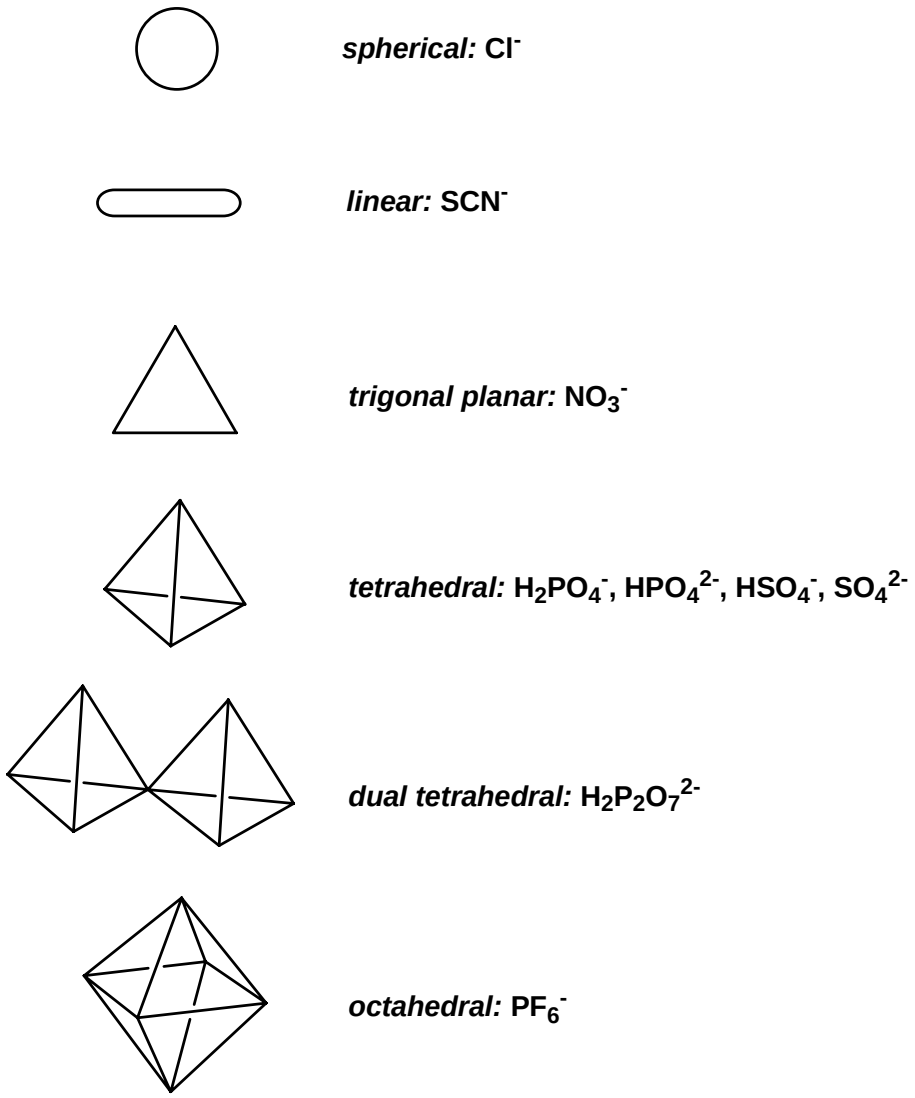

Figure 1-1. The geometry of a variety of anions.

The complementarity between anions and the binding site of the host would play a crucial role in designing such anion hosts. The fundamental characteristics of anions, such as negative charge, basicity, and salvation, should also be taken into account in designing host molecules. If the designed hosts are positively charged, it would be potential to bind to negatively charged anions, since the charge difference between the hosts and the anions would give rise to attractive electrostatic interactions. If the designed hosts contain acidic hydrogen atoms, they would make a good basis for the formation of hydrogen bonds with the anions, since almost all anions are basic and hence serve as suitable hydrogen bond acceptors. In addition, the solvents, in which the host/anion complexation would take place, will strongly affect the binding properties of the host and anions, since anions possess large solvation energies. Thus, it is important to select a suitable solvent as the complexation medium.

Considerations of molecular structures and properties of enormous variety of hosts reported allow us to realize the basic designing principle — the separation of the anion binding site and the signaling subunit in one host molecule.[9] The schematic illustration of the concept is shown in Figure 1-2. The anion binding site and the signaling subunit is coupled by covalent bond in a host molecule. When the binding site of the host molecule would complex an anion guest, the signaling subunit would respond to the anion complexation process to show signal changes in color, absorbance, chemical shift, and/or fluorescence.

The binding site would alternatively possess positive charge, acidic hydrogen, and complemental position or cavity to match the anion geometry so that it would selectively complex with the target anion guest. In this sense, the binding forces such as electrostatic interactions, formations of intermolecular hydrogen bonds, or combinations of these interactions working together have frequently been applied during

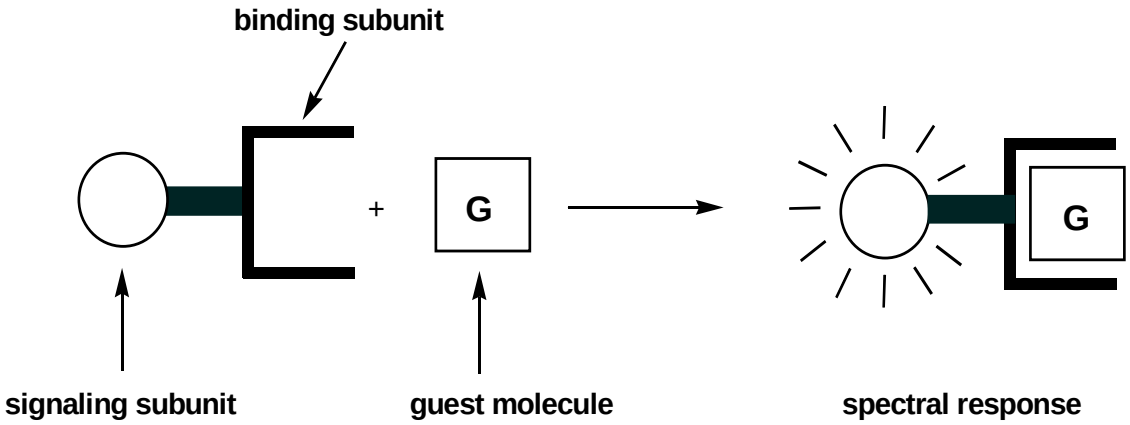

Figure 1-2. Binding subunit-signaling subunit method for anion recognition.

complexation process.[10] Concretely, electrostatic interactions have been the simplest and most obvious ways for a positively charged host to bind a negatively charged anion. Hydrogen bonding interactions also have been widely used as binding sites for recognizing oxyanions. The combinations of the electrostatic attractions and the hydrogen bonding interactions can enhance both the strength and the selectivity of hosts toward anion guests as compared with the cases that electrostatic attraction or hydrogen bonding is independently used to bind anionic guests. Guanidinium groups[11] and quaternary ammonium ions[12] are representative binding sites for anion recognition using electrostatic interactions. Typical hydrogen-bonding sites are ureas,[13] thioureas,[14] calyx[4]pyrroles, [15] sapphyrins, [16] porphyrins, [17] and guanidinium ions,[15] and polyamides.[18] Moreover, polyamine macrocycles, guanidinium groups, porphyrins, and protonated sapphyrins serve as binding sites through both the electrostatic interactions and the hydrogen bonding interactions simultaneously upon complexation with guest anions. Some representative anion recognition systems by using the electrostatic interactions and the hydrogen bonding simultaneously are presented in Figure 1-3, which are Simmons and Park's katapinand (**1**), Graf and Lehn's cryptand (**2**),[19] de

Mendoza and Lehn's guanidinium host **3**, Sessler's sapphyrin (**4**).

On the other hand, signaling of the anion recognition process is of significant importance in the estimation of the complexation behavior of hosts towards anions. The role of the signaling subunit is to act as a signal transducer. Thus, chromogentic and fluorogenic functional groups are combined into the designed host molecules. Chromophores, such as nitrophenyl,[20] anthraquinone,[21] azo dye derivatives,[22]

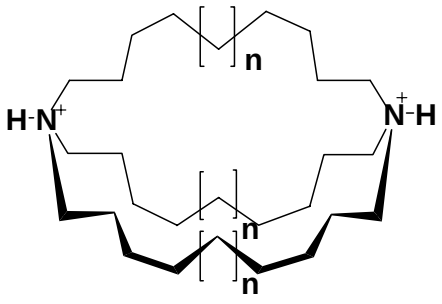

1 **n = 0: (1a)**
n = 1: (1b)
n = 2: (1c)

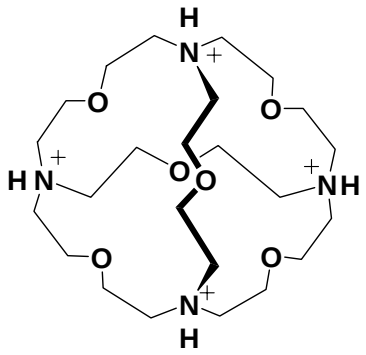

2

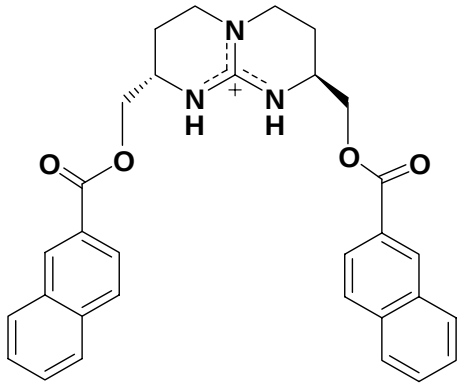

3

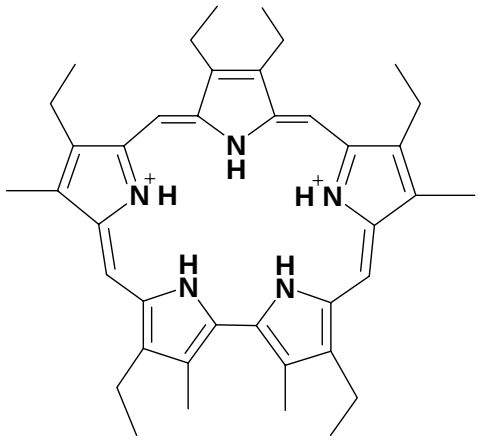

4

Figure 1-3. Representative hosts using electrostatic interactions and hydrogen bonding as binding forces.

porphyrins,[23] and sapphyrins[24], and fluorophores, such as polycyclic aromatic compounds[25] and transition metal complexes with bipyridine derivatives[26] have been applied for this purpose as signaling subunits to show absorption changes, color changes or fluorescent changes, which would provide clear binding information. Some of the representative signaling subunits with nitrophenyl derivative **5**, azo dye derivative **6**, anthraquinone derivative **7**, and polycyclic aromatic derivative **8** are presented in Figure 1-4.

In fact, Kobiro and Inoue utilized the advantages of the guanidinium ion moiety to efficiently bind anions for designing a novel host molecule **9**,[27] in which the chromogenic and fluorogenic, 4-(*N*,*N*-dimethylamino)benzoate (DMAB) group was employed as a signaling subunit to show the binding information. Their research demonstrated that the guanidinium ion moiety was a perfect binding site and the DMAB group was an excellent signaling subunit in complexation with sulfate anion through both of the dual hydrogen bonding and electrostatic interactions. Electronic absorption spectra of host **9** revealed that a strong intramolecular hydrogen bonding was present between the carbonyl oxygen atom of DMAB group and one of the N-H groups of the guanidinium ion moiety even in a highly polar solvent such as acetonitrile. The stepwise 1:1 (host **9**: sulfate anion) and 2:1 complexation constants (log $K_{1:1}$ = 6.2 and log $K_{2:1}$ = 4.7, respectively) were determined by ^{1}H NMR titration. The CD exciton chirality method allowed us to know the chiral sense of the two DMAB groups in the

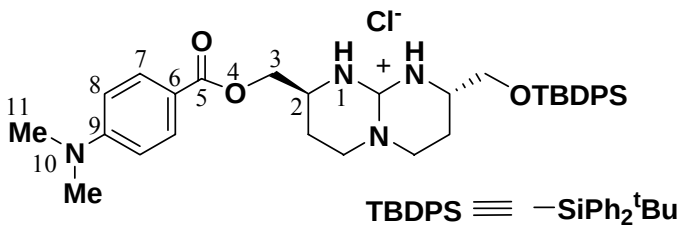

9

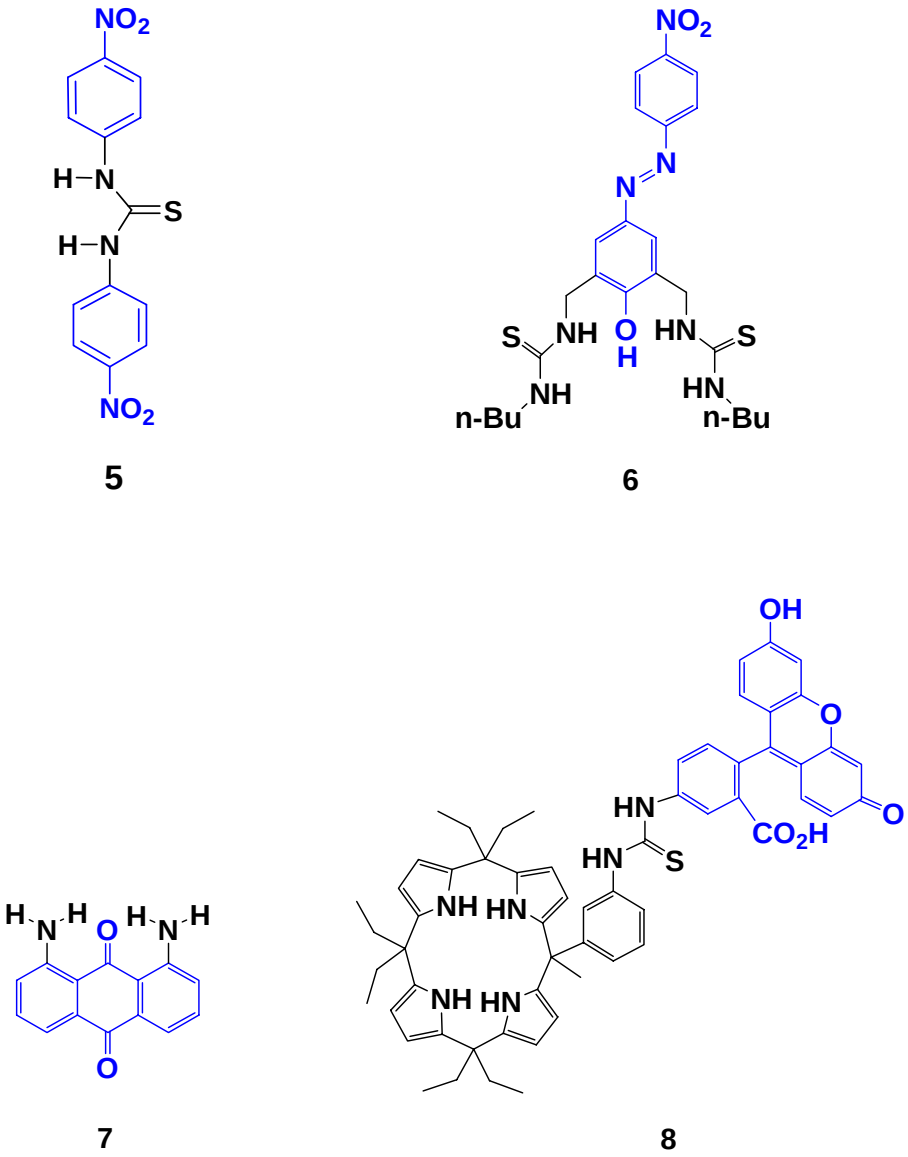

Figure 1-4. Hosts with representative signaling subunits.

2:1 complex as negative. The dual fluorescence behavior of the DMAB group showed not only the same binding stoichoimitry as in ^{1}H NMR titrations but also the role of the countercation tetrabutylammonium (TBA) upon complexation of host **9** with the sulfate anion.

In the thesis, the complexation behavior of host **9** with expanded variety of anions was studied by means of ^{1}H NMR, CD, and fluorescence spectroscopy.[28] These anions

possess monovalent or divalent negative charge with trigonal planar, tetrahedral, dual-tetrahedral, or octahedral geometry, including divalent anions, HPO_4^{2-}, $H_2P_2O_7^{2-}$, and AMP^{2-}, and monovalent anions, ClO_4^-, NO_3^-, BF_4^-, HSO_4^-, PF_6^-, and $H_2PO_4^-$. The purposes are to clarify the scope and limitations of the DMAB signaling subunit in host **9** upon complexation with a variety of divalent and monovalent anions and to demonstrate the versatility of DMAB signaling subunit for anion recognition.

Although numerous efforts have currently been contributed to the design and synthesis of anion receptors in molecular recognition field according to the binding site-signaling approach, the efforts resulted in not simple but quite massive and complicated molecular features of the hosts to accomplish such selective recognition and sensitive signaling on the specific anions.[29] Thus, the author has embarked on developing simple, efficient, and, if possible, commercially available chromogenic and fluorogenic reagents for anion hosts. One candidate suitable for this purpose is the aromatic acid derivative, for instance, 4-(*N*,*N*-dimethylamino)benzoic acid (**10**). Since such aromatic acid derivative has acidic hydrogen atom to be transferred to guest anions to form intermolecular hydrogen bonding and its aromatic moiety would show spectral response upon complexation with anions.

In the thesis, simple and commercially available 4-(*N*,*N*-dimethylamino)benzoic acid (**10**) as a new class of anion host was directly applied to recognize a variety of

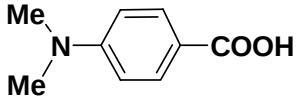

10

anions,[30] all of which possess monovalent or divalent negative charge with trigonal planar, tetrahedral, dual-tetrahedral, or octahedral geometry, including divalent anions, SO_4^{2-}, HPO_4^{2-}, $H_2P_2O_7^{2-}$, and monovalent anions, $H_2PO_4^-$, HSO_4^-, ClO_4^-, BF_4^-, PF_6^-, and NO_3^-. The complexation behavior of host **10** with these anions was studied by means of UV-vis and fluorescence spectroscopies. The purposes in the thesis are to demonstrate the availability of the simple acid **10** as a new class of anion host and the versatility of the DMAB signaling subunit for anion recognition.

The details of the research are presented in Chapter 2 and Chapter 3. Chapter 2 treats with the investigation on the scope and limitations as well as the versatility of DMAB signaling subunit in host **9** upon complexation with a variety of anions by means of ^{1}H NMR, CD, and fluorescence spectroscopic studies. Chapter 3 describes the availability of utilizing commercially available **10** as a new class of anion host and the versatility of the DMAB signaling subunit for anion recognition by means of UV-vis and fluorescence spectroscopic studies.

References

1. J. W. Steed and J. L. Atwood, *Supramolecular Chemistry.* John Wiley & Sons, Ltd.: West Sussex, 2000.
2. For reviews, see: (a) F. P. Schmidtchen and M. Berger, *Chem. Rev.* **1997**, *97*, 1609. (b) P. A. Gale, *Coord. Chem. Rev.* **2001**, *213*, 79. (c) R. Martínez-Máñez and F. Sancenón, *Chem. Rev.* **2003**, *103*, 4419.
3. A. Bianchi, K. Bowman-James, and E. Garcia-España, Eds. *Supramolecular Chemistry of Anions.* WILEY-VCH: New York, 1997.
4. P. D. Beer, P. A. Gale, and D. K. Smith, *Supramolecular Chemistry*, Oxford University Press: New York, 1999.
5. D. W. Christianson and W. N. Lipscomb, *Acc. Chem. Res.* **1989**, *22*, 62.
6. D. B. Enders and R. K. Rude, Mineral and Bone Metabolism. In *Tietz Textbook of Clinical Chemistry*; C. A. Burtis and E. R. Ashwood, Eds. W.B. Saunders Company: Philadelphia, PA, 1999; pp 1406-1408 and 1439-1440.
7. B. Moss, *Chem. Ind.* **1996**, 407.
8. R. D. Shannon, *Acta Crystallogr. Sect. A*, **1976**, *32*, 751.
9. X.-H. Hou and K. Kobiro, *Tetrahedron*, **2005**, *61*, 5866.
10. For reviews, see: (a) P. D. Beer and P. A. Gale, *Angew. Chem., Int. Ed.* **2001**, *40*, 486. (b) R. Martínez-Máñez and F. Sancenón, *Chem. Rev.* **2003**, *103*, 4419.
11. (a) A. Echevarren, A. Galañ, J. M. Lehn, and J. de Mendoza, *J. Am. Chem. Soc.* **1989**, *111*, 4994. (b) S. Camiolo, P. A. Gale, M. I. Ogden, B. W. Skelton, and A. H. White, *J. Chem. Soc., Perkin Trans. 2*, **2001**, 1294.
12. (a) S. Shinoda, M. Tadokoro, H. Tsukube, and R. Arakawa, *Chem. Commun.* **1998**,

181. (b) L. O. Abouderbala, W. J. Belcher, M. G. Boutelle, P. J. Cragg, J. Dhaliwal, M. Fabre, J. W. Steed, D. R. Turner, and K. J. Wallace, *Chem. Commun.* **2002**, 358.

13. (a) H. Boerrigter, L. Grave, J. W. M. Nissink, L. A. J. Chrisstoffels, J. H. van der Maas, W. Verboom, F. de Jong, and D. N. Reinhoudt, *J. Org. Chem.* **1998**, *63*, 4174. (b) F. Werner and H. J. Schneider, *Helv. Chim. Acta* **2000**, *83*, 465.

14. (a) P. Bühlmann, S. Nishizawa, K. P. Xiao, and Y. Umezawa, *Tetrahedron*, **1997**, *53*, 1647. (b) S. Sasaki, M. Mizuno, K. Naemura, and Y. Tobe, *J. Org. Chem.* **2000**, *65*, 275.

15. (a) P. A. Gale, J. L. Sessler, and V. Král, *Chem. Commun.* **1998**, 1. (b) C. Bucher, R. S. Zimmerman, V. Lynch, and J. L. Sessler, *J. Am. Chem. Soc.* **2001**, *123*, 9716. (c) C. J. Woods, S. Camiolo, M. E. Light, S. J. Coles, M. B. Hursthouse, M. A. King, P. A. Gale, and J. W. Essex, *J. Am. Chem. Soc.* **2002**, *124*, 8644.

16. J. L. Sessler and J. M. Davis, *Acc. Chem. Res.* **2001**, *34*, 989.

17. (a) J. L. Sessler, M. Cyr, H. Furuta, V. Král, T. D. Mody, T. Morishima, M. Shionoya, and S. Weghorn, *Pure Appl. Chem.* **1993**, *65*, 393. (b) M. Takeuchi, T. Shioya, and T. M. Swager, *Angew. Chem., Int. Ed.* **2001**, *40*, 3372.

18. (a) P. A. Gale, S. Camiolo, C. P. Chapman, M. E. Light, and M. B. Hursthouse, *Tetrahedron Lett.* **2001**, *42*, 5095. (b) M. Dudič, P. Lhoták, I. Stibor, K. Lang, and P. Prošková, *Org. Lett.* **2003**, *5*, 149.

19. E. Graf and J. M. Lehn, *J. Am. Chem. Soc.* **1976**, *98*, 6403.

20. (a) H. Miyaji, W. Sato, J. L. Sessler, and V. M. Lynch, *Tetrahedron Lett.* **2000**, *41*, 1369. (b) P. Piatek and J. Jurczak, *Chem. Commun.* **2002**, 2450. (c) H. Miyaji, S. R. Collinson, I. Prokeŝ, and J. H. R. Tucker, *Chem. Commun.* **2003**, 64.

21. (a) H. Miyaji, W. Sato, and J. L. Sessler, *Angew. Chem., Int. Ed.* **2000**, *39*, 1777. (b) H. Miyaji and J. L. Sessler, *Angew. Chem., Int. Ed.* **2001**, *40*, 154. (c) D. Jiménez, R. Martínez-Máñez, F. Sancenón, and J. Soto, *Tetrahedron Lett.* **2002,** *43*, 2823.

22. (a) C. Lee, D. H. Lee, and J. I. Hong, *Tetrahedron Lett.* **2001**, *42*, 8665. (b) F. Sancenón, R. Martínez-Máñez, and J. Soto, *Angew. Chem., Int. Ed.* **2002,** *41*, 1416. (c) D. H. Lee, J. H. Im, S. U. Son, Y. K. Chung, and J. I. Hong, *J. Am. Chem. Soc.* **2003**, *125*, 7752.

23. (a) S. B. Starnes, S. Arungundram, and C. H. Saundars, *Tetrahedron Lett.* **2002**, *43*, 7785. (b) Y. H. Kim and J. I. Hong, *Chem. Commun.* **2002**. 512.

24. J. L. Sessler and J. M. Davis, *Acc. Chem. Res.* **2001**, *34*, 989.

25. (a) Y. Kubo, S. Ishihara, M. Tsukahara, and S. Tokita, *J. Chem. Soc., Perkin Trans. 2*, **2002**, 1455. (b) S. K. Kim and J. Yoon, *Chem. Commun.* **2002**, 770. (c) J. Y. Kwon, Y. J. Jang, S. K. Kim, K. H. Lee, J. S. Kim, and J. Yoon, *J. Org. Chem.* **2004**, *69*, 5155.

26. (a) S. Watanabe, N. Higashi, M. Kobayashi, K. Hamanaka, Y. Takata, and K. Yoshida, *Tetrahedron Lett.* **2000**, *41*, 4583. (b) M. E. Padilla-Tosta, J. M. Lloris, R. Martínez-Máñez, T. Pardo, J. Soto, A. Benito, and M. D. Marcos, *Inorg. Chem. Commun.* **2000**, *3*, 45.

27. K. Kobiro and Y. Inoue, *J. Am. Chem. Soc.* **2003**, *125*, 421.

28. X.-H. Hou and K. Kobiro, *Tetrahedron*, **2005**, *61*, 5866.

29. For reviews, see: (a) F. P. Schmidtchen and M. Berger, *Chem. Rev.* **1997**, *97*, 1609. (b) P. A. Gale, *Coord. Chem. Rev.* **2000**, *199*, 181. (c) P. A. Gale, *Coord. Chem. Rev.* **2001**, *213*, 79. (d) P. D. Beer and P. A. Gale, *Angew. Chem., Int. Ed.* **2001**,

40, 486. (e) R. Martínez-Máñez and F. Sancenón, *Chem. Rev.* **2003**, *103*, 4419. (f) K. A. Schug, and W. Lindner, *Chem. Rev.* **2005**, *105*, 67.

30. X.-H. Hou and K. Kobiro, *Chem. Lett.* **2006**, *35*, 116.

Chapter 2.

Versatility of an Intramolecularly Hydrogen-bonded 4-(*N*,*N*-Dimethylamino)benzoate Group as a Signaling Subunit for Anion Recognition

2-1 Introduction

The design of artificial receptors (hosts) for recognition of anionic species is a subject of current interest due to their importance in a wide area ranging from chemical, biological, and environmental fields.[1] Central to the designing of the receptors with high complexation ability as well as excellent selectivity in anion recognition has been the development of new binding principles.[2] In order to estimate the complexation behavior of receptors toward anions, signaling of the anion coordination process is of great importance. In this sense, separation of the signaling subunit and the binding subunit in a receptor would lead to more intelligent and sophisticated systems to obtain clear binding information (Figure 2-1).

Kobiro and Inoue have designed and synthesized a new type of simple host molecule **9** having a 4-(*N*,*N*-dimethylamino)benzoate (DMAB) group as a signaling

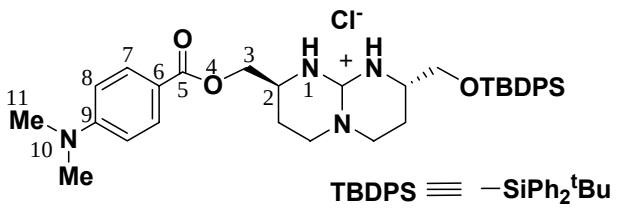

9

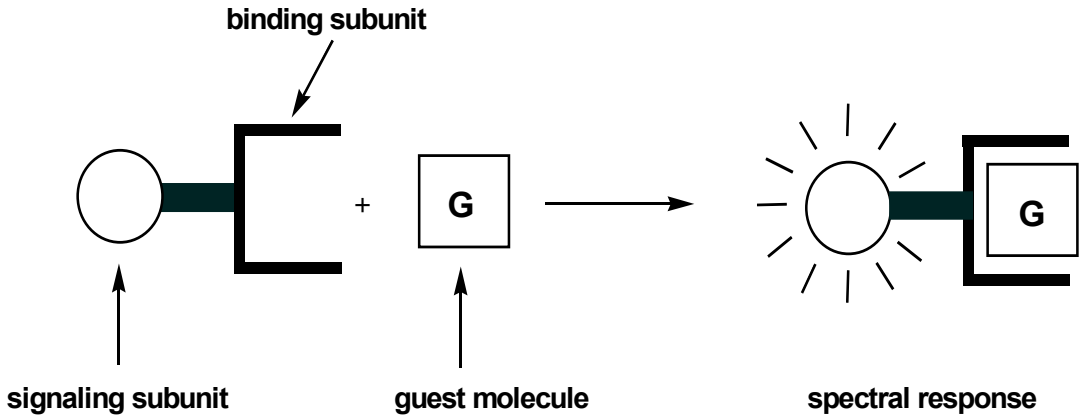

Figure 2-1. Binding subunit-signaling subunit method for anion recognition.

subunit and a chiral bicyclic guanidinium ion moiety as a binding subunit.[3] In the complexation of host **9** with sulfate anion, the guanidinium group was employed as a suitable binding site through both of dual hydrogen bonding and electrostatic interactions. The DMAB signaling subunit provided spectral information upon complexation process. Electronic absorption spectra of **9** revealed that strong intramolecular hydrogen bonding was present between the carbonyl oxygen atom of the DMAB group and one of the N-H groups of the guanidinium ion moiety even in a polar solvent such as acetonitrile. The stepwise 1:1 (host **9** : sulfate anion) and 2:1 complexation constants (log $K_{1:1}$ = 6.2 and log $K_{2:1}$ = 4.7, respectively) were determined by ^{1}H NMR titrations. The CD exciton chirality method allowed us to determine the chiral sense of the two DMAB groups in the 2:1 complex as negative. The dual fluorescence behavior of the DMAB group demonstrated not only the binding information but also the role of the counteraction tetrabutylammonium (TBA) upon complexation of host **9** with the sulfate anion.

In order to know whether the DMAB signaling subunit is versatile to give clear binding information and to clarify whether the host **9** shows selective complexation

with expanded variety of anions or not, ^{1}H NMR, CD, and fluorescence titration experiments of host **9** toward a variety of anions were carried out. Divalent anions such as hydrogenphosphate (HPO_4^{2-}, tetrahedral), dihydrogenpyrophosphate ($H_2P_2O_7^{2-}$, dual tetrahedral), and adenosine 5'-monophospate (AMP^{2-}, tetrahedral) which is a biologically important derivative of hydrogenphosphate, and monovalent anions, such as dihydrogenphosphate ($H_2PO_4^-$, tetrahedral), perchlorate (ClO_4^-, tetrahedral), nitrate (NO_3^-, trigonal planar), tetrafluoroborate (BF_4^-, tetrahedral), hydrogensulfate (HSO_4^-, tetrahedral), and hexafluorophosphate (PF_6^-, hexagonal), were selected. All anions were used as tetrabutylammonium (TBA) salts.

In this chapter, the scope and limitations of the DMAB signaling subunit in host **9** upon complexation with a variety of anions possessing monovalent or divalent negative charge with trigonal planar, tetrahedral, dual-tetrahedral, or octahedral geometry are discussed. The versatility of the DMAB signaling subunit for anion recognition is also studied by means of ^{1}H NMR, CD, and fluorescence spectroscopy.

2-2 Results and Discussion

2-2-1 ^{1}H NMR spectral titrations

2-2-1-2 ^{1}H NMR spectral titrations

^{1}H NMR spectral titration method is a useful and powerful technique to investigate complexation behavior between hosts and guests, especially in the case that hosts have no chromophore or fluorophore.[4] Kobiro and Ionue reported that clear chemical shift changes of aromatic protons (H7 and H8) and *N*-methyl proton (H11) of the signaling subunit in host **9** were observed by ^{1}H NMR titration in CD_3CN, when bistetrabutylammonium sulfate $(TBA)_2SO_4$ was added to host **9**. All of the H7, H8, and H11 signals first shifted to high field almost proportionally to the amount of added sulfate until the SO_4^{2-}/**9** ratio reached 0.5, and then they moved to the opposite direction until the ratio reached 1-1.2 and finally leveled off thereafter, as can be seen in Figure 2-2. The observation of the clear chemical shift changes is quite interesting, since these protons (H7, H8, and H11) are quite distant from the NH group of the binding site and the existence of three single bonds between N1 and O4 would make it difficult to transmit any electronic effect from the NH groups in the binding subunit to the DMAB chromophore through the bonds. The clear chemical shift changes observed are, therefore, rationalized by fission of the intramolecular hydrogen bonding (Figure 2-3), the existence of which was indicated by electronic absorption spectra of host **9** in the paper.[3] When a guest anion binds to the guanidinium ion moiety of host **9** with "covered" structure, the intramolecular hydrogen bonding will be broken to release a free carbonyl group with an "open" structure, which will influence the electronic and/or steric environment on the DMAB group.

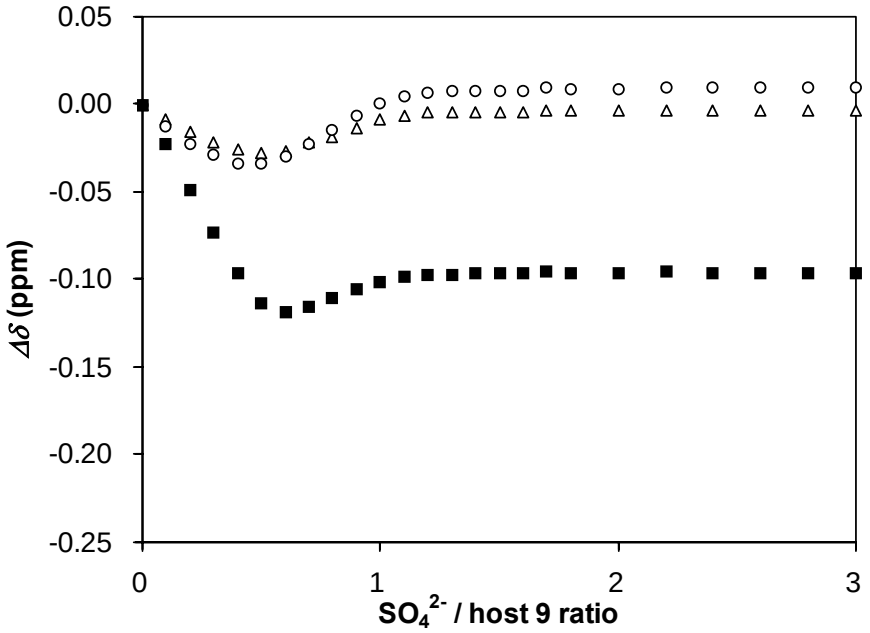

Figure 2-2. Chemical shift changes of aromatic (■ : H7 and ○ : H8) and *N*-methyl (△ : H11) protons of host **9** upon ^{1}H NMR titrations with $(TBA)_2SO_4$ in CD_3CN.

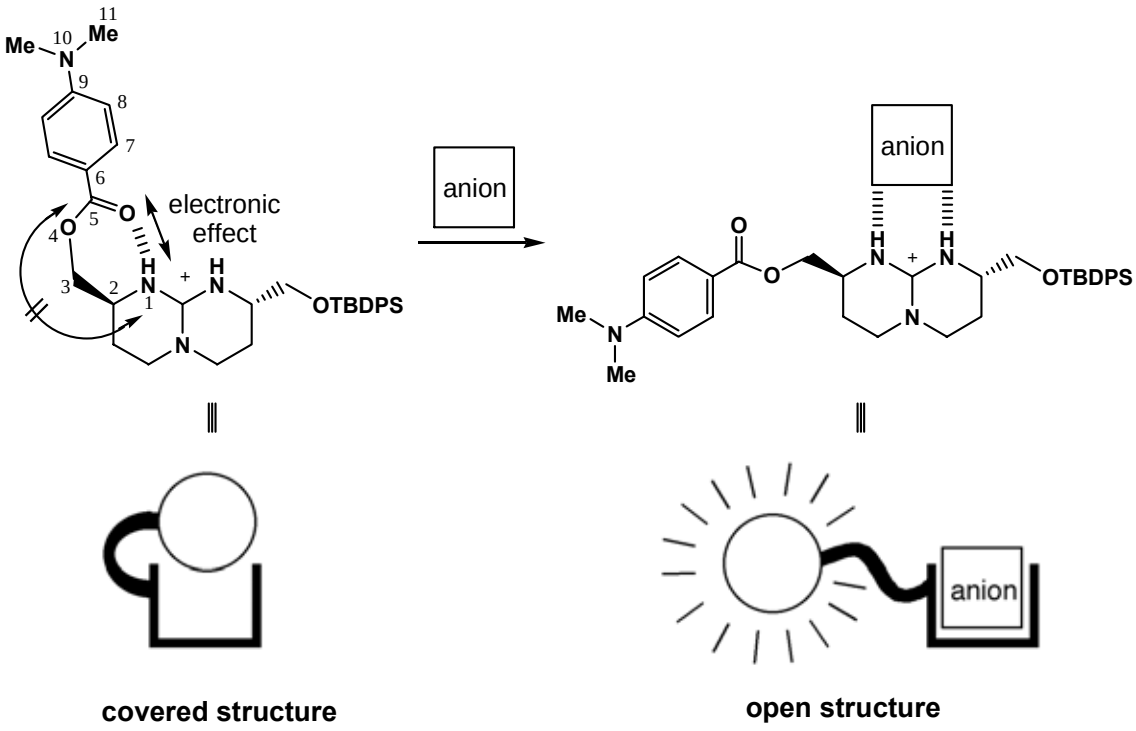

Figure 2-3. The schematic expressions of 'covered' and 'open' structures of host **9**.

In order to make it clear whether the chemical shift changes are a common aspect of anion binding in host **9** or not, a variety of anions, such as divalent anions, HPO_4^{2-}, $H_2P_2O_7^{2-}$, and AMP^{2-}, and monovalent anions, ClO_4^-, NO_3^-, BF_4^-, HSO_4^-, PF_6^-, and $H_2PO_4^-$, were selected, all of which are potentially able to bind to the guanidinium ion moiety.

At first, the complexation behavior of host **9** with the divalent anions was studied by the ^1H NMR titration method in CD_3CN at 25°C. The chemical shifts of aromatic protons (H7 and H8) and N-methyl proton (H11) were monitored during the titrations. As can be seen in Figure 2-4, when host **9** was titrated with HPO_4^{2-}, a representative anion having a tetrahedral array of four oxygen atoms with divalent negative charges, similar titration curves were obtained as compared with those for SO_4^{2-}. All of the H7, H8, and H11 signals, namely, first decreased almost linearly toward high field along with the increasing of the amount of added HPO_4^{2-} till the HPO_4^{2-}/**9** ratio reached 0.5, then they oppositely increased toward low field until the ratio reached almost 2, and finally leveled off thereafter. In the case of $H_2P_2O_7^{2-}$, which contains dual phosphate moieties in a molecule, the titration curves were close to the cases of SO_4^{2-} and HPO_4^{2-}, irrespective of a dual tetrahedral array of seven oxygen atoms (Figure 2-5). All of the H7, H8, and H11 signals shifted to high field first and then low field and maintained no changes to the end of titrations, while the chemical changes appeared around the 0.5 equivalent amounts of addition of $H_2P_2O_7^{2-}$ was much smoother than those observed for SO_4^{2-} and HPO_4^{2-}. With respect to AMP^{2-} having the phosphate moiety as a partial structure, the chemical shift changes were quite similar to those recorded in the cases of SO_4^{2-} and HPO_4^{2-}, irrespective of a large volume of an organic residue on one of the oxygen atoms of the phosphate anion (Figure 2-6). The characteristic titration curves

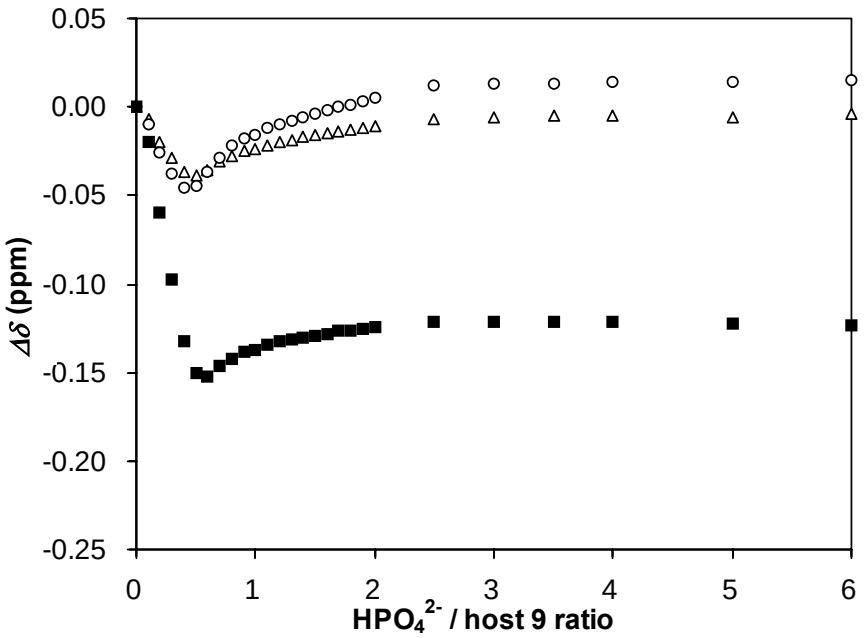

Figure 2-4. Chemical shift changes of aromatic (■ : H7 and ○ : H8) and N-methyl (△ : H11) protons of host **9** upon ^{1}H NMR titrations with $(TBA)_2HPO_4$ in CD_3CN.

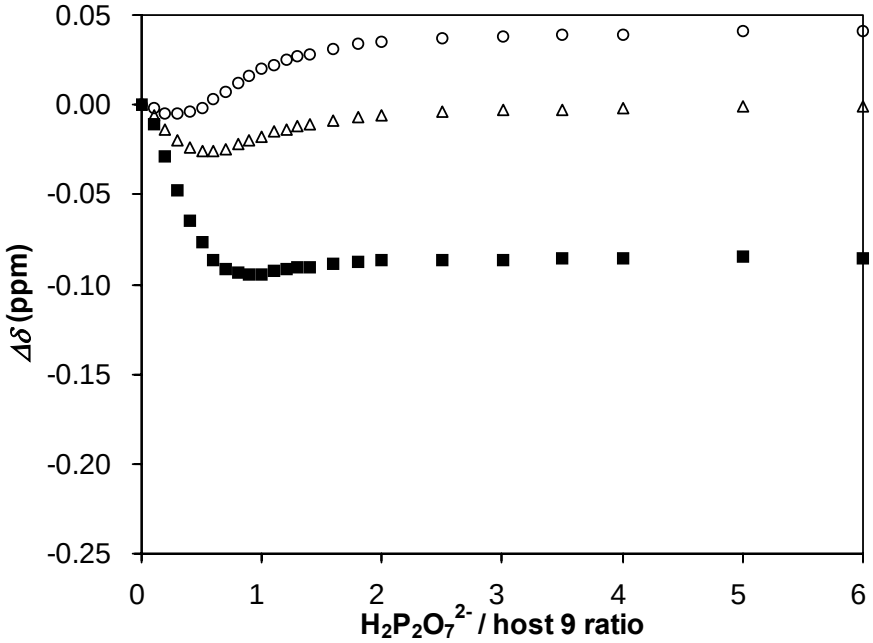

Figure 2-5. Chemical shift changes of aromatic (■ : H7 and ○ : H8) and N-methyl (△ : H11) protons of host **9** upon ^{1}H NMR titrations with $(TBA)_2H_2P_2O_7$ in CD_3CN.

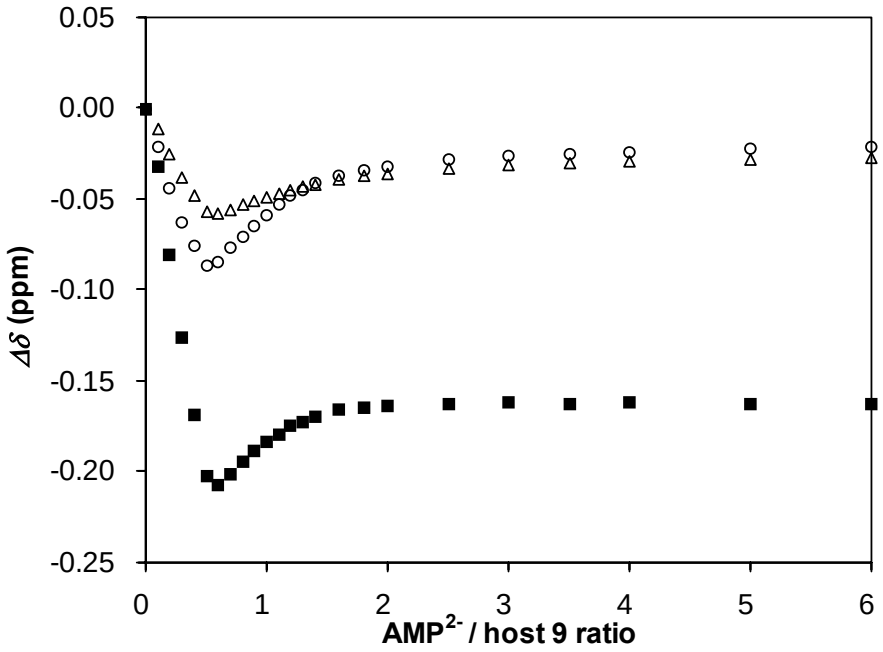

Figure 2-6. Chemical shift changes of aromatic (■ : H7 and ○ : H8) and *N*-methyl (△ : H11) protons of host **9** upon ^{1}H NMR titrations with $(TBA)_2AMP$ in CD_3CN.

clearly indicate that 2:1 (host **9** : anion) complexes were formed at the initial stages of titrations up to the anion/**9** ratio equal to 0.5 and then they were gradually replaced by the 1:1 complexes with increasing the anion/**9** ratio ranging from 0.5 to 2, and finally the 1:1 complexes dominated thereafter.

Next, the complexation behavior of host **9** toward the monovalent anions was also studied by ^{1}H NMR titrations in CD_3CN at 25°C via monitoring the chemical shift changes of H7, H8, and H11 protons. Upon addition of ClO_4^-, one of the most representative monovalent anions which have a tetrahedral array of four oxygen atoms with monovalent negative charge, the chemical shift changes of host **9** monitored in H7 proton was quite slight, while almost no changes were observed in H8 and H11 protons, even though excess amounts of ClO_4^- were added, as shown in Figure 2-7. Similar results were obtained in the cases of other monovalent anions such as NO_3^- (Figure 2-8),

BF_4^- (Figure 2-9), HSO_4^- (Figure 2-10) and PF_6^- (Figure 2-11). Unfortunately, precipitation was observed during ^1H NMR titration of **9** with $H_2PO_4^-$. The observed simple and moderate upfield shift suggested that weak 1:1 complexation occurred between host **9** and ClO_4^- as well as NO_3^-, BF_4^-, HSO_4^-, and PF_6^-.

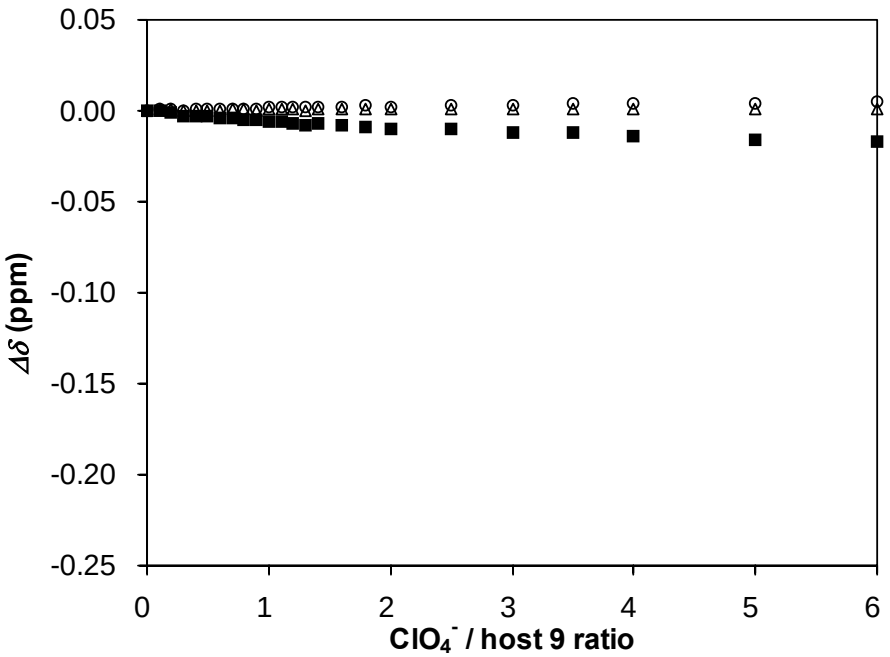

Figure 2-7. Chemical shift changes of aromatic (■ : H7 and ○ : H8) and *N*-methyl (△ : H11) protons of host **9** upon ^1H NMR titrations with (TBA)ClO_4 in CD_3CN.

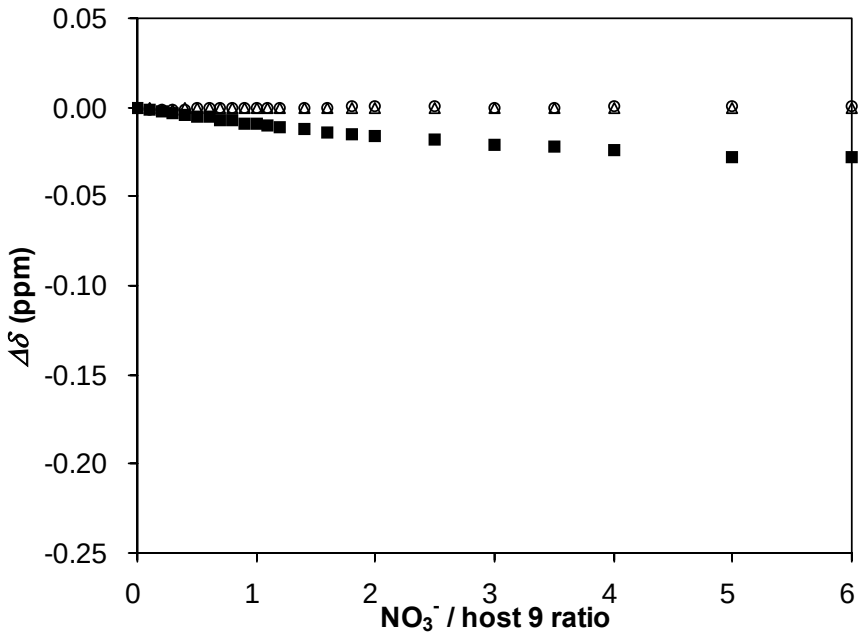

Figure 2-8. Chemical shift changes of aromatic (■ : H7 and ○ : H8) and *N*-methyl (△ : H11) protons of host **9** upon ^{1}H NMR titrations with (TBA)NO_3 in CD_3CN.

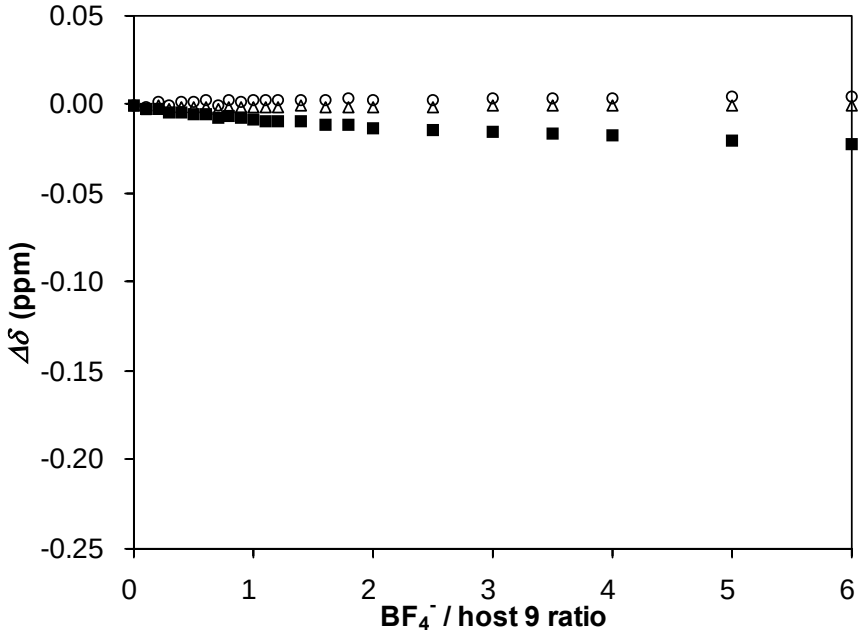

Figure 2-9. Chemical shift changes of aromatic (■ : H7 and ○ : H8) and *N*-methyl (△ : H11) protons of host **9** upon ^{1}H NMR titrations with (TBA)BF_4 in CD_3CN.

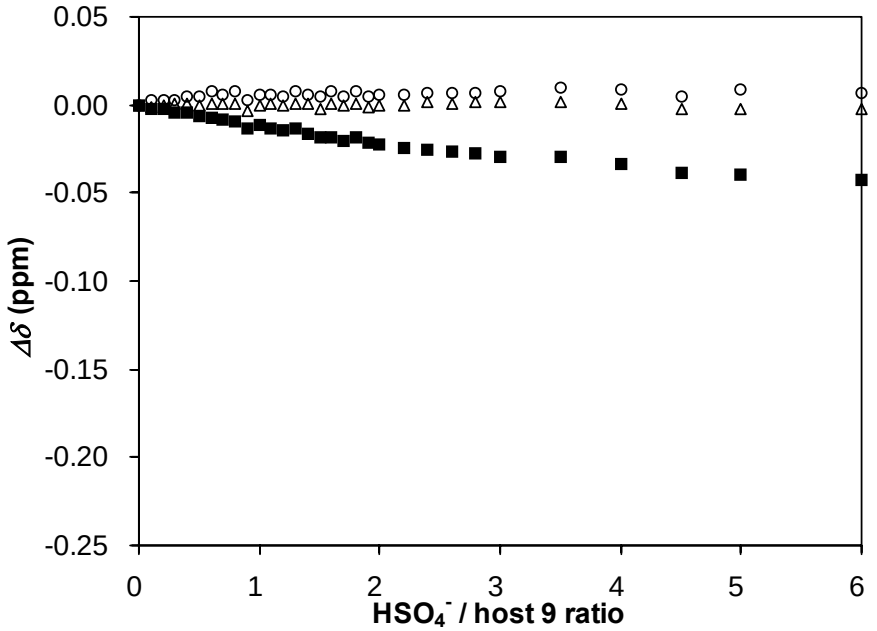

Figure 2-10. Chemical shift changes of aromatic (■ : H7 and ○ : H8) and *N*-methyl (△ : H11) protons of host **9** upon ^{1}H NMR titrations with (TBA)HSO_4 in CD_3CN.

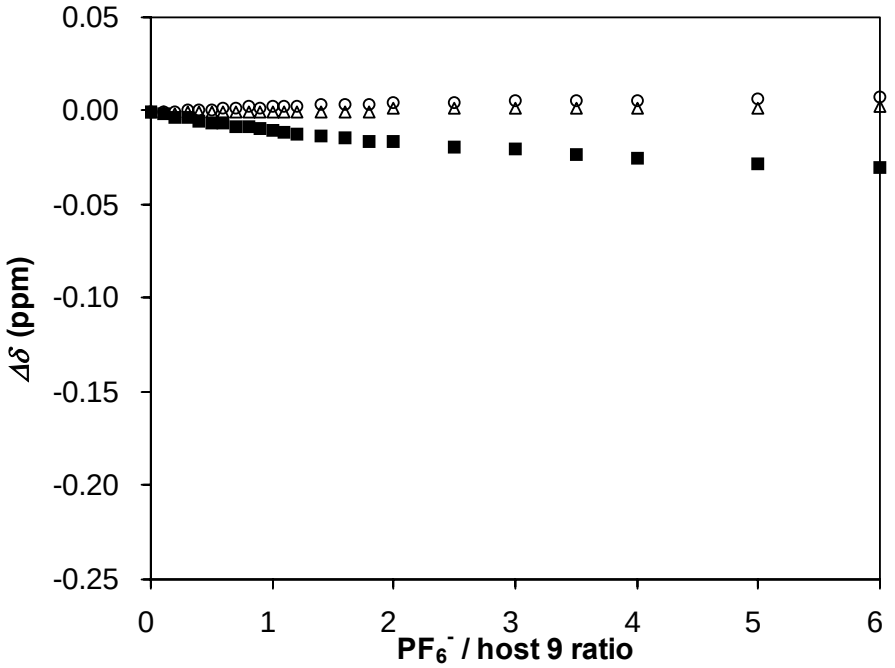

Figure 2-11. Chemical shift changes of aromatic (■ : H7 and ○ : H8) and *N*-methyl (△ : H11) protons of host **9** upon ^{1}H NMR titrations with (TBA)PF_6 in CD_3CN.

For easy comparison of the titration behavior of host **9** toward the anions, the chemical shift changes of aromatic H7 and H8 as well as *N*-methyl H11 protons were summarized into Figures 2-12, Figure 2-13 and Figure 2-14 for H7, H8, and H11, respectively. As can be seen in three figures, the titration profiles of host **9** upon complexation with the divalent anions (SO_4^{2-}, HPO_4^{2-}, $H_2P_2O_7^{2-}$, and AMP^{2-}) were quite different from those upon complexation with the monovalent anions (NO_3^-, BF_4^-, ClO_4^-, HSO_4^-, and PF_6^-). Furthermore, the inflection points around 0.5 equivalent amounts of addition of the divalent anions in titration profiles ensure that host **9** leads to stepwise 2:1 and 1:1 complexation with the divalent anions. In the cases of the monovalent anions, the chemical shift changes were so simple and quite small that host **9** would show only 1:1 complexation with the monovalent anions. The observation obviously demonstrates that host **9** exhibited highly selective complexation behavior with the divalent anions over the monovalent anions.

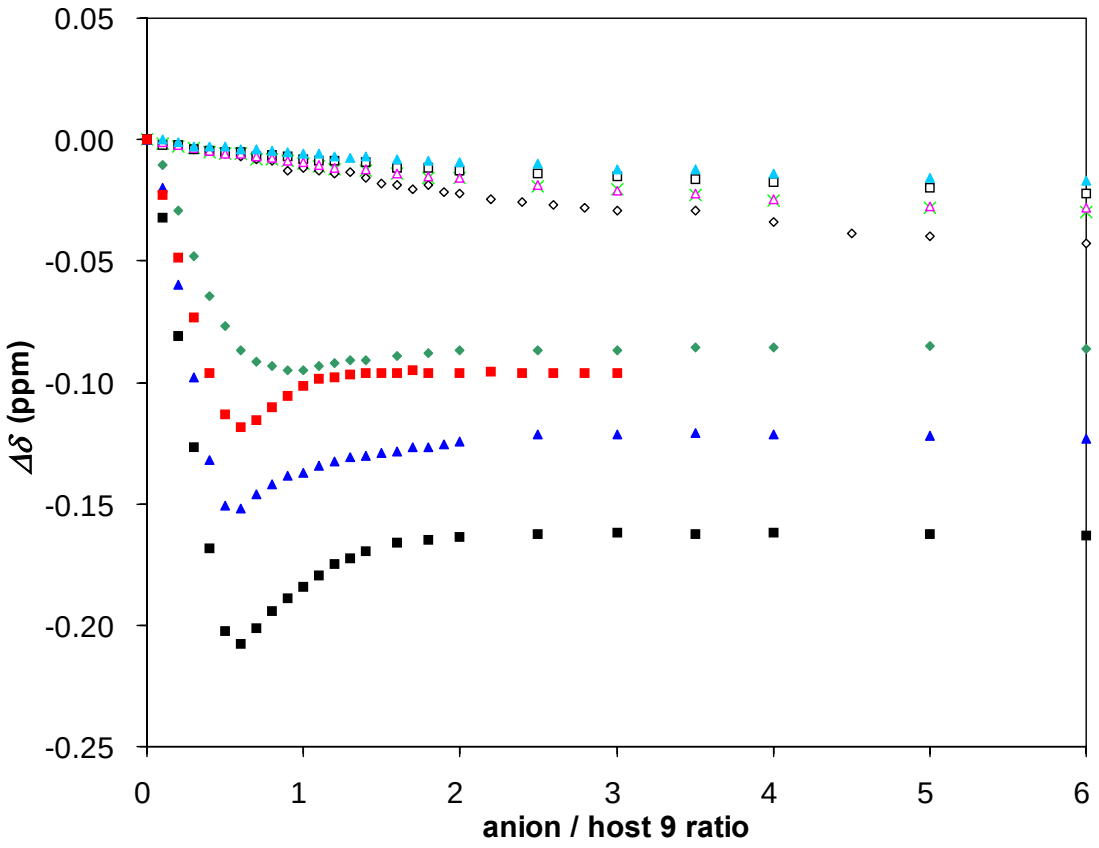

Figure 2-12. Chemical shift changes of aromatic H7 protons of host **9** upon ^{1}H NMR titrations with $(TBA)_2SO_4$ (■), $(TBA)_2HPO_4$ (▲), $(TBA)_2H_2P_2O_7$ (●), $(TBA)_2AMP$ (■), $(TBA)ClO_4$ (▲), $(TBA)NO_3$ (△), $(TBA)BF_4$ (□), $(TBA)HSO_4$ (◇) and $(TBA)PF_6$ (×) in CD_3CN.

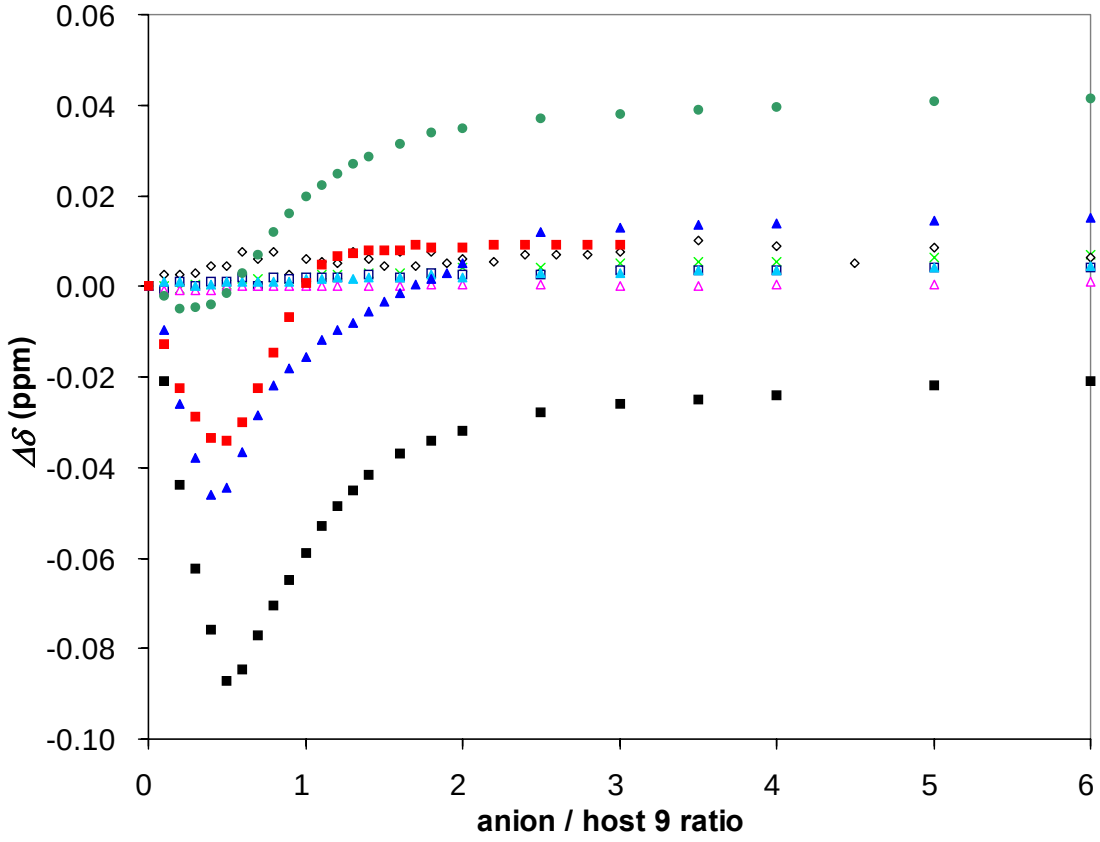

Figure 2-13. Chemical shift changes of aromatic H8 protons of host **9** upon ^{1}H NMR titrations with $(TBA)_2SO_4$ (■), $(TBA)_2HPO_4$ (▲), $(TBA)_2H_2P_2O_7$ (●), $(TBA)_2AMP$ (■), $(TBA)ClO_4$ (▲), $(TBA)NO_3$ (△), $(TBA)BF_4$ (□), $(TBA)HSO_4$ (◇) and $(TBA)PF_6$ (×) in CD_3CN.

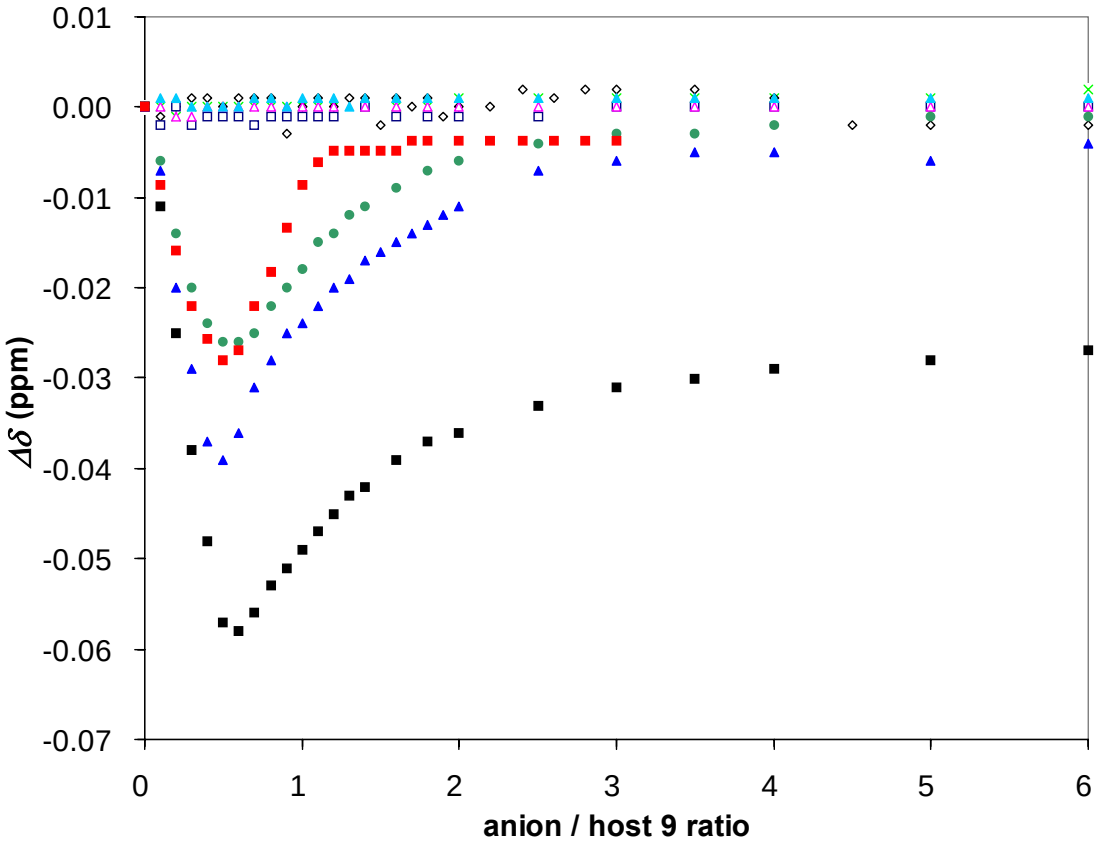

Figure 2-14. Chemical shift changes of aromatic *N*-methyl H11 protons of host **9** upon ^{1}H NMR titrations with $(TBA)_2SO_4$ (■), $(TBA)_2HPO_4$ (▲), $(TBA)_2H_2P_2O_7$ (●), $(TBA)_2AMP$ (■), $(TBA)ClO_4$ (▲), $(TBA)NO_3$ (△), $(TBA)BF_4$ (□), $(TBA)HSO_4$ (◇) and $(TBA)PF_6$ (×) in CD_3CN.

2-2-1-2 Binding constants and anion selectivity of host 9

As concluded in the former section, host **9** showed 1:1 binding stoichiometry toward the monovalent anions and stepwise 1:1 and 2:1 binding stoichiometry toward the divalent anions. (Figure 2-15). The binding constant $K_{1:1}$ for the 1:1 complexation is, therefore, defined by equation (1),

$$\mathbf{9}^{+} + A^{-} \underset{}{\overset{K_{1:1}}{\rightleftharpoons}} \mathbf{9}^{+}\bullet A^{-} \qquad K_{1:1} = [\mathbf{9}^{+}\bullet A^{-}]/([\mathbf{9}^{+}][A^{-}]) \qquad (1)$$

where A^{-} denotes a monovalent anion. In the case of a divalent anion, on the other hand, not only 1:1 complex (**B**) but also 2:1 complex (**A**) will be formed by addition of the anion as illustrated in Figure 2-15. The stepwise binding constants $K_{1:1}$ and $K_{2:1}$ for the 1:1 and 2:1 complexes, therefore, are defined by equations (2) and (3), respectively,

$$\mathbf{9}^{+} + A^{2-} \underset{}{\overset{K_{1:1}}{\rightleftharpoons}} \mathbf{9}^{+}\bullet A^{2-} \qquad K_{1:1} = [\mathbf{9}^{+}\bullet A^{2-}]/([\mathbf{9}^{+}][A^{2-}]) \qquad (2)$$

$$\mathbf{9}^{+}\bullet A^{2-} + \mathbf{9}^{+} \underset{}{\overset{K_{2:1}}{\rightleftharpoons}} (\mathbf{9}^{+})_2\bullet A^{2-} \qquad K_{2:1} = [(\mathbf{9}^{+})_2\bullet A^{2-}]/([\mathbf{9}^{+}\bullet A^{2-}]\,[\mathbf{9}^{+}]) \qquad (3)$$

where A^{2-} denotes a divalent anion. The titration data obtained with the H7 proton of **9** were submitted to the non-linear least square curve-fitting[4a,5] to calculate $K_{1:1}$ and $K_{2:1}$ values, because the H7 proton exhibited the largest chemical shift changes among three protons upon titrations. The calculation results of binding constants are summarized in Table 2-1.

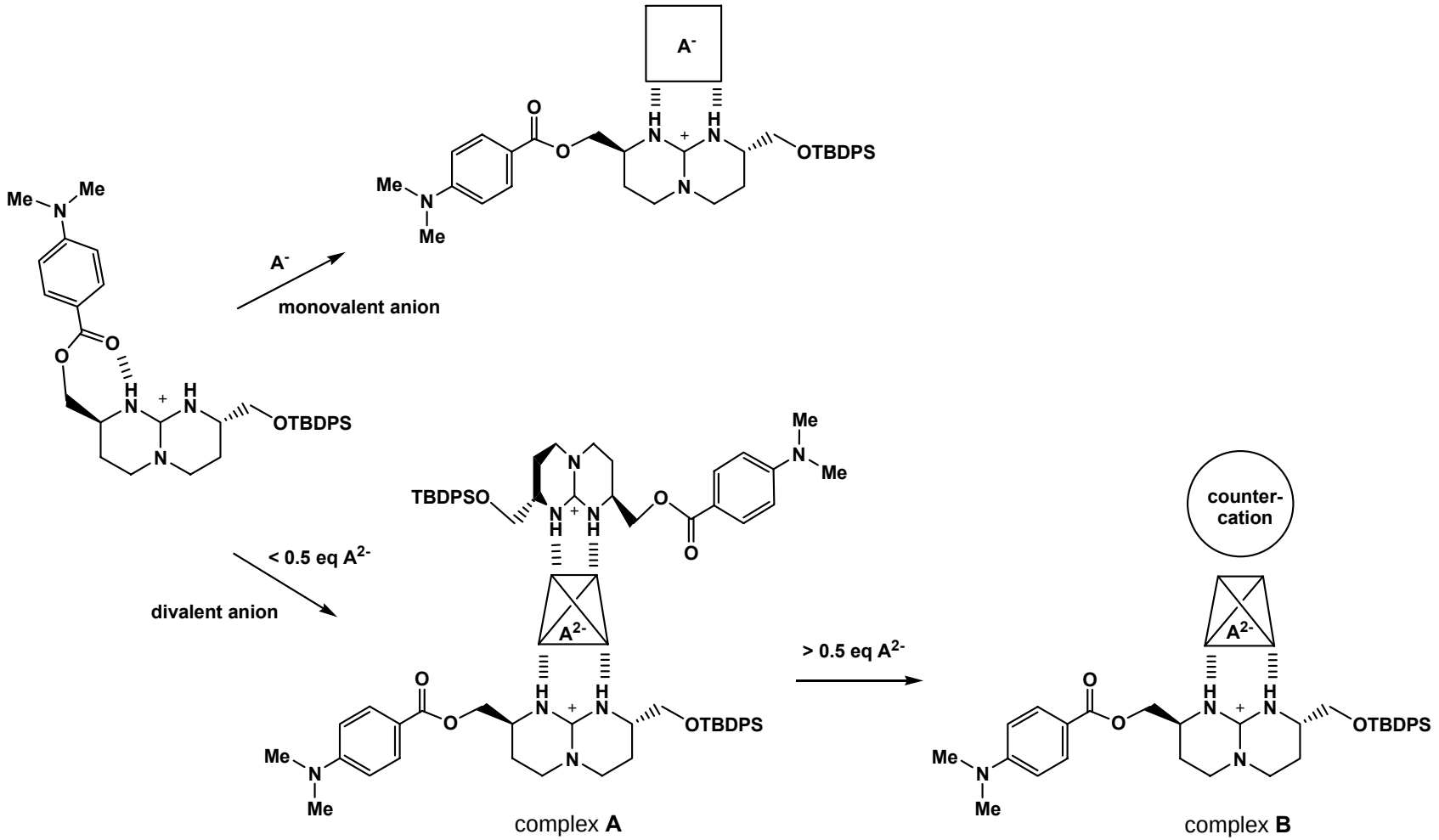

Figure 2-15. The complexation stoichiometry of host **9** toward monovalent anions and divalent anions.

Table 2-1. Binding Constants of Host **9** with Anions in CD_3CN

anion	binding constants (log M^{-1})	
	log $K_{1:1}$	log $K_{2:1}$
HPO_4^{2-}	6.2	4.9
$H_2P_2O_7^{2-}$	4.4	1.8
AMP^{2-}	> 7[a]	> 5[a]
SO_4^{2-}	6.2[b]	4.7[b]
NO_3^-	< 2[c]	—
BF_4^-	< 2[c]	—
ClO_4^-	< 2[c]	—
$H_2PO_4^-$	4.4[d]	—
HSO_4^-	< 2[c]	—
PF_6^-	< 2[c]	—

[a] Binding constants $K_{1:1}$ and $K_{2:1}$ are too large to be accurately determined.

[b] Taken from reference 3.

[c] Binding constant $K_{1:1}$ is not determined accurately because chemical shift changes were so small (< 0.03 ppm) and clear endpoint of titration was not obtained.

[d] The binding constant of $K_{1:1}$ was calculated, instead, by the use of titration data on CD shown in Figure 2-22, because precipitation occurred during ^1H NMR titration of **9** with $H_2PO_4^-$.

The tetrahedral divalent anion HPO_4^{2-} exhibited quite large binding affinities (log $K_{1:1}$ = 6.2 and log $K_{2:1}$ = 4.9) and these binding constants are almost identical with those for SO_4^{2-} (log $K_{1:1}$ = 6.2 and log $K_{2:1}$ = 4.7). With respect to $H_2P_2O_7^{2-}$ having divalent negative charge with dual tetrahedral array of seven oxygen atoms, the binding constants of log $K_{1:1}$ (4.4) and log $K_{2:1}$ (1.8) are relatively large. Binding constants, $K_{1:1}$ and $K_{2:1}$, for AMP^{2-} were too large to be calculated accurately. On the other hand, the binding constants for monovalent anions ClO_4^-, NO_3^-, BF_4^-, HSO_4^-, and PF_6^-, the geometries of which are tetrahedral, trigonal planer, and octahedral, as illustrated in

Figure 1-1, turned out to be small (log $K_{1:1}$ < 2.0). Interestingly, $H_2PO_4^-$ (tetrahedral) showed relatively strong binding affinity (log $K_{1:1}$ = 4.4). Host **9**, therefore, showed strong complexation affinities toward the divalent anions over the monovalent anions.

Anions, indeed, must compete with and then overcome the inherent strong internal hydrogen bonding existing between one of the NH groups of the guanidinium moiety and the carbonyl oxygen atom of the DMAB group to give complexes. Geometric matching between the binding site of host **9** and anions as well as charge densities on O or F atoms of guest anions must play a crucial role in complexation in this regard, because host **9** binds the anions through both dual-hydrogen-bonding and ion-pairing interactions.[3] The geometric matching can be estimated by comparison of the interatomic distance of two NH groups of host **9** and those of O atoms or F atoms of the anions. Thus, semiempirical AM1 calculations[6] of anions were performed in order to determine the interatomic distances of O atoms or F atoms and charges on the anions. The calculation results were presented in Table 2-2. The interatomic distance of and charges on hydrogen atoms of cyclic guanidinium ion, a simplified model compound **11** for host **9**, were also calculated to give the values of 2.37 Å and +0.273 au, respectively.

Several interesting trends can be gleaned from the data of Tables 2-1 and 2-2. Host **9** showed much higher complexation affinities to the divalent anions, SO_4^{2-}, HPO_4^{2-}, $H_2P_2O_7^{2-}$, and AMP^{2-}, than those to the monovalent anions, ClO_4^-, NO_3^-, BF_4^-, HSO_4^-, and PF_6^-. The higher affinities of host **9** to the divalent anions, HPO_4^{2-} and SO_4^{2-},

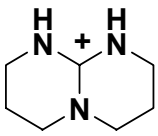

11

Table 2-2. Calculated Interatomic Distances between Oxygen Atoms or Fluorine Atoms, Charges on Oxygen or Fluorine Atoms, and Heat of Formation

anion	O---O or F---F distances (Å)	charges on O or F atom (au)	ΔH_f (kcal·mol^{-1})
HPO_4^{2-}	2.56×2, 2.55, 2.54×2, 2.41	-1.29, -1.27×2, -0.85	-205
SO_4^{2-}	2.39×6	-1.20×4	-133
NO_3^-	2.12×3	-0.57×3	-89
BF_4^-	2.12×6	-0.32×4	-397
ClO_4^-	2.89×6	-0.50×4	166
$H_2PO_4^-$	2.66, 2.56×2, 2.47, 2.44×2	-1.17×2, -0.82×2	-316
HSO_4^-	2.44×2, 2.37×2, 2.36×2	-1.11, -1.08×2, -0.82	-234
PF6-	2.22×15	-0.65×6	-504

should be attributable to the large negative charges on the O atoms (-1.29 — -0.85 au: HPO_4^{2-} and SO_4^{2-}). The distances between the O atoms in SO_4^{2-} (2.39 Å) are almost equal to that of the H atoms of the guanidinium NH groups (2.37 Å) in the model compound **11**. Similarly, the corresponding distances of HPO_4^{2-} are almost equal to or only a little bit longer (2.56 — 2.41 Å) than that of the calculated distance of the guanidinium NH groups (2.37 Å). By contrast with the divalent anions, monovalent anions, ClO_4^-, NO_3^-, BF_4^-, and PF_6^-, exhibiting very low affinity toward host **9**, have smaller negative charges on their O or F atoms (-0.65 — -0.32 au) as well as a little bit shorter (2.22 — 2.12 Å: NO_3^-, BF_4^-, and PF_6^-) or quite longer (2.89 Å: ClO_4^-) interatomic distances between the O atoms or F atoms than that of the NH groups in the model compound **11**(2.37 Å). The low affinity of host **9** to the anions is most probably due to small charges on the O or F atoms of the anions and the geometric disagreement between the binding site of host **9** and guest anions. The exceptionally high affinity of $H_2PO_4^-$ is presumably due to the significantly large charge of the O atoms (-1.17 —

-0.82 au) among monovalent anions. On the contrary, HSO_4^- has comparable negative charge on the O atoms (-1.11 — -0.82 au) to those of HPO_4^{2-} and SO_4^{2-} (-1.29 — -0.85 au) and interatomic distances between the O atoms (2.44 — 2.36 Å) are almost equal to the NH distance of the guanidinium ion (2.37 Å), while the binding affinity resulted in unexpectedly low value.[7]

2-2-1-3 Conclusions

The DMAB signaling subunit provided quantitative information on complexation of host **9** with a variety of anions in terms of ^{1}H NMR titrations. The titration profiles of host **9** monitored at H7, H8, and H11 protons upon complexation with the divalent anions were remarkably different from those with the monovalent anions. The binding constants of host **9** with the divalent anions were quite larger (SO_4^{2-}: log $K_{1:1}$ = 6.2 and log $K_{2:1}$ = 4.7, HPO_4^{2-}: log $K_{1:1}$ = 6.2 and log $K_{2:1}$ = 4.9, $H_2P_2O_7^{2-}$: log $K_{1:1}$ = 4.4 and log $K_{2:1}$ = 1.8, AMP^{2-}: log $K_{1:1}$ > 7 and log $K_{2:1}$ > 5) than those with the monovalent anions (log $K_{1:1}$ < 2.0, exceptional case of $H_2PO_4^-$: log $K_{1:1}$ = 4.4). Host **9** showed successive 1:1 and 2:1 complexation with SO_4^{2-}, HPO_4^{2-}, $H_2P_2O_7^{2-}$, and AMP^{2-}, while 1:1 complexation with ClO_4^-, NO_3^-, BF_4^-, HSO_4^-, PF_6^-, and $H_2PO_4^-$. It is noteworthy that the dual tetrahedral structure of $H_2P_2O_7^{2-}$ and the existence of an extraordinarily large organic residue of AMP^{2-} did not influence their complexation behavior with host **9**. Therefore, the complexation information offered by DMAB signaling subunit indicated that host **9** exhibited strong binding ability and high selectivity toward SO_4^{2-}, HPO_4^{2-}, $H_2P_2O_7^{2-}$, and AMP^{2-} having a tetrahedral array of oxygen atoms with divalent negative charges over monovalent anions such as NO_3^-, BF_4^-, ClO_4^-, HSO_4^-, and PF_6^-, except for $H_2PO_4^-$.

2-2-2 CD spectral titrations

2-2-2-1 CD spectral titrations[8]

The exciton chirality method is a simple and practical approach for establishing absolute configurations and conformations of organic compounds in solution on a microscale.[9] Kobiro and Inoue reported that the two guanidinium ion moieties in 2:1 complex of host **9** with SO_4^{2-} were fixed in perpendicular arrangement (as a statistical ensemble) to each other around the SO_4^{2-} as illustrated in Figure 2-16. A closer look at this structure immediately reveals that two stereochemical possibilities exist in the complexation mode. One is complex **C** with negative chirality in which two DMAB groups are placed counterclockwise from the front-to-back, whose CD spectrum should show a negative first (at longer wavelength) and a positive second Cotton effect peaks. The other is complex **D** with positive chirality in which two DMAB groups are placed clockwise, whose CD spectrum should show a positive first (at longer wavelength) and a negative second Cotton effect peaks. Complexes **C** and **D** are diastereomers.

Host **9** showed, indeed, simple positive Cotton effect peak in CH_3CN, while the CD spectrum of host **9** was varied to show bisignated exciton coupling with negative first and positive second Cotton effect peaks upon addition of a half equivalent amount of SO_4^{2-}. Then a negative Cotton effect was observed when an excess amount of SO_4^{2-} was added, as shown in Figure 2-17. The observation of the exciton coupling peaks clearly indicates that the spatial array of the two DMAB chromophores in the 2:1 complex should be a counterclockwise arrangement (complex **C**) rather than a clockwise arrangement (complex **D**).

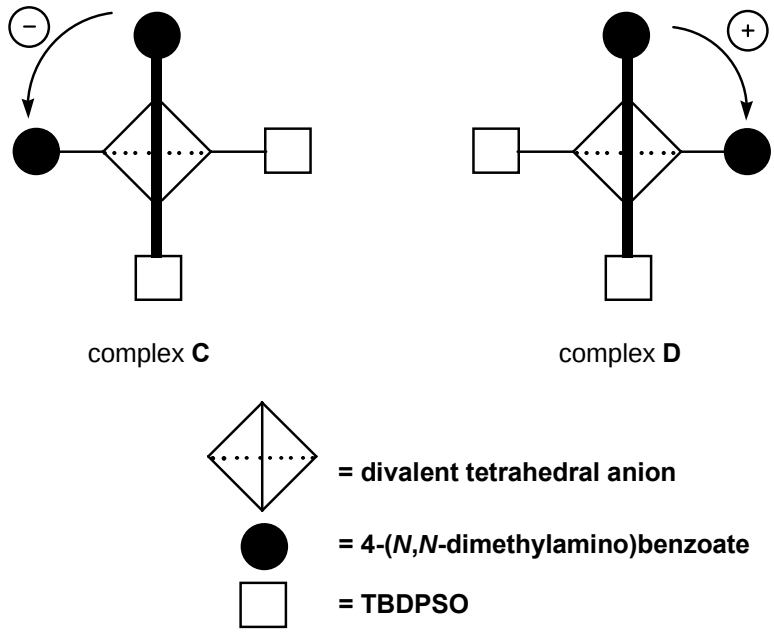

Figure 2-16. Schematic expressions of the exciton chirality of the 2:1 complex between host **9** and divalent anion.

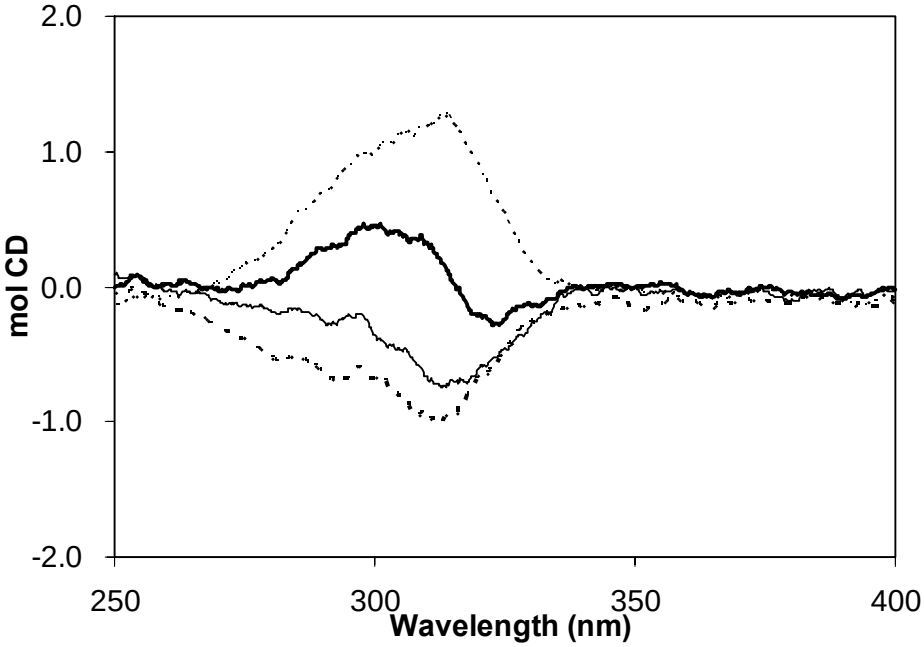

Figure 2-17. CD spectra of acetonitrile solution of host **9** in the absence of (thin dashed line) and in the presence of 0.5 (thick solid line), 1 (thin solid line), and 3 (thick dashed line) equivalents of $(TBA)_2SO_4$.

In order to clarify whether the favorable formation of complex **C** is an intrinsic aspect in the complexation of host **9** with divalent anions possessing a tetrahedral array of four oxygen atoms, the titrations of host **9** with several anions on CD spectra were carried out in acetonitrile. The titrations of host **9** by HPO_4^{2-} and AMP^{2-}, which are divalent anions with a tetrahedral array of four oxygen atoms, exhibited similar results to SO_4^{2-}. In the case of HPO_4^{2-} (Figure 2-18), for example, simple positive Cotton effect peaks were observed in the absence of the anion and, then, the profile of CD spectral varied to show negative first and positive second Cotton effect peaks upon addition of a half amount of HPO_4^{2-}. Finally, a negative Cotton effect peak appeared on addition of an excess amount of HPO_4^{2-}. The observed weak but clear negative first and positive second Cotton effect peaks indicate that two DMAB groups in the 2:1 complex are arranged counterclockwisely. Similar results were given in the case of AMP^{2-} (Figure 2-19), regardless of the sterically bulky organic residue on the oxygen atom of the

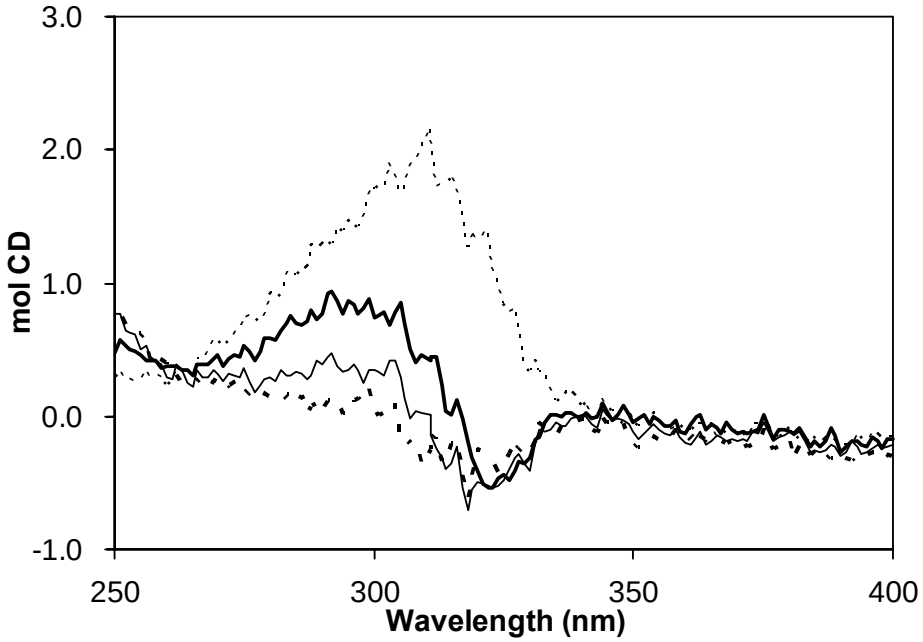

Figure 2-18. CD spectra of acetonitrile solution of host **9** in the absence of (thin dashed line) and in the presence of 0.5 (thick solid line), 1 (thin solid line), and 3 (thick dashed line) equivalents of $(TBA)_2HPO_4$.

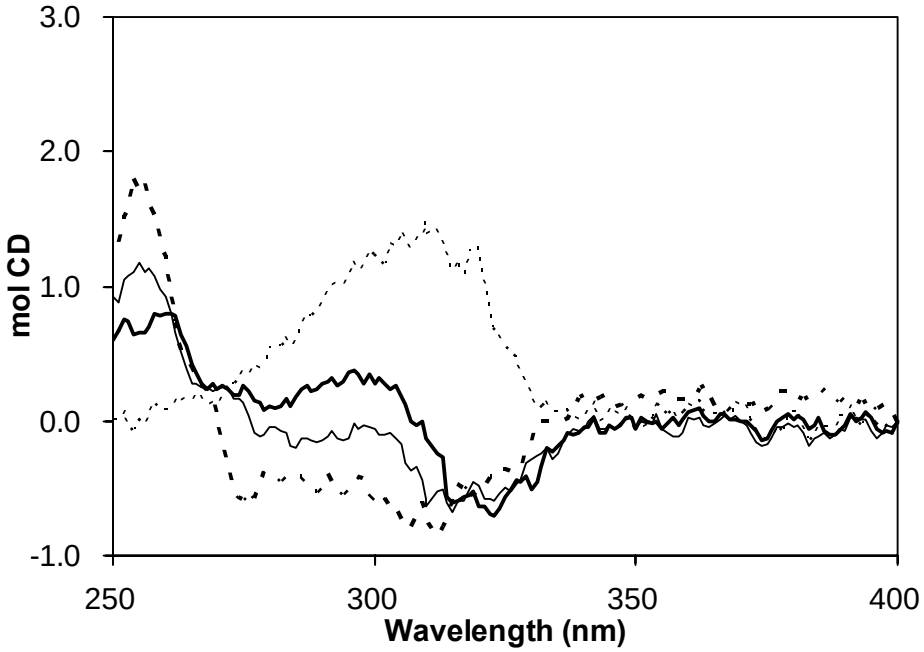

Figure 2-19. CD spectra of acetonitrile solution of host **9** in the absence of (thin dashed line) and in the presence of 0.5 (thick solid line), 1 (thin solid line), and 3 (thick dashed line) equivalents of $(TBA)_2AMP$.

phosphate moiety. The formation of complex **C**, therefore, is certainly favorable in 2:1 complexations of host **9** with both HPO_4^{2-} and AMP^{2-}.

In contrast, addition of a half amount of $H_2P_2O_7^{2-}$, having a "dimer" structure of HPO_4^{2-}, to host **9** resulted in simple decrease of CD intensity (Figure 2-20) rather than exciton coupling peaks, though host **9** tends to give the 2:1 complex with the anion as demonstrated by ^1H NMR titration. The different titration profiles of HPO_4^{2-} and $H_2P_2O_7^{2-}$ could be explained by the flexibility of the 2:1 complexes. Since the 2:1 complex (Figure 2-21) of **9** with $H_2P_2O_7^{2-}$ has P-O-P single bonds leading to a number of conformers by rotation, the relative position of the two DMAB groups in the complex would not be fixed well, while the 2:1 complex of **9** with HPO_4^{2-} has no such single bond in the corresponding complex. Further addition of an excess amount of $H_2P_2O_7^{2-}$

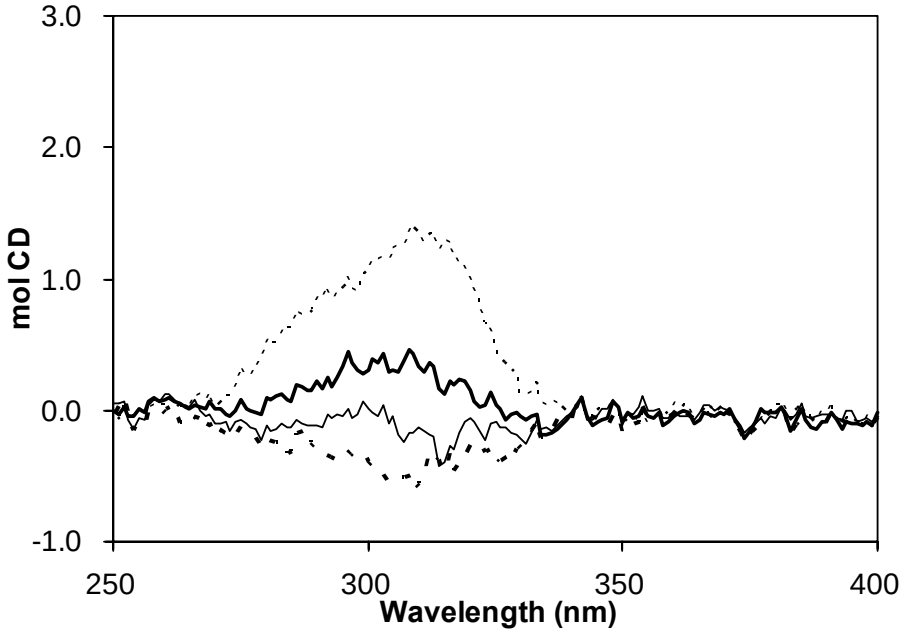

Figure 2-20. CD spectra of acetonitrile solution of host **9** in the absence of (thin dashed line) and in the presence of 0.5 (thick solid line), 1 (thin solid line), and 3 (thick dashed line) equivalents of $(TBA)_2H_2P_2O_7$.

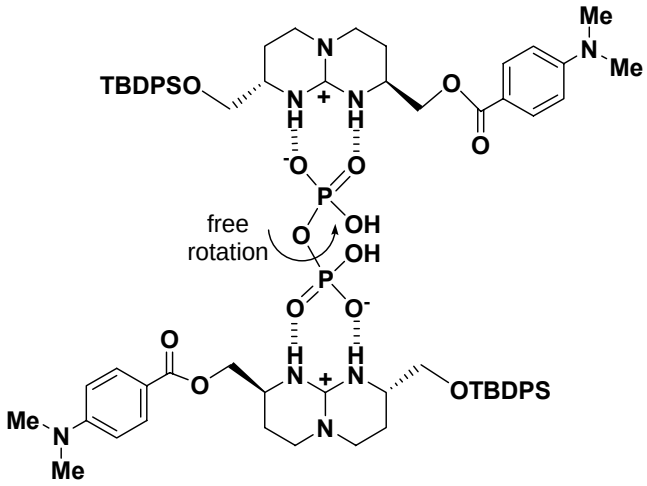

Figure 2-21. The postulated structure of the 2:1 complex of host **9** with $H_2P_2O_7^{2-}$.

finally led to a negative Cotton effect peak. Similarly, addition of monovalent anion $H_2PO_4^-$ led to a simple decrease of CD intensity and finally an almost flat line (Figure 2-22). The simple change in Cotton effect peaks on addition of $H_2P_2O_7^{2-}$ or $H_2PO_4^-$ to host **9** could be ascribed to some conformational changes around the DMAB groups caused by anion coordination, which would drive the DMAB chromophores from the original position to a different sector of the chiral field created by the chiral guanidinium skeleton. In the case of ClO_4^-, having quite weak complexation ability as shown by ^1H NMR titrations, no change in CD profiles was observed on addition of even excess amount of ClO_4^-, as expected (Figure 2-23).

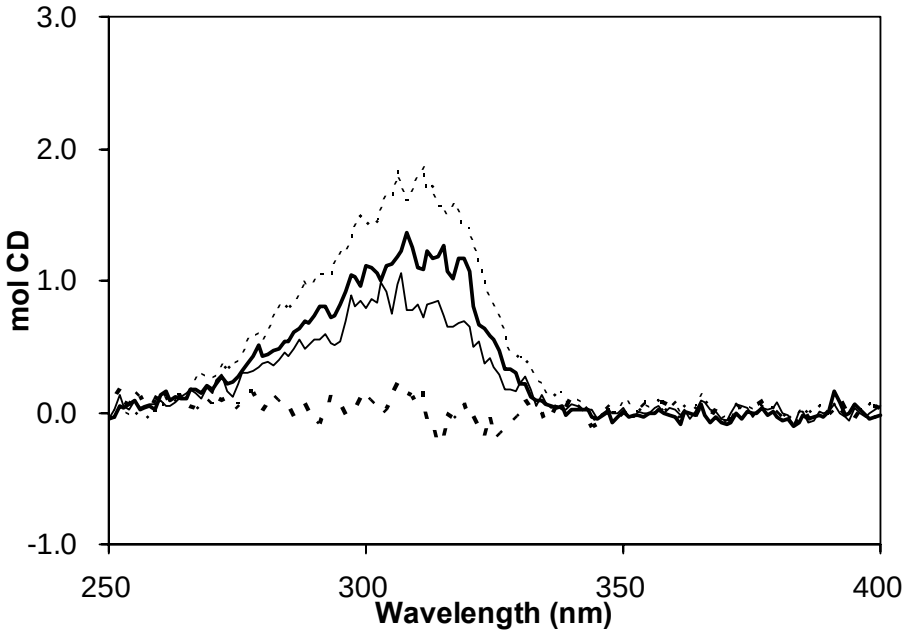

Figure 2-22. CD spectra of acetonitrile solution of host **9** in the absence of (thin dashed line) and in the presence of 0.5 (thick solid line), 1 (thin solid line), and 3 (thick dashed line) equivalents of $(TBA)H_2PO_4$.

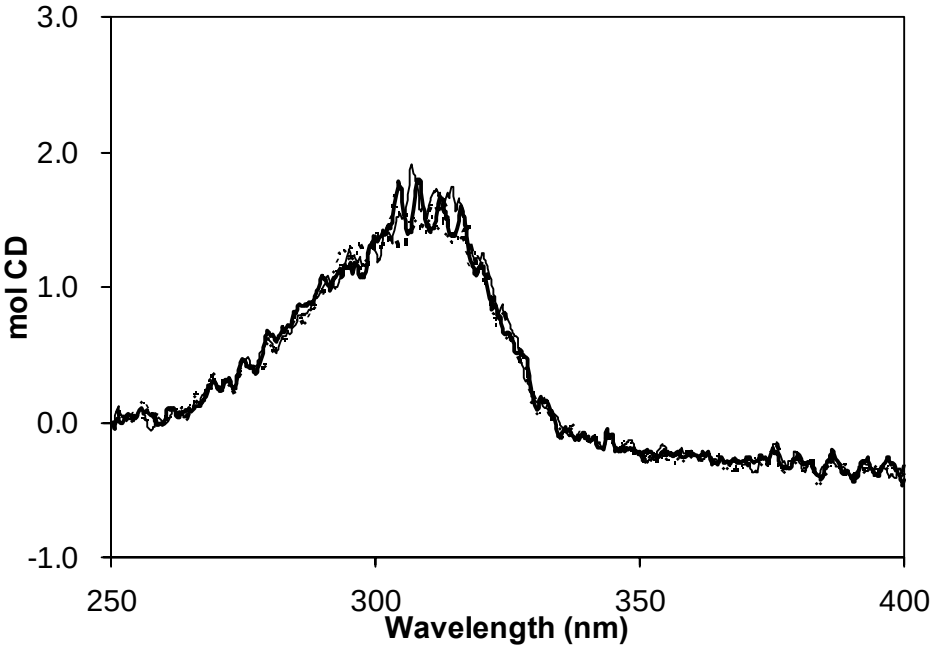

Figure 2-23. CD spectra of acetonitrile solution of host **9** in the absence of (thin dashed line) and in the presence of 0.5 (thick solid line), 1 (thin solid line), and 3 (thick dashed line) equivalents of (TBA)ClO_4.

2-2-2-2 Conclusions

The DMAB signaling subunit successfully provided the complexation information for host **9** with some anions in terms of the exciton chirality method. Divalent anions, SO_4^{2-}, HPO_4^{2-}, and AMP^{2-} exhibited clear intensity changes with exciton coupling peaks. In addition, the observation of the bisignate negative first and positive second Cotton effect peaks in the 2:1 complexes indicates that the two DMAB groups in the corresponding 2:1 complexes are arranged with negative chirality (counterclockwise) rather than positive chirality (clockwise). Divalent anion $H_2P_2O_7^{2-}$ and monovalent anion $H_2PO_4^-$ showed simple decreases in CD intensities. Monovalent anion ClO_4^- with weak coordination ability exhibited no change. Thus, anions having strong affinity for host **9** gave the characteristic intensity changes in CD profiles during titrations. The combination of the DMAB signaling subunit and the chiral guanidinium binding site makes it possible to obtain detailed information on the complexation process of host **9** with anions as well as on the absolute configuration of the 2:1 complexes of host **9** with the divalent anions using CD spectroscopy.

2-2-3 Fluorescence titrations

2-2-3-1 Fluorescence titrations

Fluorescence detection has been widely used as a powerful tool in various fields due to its high sensitivity.[10] An excellent fluorophore, 4-(*N*,*N*-dimethylamino)benzoate group has been known to have the dual fluorescence emission feature, which is emitted from the locally excited (LE) state and twisted intramolecular charge transfer (TICT) state. Since the dual fluorescence property of DMAB group is quite susceptible to the media polarity, it has been applied for the probe of media polarity[11] as well as of signaling group of the artificial anion receptor.[12] Figure 2-24 depicts the energy diagram of ethyl 4-(*N*,*N*-dimethylamino)benzoate (**12**) with LE (at the coplanar conformation) and TICT (at the twisted conformation) states.

Kobiro and Inoue reported[3] that the DMAB in host **9** showed two fluorescence emissions at 346 nm and 491 nm in acetonitrile upon excitation at 280 nm, which were attributable to the LE and TICT emissions, respectively. However, the relative intensity of TICT and LE bands of host **9** was greatly smaller than that of ethyl 4-(*N*,*N*-dimethylamino)benzoate. The reduced relative TICT fluorescence intensity observed for host **9** was ascribed to the intramolecular hydrogen bonding between the guanidinium proton and the ester carbonyl oxygen atom as pointed out in section 2-2-1-2, Figure 2-3, which delayed the relaxation of the DMAB moiety to the TICT state even in polar acetonitrile. When fluorescence titration of host **9** with divalent sulfate anion was performed in acetonitrile, the LE intensity first dropped quickly up to a half amount of addition of SO_4^{2-}, and then increased rapidly up to addition of twice amounts. In contrast, the TICT band showed a simple increase until a half amount addition of SO_4^{2-}, and then the TICT intensity showed no appreciable increase

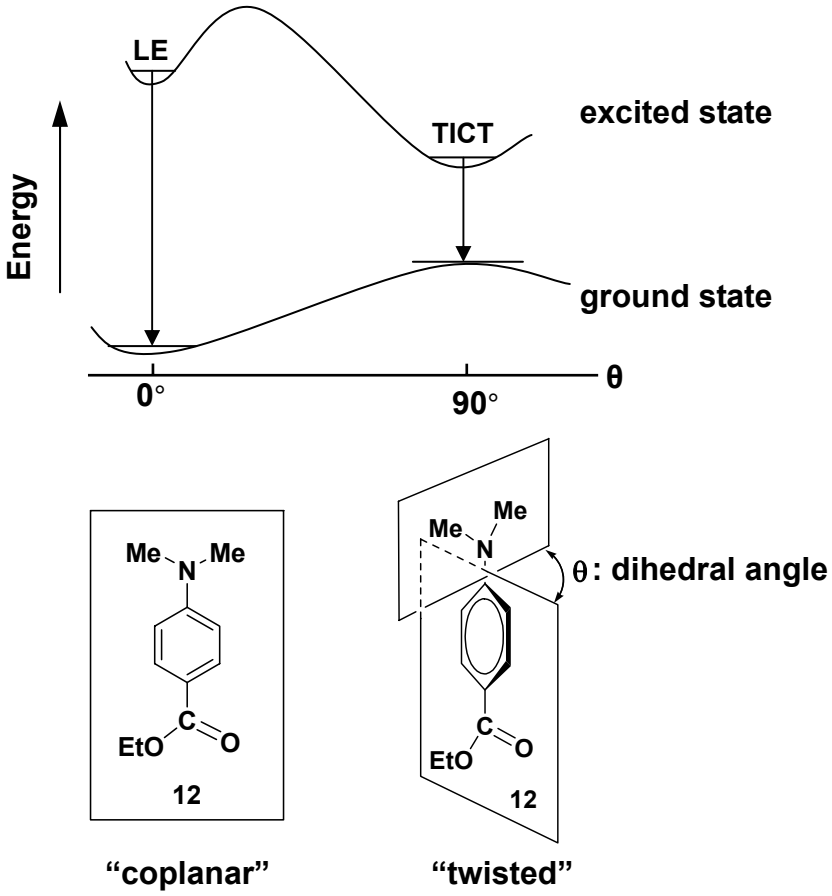

Figure 2-24. Schematic expressions of LE and TICT states of ethyl 4-(*N*,*N*-dimethylamino)benzoate.

thereafter, as can be seen in Figure 2-25. These observations were due to the formation of stepwise 2:1 and 1:1 complexes. The feasibility of rotation to give a TICT state from the LE state was hindered by the intramolecular hydrogen bonding in host **9**. When SO_4^{2-} bound to host **9**, of which the complexation ability was stronger than the intramolecular hydrogen bonding, the internal hydrogen bonding was broken to make the rotation easy and give a TICT state from the LE state with increasing TICT intensity along with the decreasing LE intensity in the 2:1 complex. On the other hand, the participation of lipophilic counteraction TBA with the DMAB chromophore, which decreased the polarity of the microenvironment around the DMAB group, gave rise to

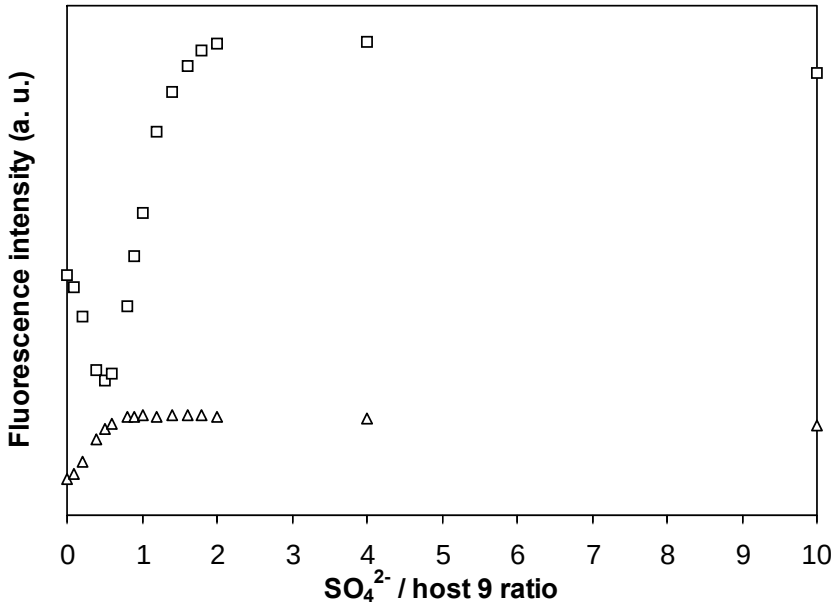

Fgure 2-25. Fluorescence intensity changes in the LE band at 346 nm (▫) and those in the TICT band at 491 nm (▵) upon titration of host **9** with $(TBA)_2SO_4$ in CH_3CN. Excitation wavelength: 280 nm.

increase of the fluorescence intensity in the 1:1 complex.

In order to investigate whether the dual fluorescence behavior of the DMAB group in host **9** is a common feature upon complexation with expanded variety of anions or not, titrations of host **9** with divalent and monovalent anions were performed on fluorescence spectra in CH_3CN. As can be seen in Figure 2-26, the titration profiles obtained with HPO_4^{2-} were very close to those with SO_4^{2-}. The LE intensity first dropped sharply on addition of up to 0.5 equivalent amounts of the anion, then gradually increased to exceed the original intensity until about 2 equivalent amounts of the anion was added, finally maintained the increasing tendency. In contrast, the TICT fluorescence showed an initial rapid increase up to HPO_4^{2-}/**1** ratio equal to 0.5, but almost no change was observed even large amount addition of the anion. The titration

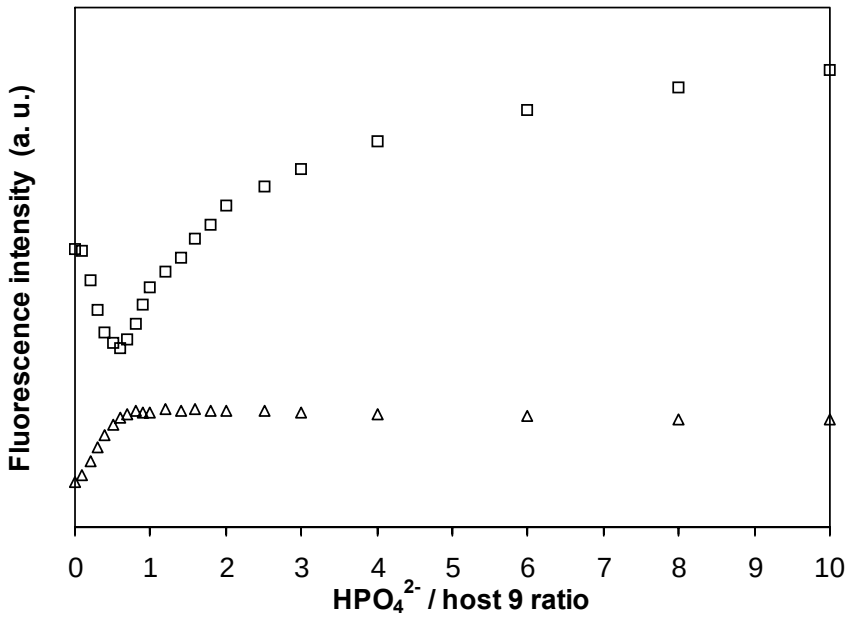

Figure 2-26. Fluorescence intensity changes in the LE band at 348 nm (□) and those in the TICT band at 491 nm (△) upon titration of host **9** with $(TBA)_2HPO_4$ in CH_3CN. Excitation wavelength: 280 nm.

profiles of host **9** by $H_2P_2O_7^{2-}$ and AMP^{2-} were also similar to those with $SO_4^{2-}$and HPO_4^{2-}. However, the tendency of the decreasing of the LE intensity and the increasing of the TICT intensity was smaller (up to 0.5 equivalent addition) in the case of $H_2P_2O_7^{2-}$ (Figure 2-27), whereas the LE and TICT intensity obviously decreased upon addition of excess amounts of AMP^{2-} (Figure 2-28). The characteristic titration profiles of the LE bands observed in divalent anions (SO_4^{2-}, HPO_4^{2-}, $H_2P_2O_7^{2-}$, and AMP^{2-}) demonstrate that the 2:1 complexation occurred on addition of up to 0.5 equivalent amounts of the divalent anions and further addition of the anions would replace the 2:1 complexes with the 1:1 complexes concomitant with lipophilic TBA cation.

It is understandable that the decreasing of LE intensity compensated the increasing of TICT intensity upon addition of 0.5 equivalent amounts of the divalent anions. Because divalent anions (SO_4^{2-}, HPO_4^{2-}, $H_2P_2O_7^{2-}$ and AMP^{2-}) having strong affinities

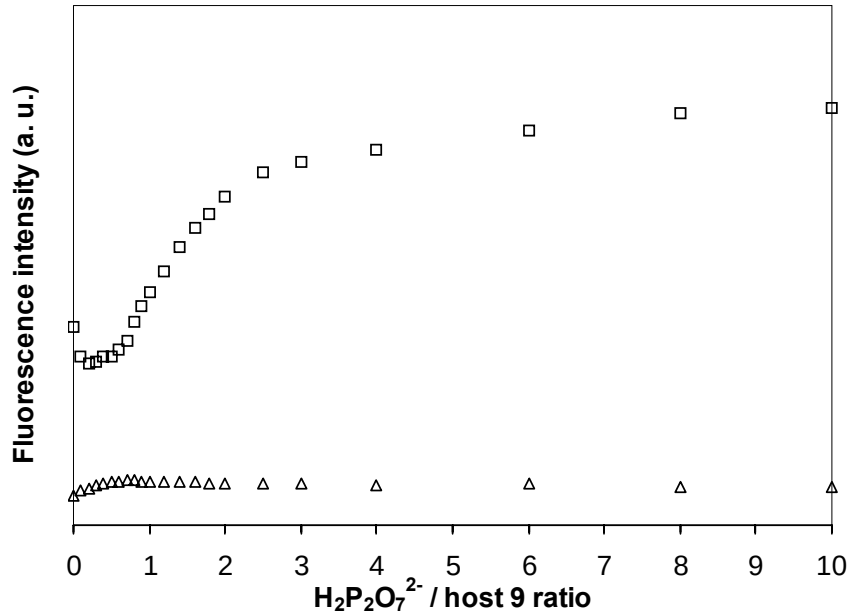

Figure 2-27. Fluorescence intensity changes in the LE band at 348 nm (▫) and those in the TICT band at 491 nm (▵) upon titration of host **9** with $(TBA)_2H_2P_2O_7$ in CH_3CN. Excitation wavelength: 280 nm.

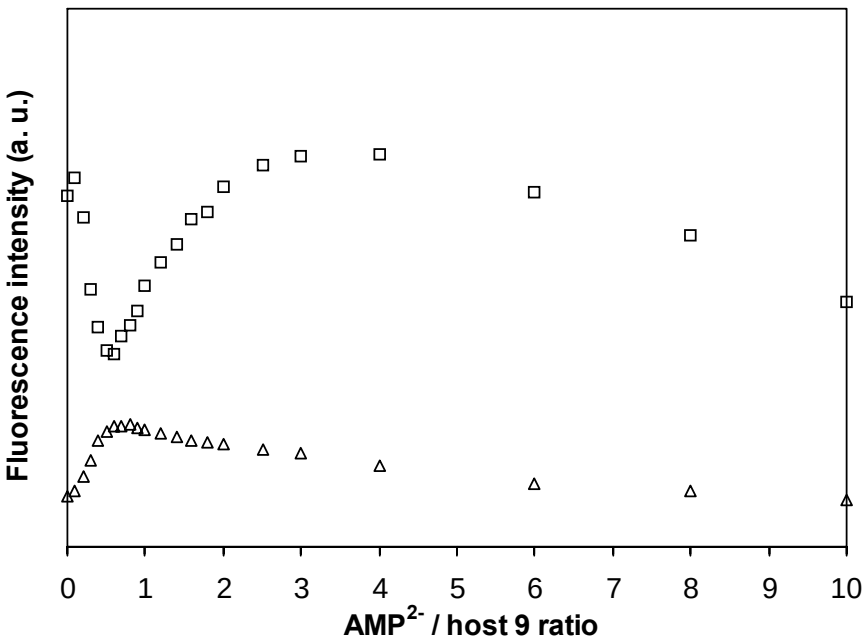

Figure 2-28. Fluorescence intensity changes in the LE band at 348 nm (▫) and those in the TICT band at 491 nm (▵) upon titration of host **9** with $(TBA)_2AMP$ in CH_3CN. Excitation wavelength: 280 nm.

for host **9** would break the intramolecular hydrogen bond upon complexation at the guanidinium moiety binding site, which allowed the rotational relaxation from the LE to TICT state. Hence, the TICT intensity increased with the loss of the LE intensity on increasing concentration of the 2:1 complex in solution. However, the LE and TICT fluorescence behaved in different ways after addition of 0.5 equivalent amounts of SO_4^{2-}, HPO_4^{2-} and $H_2P_2O_7^{2-}$. The LE intensity monotonously increased, while the TICT intensity presented almost no change. The phenomenon would ascribe to the active participation of the lipophilic TBA counteraction in the complex species, which greatly increased the microenvironmental polarity around the DMAB group. Addition of an excess amount of AMP^{2-} resulted in the decreases both at LE and TICT states, which would be caused by the influence of large amounts of quite hydrophilic AMP^{2-} salt on increasing the polarity of the microenvironment around the DMAB group.

By contraries, titration curves were quite simple in the case of ClO_4^- (Figure 2-29). The LE intensity became gradually stronger with increasing amount of added ClO_4^-, while almost no change was observed in TICT intensity. The appreciable differences in coordination affinities between the divalent anions, SO_4^{2-}, HPO_4^{2-}, $H_2P_2O_7^{2-}$, and AMP^{2-}, and the monovalent anion, ClO_4^-, should be the reason for the differences in the observed titration curves. Fission of the intrinsic internal hydrogen bonding in host **9**, namely, would increase the feasibility of rotation leading to a TICT state from the LE state. However, weak (or almost no) coordination of ClO_4^- should have no influence on the internal hydrogen bonding and, therefore, leads to almost no change in TICT intensity. The simple increase in LE emission is most likely due to the active participation of lipophilic TBA countercation to the DMAB group of host **9**, as discussed above. Furthermore, quite similar results to ClO_4^- were obtained in the

titrations of host **9** with NO_3^-, BF_4^-, HSO_4^-, and PF_6^-, all of which have low affinities for host **9** as indicated by ^1H NMR titrations (Figure 2-30 for NO_3^-, Figure 2-31 for BF_4^-, Figure 2-32 for HSO_4^-, Figure 2-33 for PF_6^-).

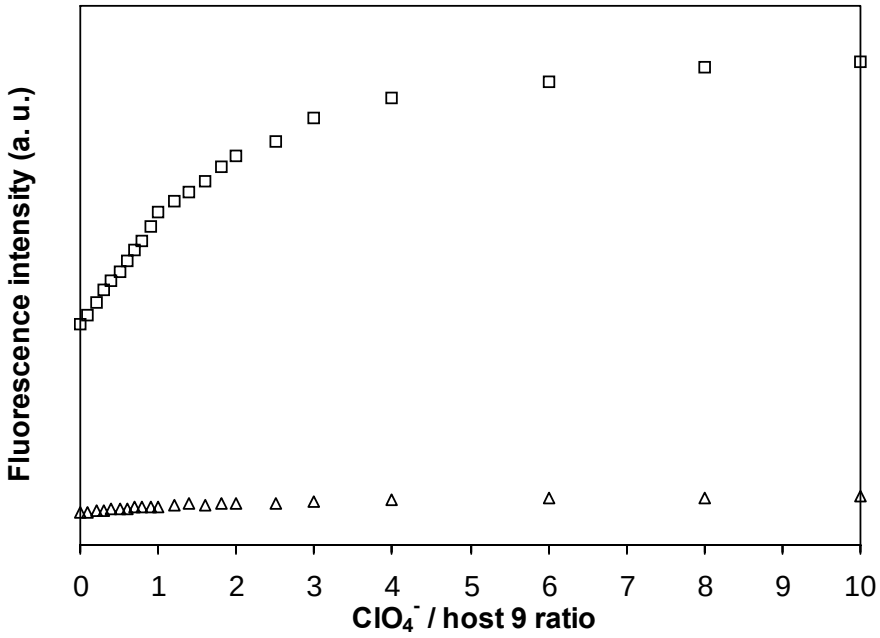

Figure 2-29. Fluorescence intensity changes in the LE band at 348 nm (▫) and those in the TICT band at 491 nm (▵) upon titration of host **9** with (TBA)ClO_4 in CH_3CN. Excitation wavelength: 280 nm.

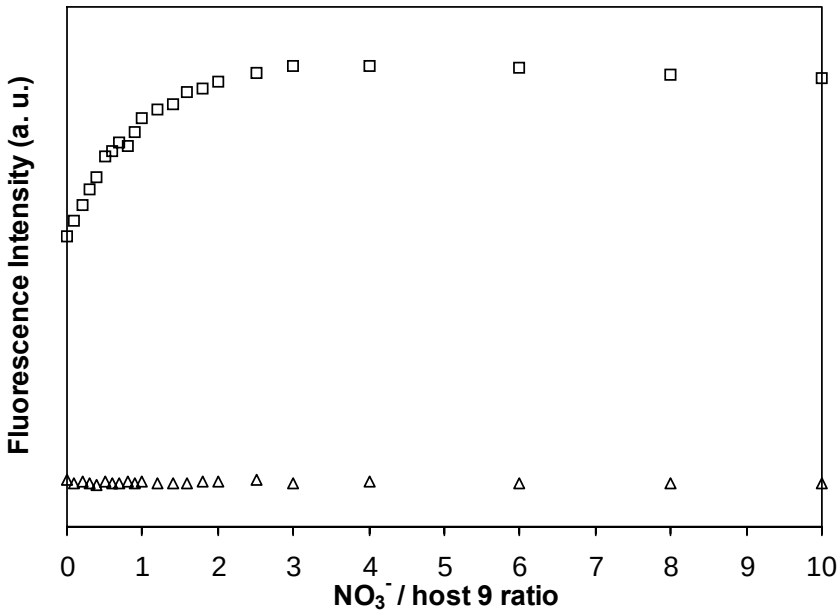

Figure 2-30. Fluorescence intensity changes in the LE band at 348 nm (▫) and those in the TICT band at 491 nm (△) upon titration of host **9** with (TBA)NO_3 in CH_3CN. Excitation wavelength: 280 nm.

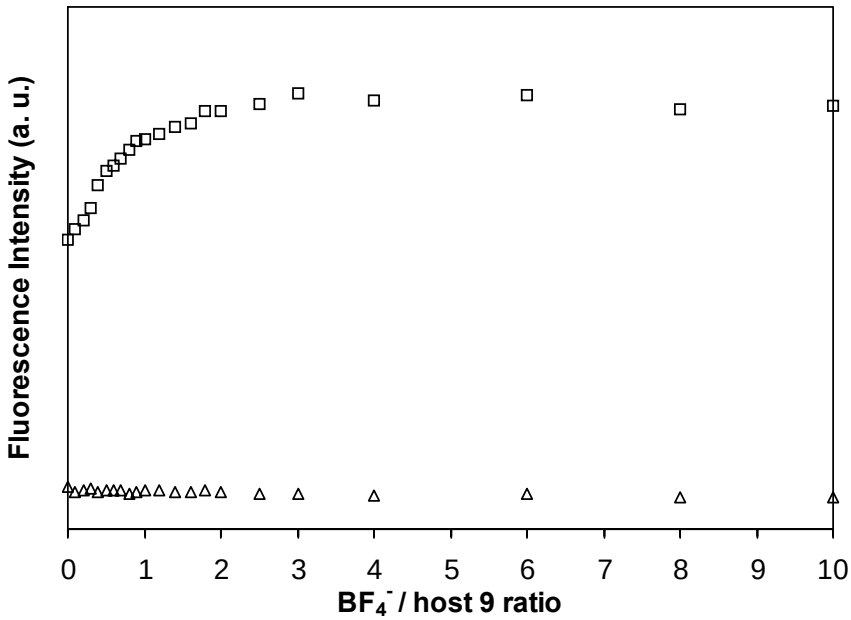

Figure 2-31. Fluorescence intensity changes in the LE band at 348 nm (▫) and those in the TICT band at 491 nm (△) upon titration of host **9** with (TBA)BF_4 in CH_3CN. Excitation wavelength: 280 nm.

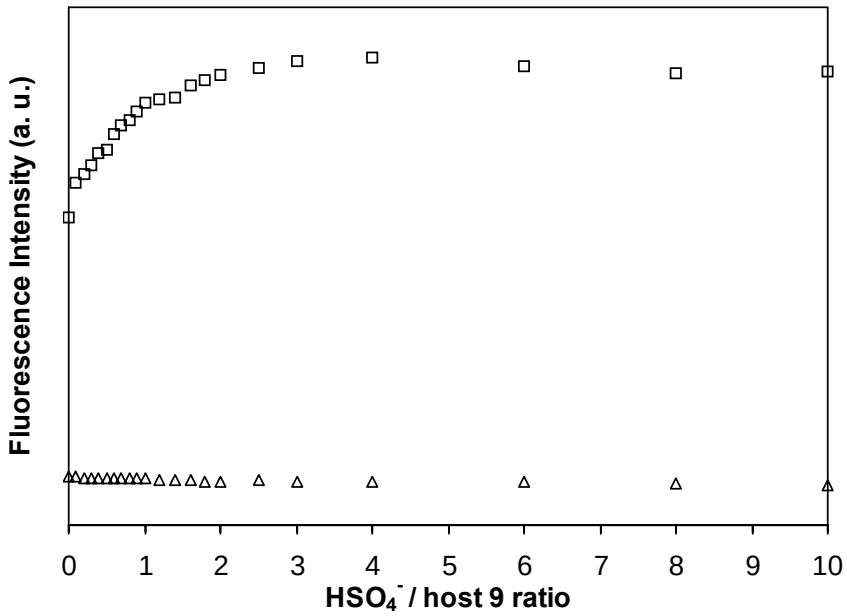

Figure 2-32. Fluorescence intensity changes in the LE band at 348 nm (▫) and those in the TICT band at 491 nm (△) upon titration of host **9** with (TBA)HSO_4 in CH_3CN. Excitation wavelength: 280 nm.

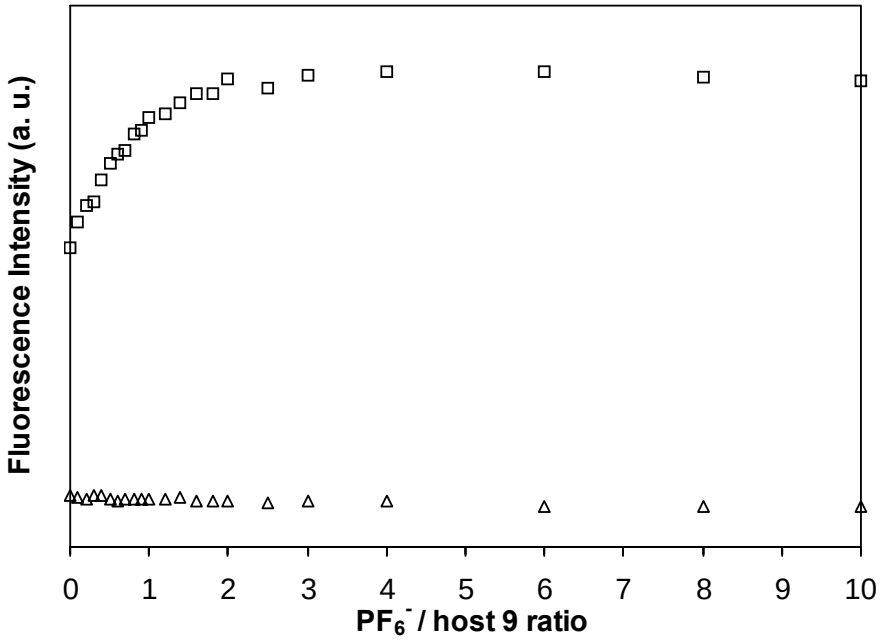

Figure 2-33. Fluorescence intensity changes in the LE band at 348 nm (▫) and those in the TICT band at 491 nm (△) upon titration of host **9** with (TBA)PF_6 in CH_3CN. Excitation wavelength: 280 nm.

Particularly, the titration profiles of the LE and TICT intensity of host **9** by addition of $H_2PO_4^-$ (Figure 2-34) were quite different from those of the divalent anions and the other monovalent anions. The LE intensity exhibited an intricate increase with increasing amount of $H_2PO_4^-$, while the TICT intensity increased slightly till the ratio of anion/**9** reached about 1 and, then, became almost flat. Relatively strong complexation ability of $H_2PO_4^-$ with host **9** would lead to decrease of the LE intensity along with increase of the TICT intensity. Judging from the increment of the TICT intensity, the decrease of the LE intensity seems to be very small. The expected slight decrease of the LE intensity could overlap with the large increase of the LE intensity which is caused by the active participation of the lipophilic TBA to show the observed intricate increase of the LE profile.

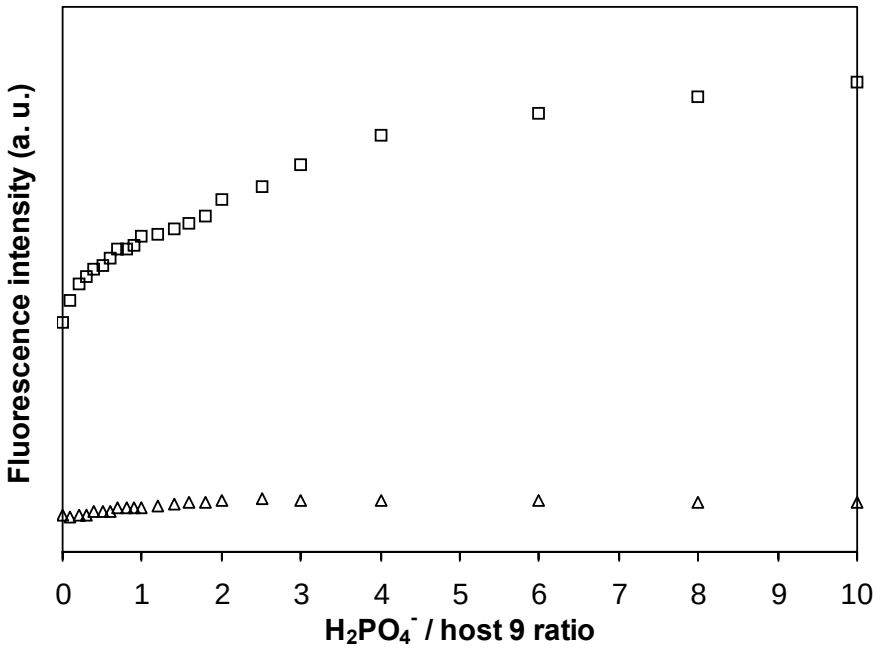

Figure 2-34. Fluorescence intensity changes in the LE band at 348 nm (▫) and those in the TICT band at 491 nm (△) upon titration of host **9** with (TBA)H_2PO_4 in CH_3CN. Excitation wavelength: 280 nm.

All the intensity data monitored at LE state (348 nm) and TICT state (491 nm) were put together into two graphics respectively for easy comparison of the complexation behavior of host **9** upon addition of divalent anions, SO_4^{2-}, HPO_4^{2-}, $H_2P_2O_7^{2-}$, and AMP^{2-} as well as monovalent anions, ClO_4^-, NO_3^-, BF_4^-, HSO_4^-, PF_6^-, and $H_2PO_4^-$ (Figure 2-35 for LE and Figure 2-36 for TICT). As can be seen, the titration profiles of host **9** by divalent anions (SO_4^{2-}, HPO_4^{2-}, $H_2P_2O_7^{2-}$, and AMP^{2-}) were quite different from those by monovalent anions (ClO_4^-, NO_3^-, BF_4^-, HSO_4^-, PF_6^-, and $H_2PO_4^-$). The results obtained from the dual fluorescence emissions of the DMAB signaling subunit upon complexation with the anions are highly in agreement with those obtained in ^1H NMR titrations.

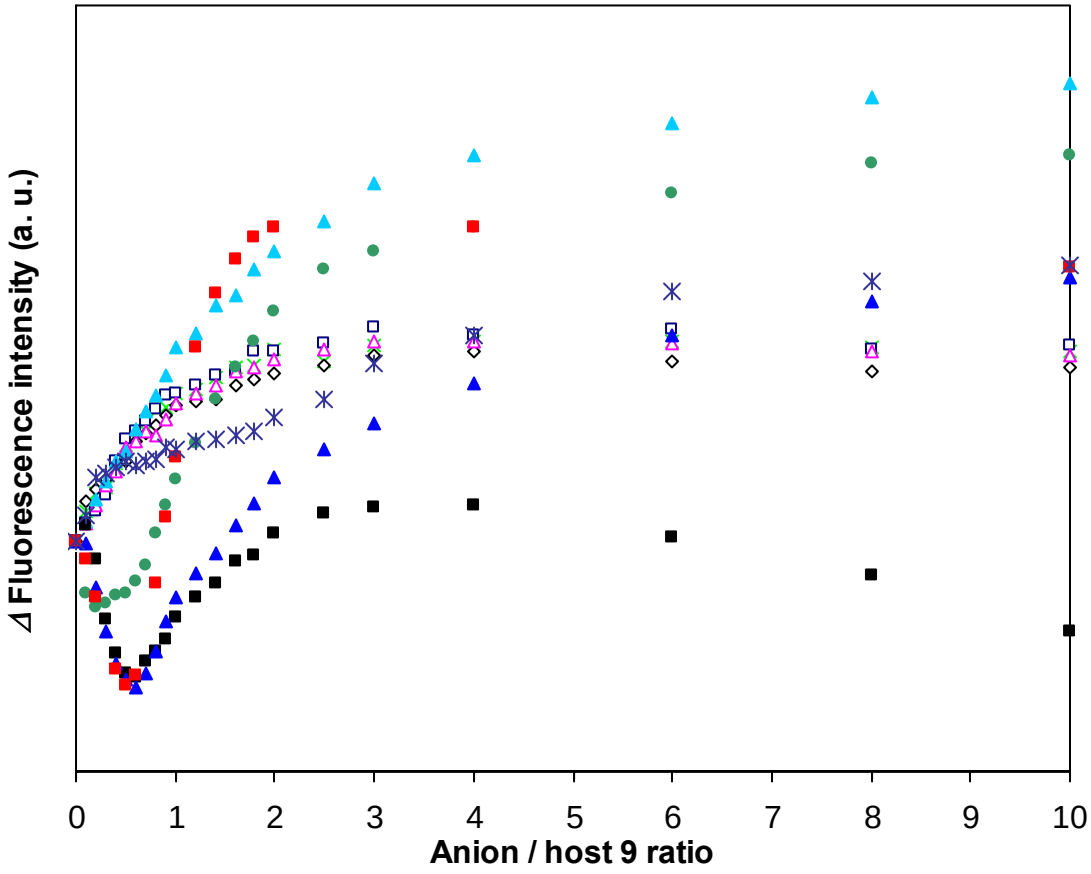

Figure 2-35. LE intensity changes (348 nm) upon fluorescence titrations of host **9** with $(TBA)_2SO_4$ (■), $(TBA)_2HPO_4$ (▲), $(TBA)_2H_2P_2O_7$ (●), $(TBA)_2AMP$ (■), $(TBA)ClO_4$ (▲), $(TBA)NO_3$ (△), $(TBA)BF_4$ (□), $(TBA)HSO_4$ (◇), $(TBA)PF_6$ (×), and $(TBA)H_2PO_4$ (*) in CH_3CN. Excitation wavelength: 280 nm.

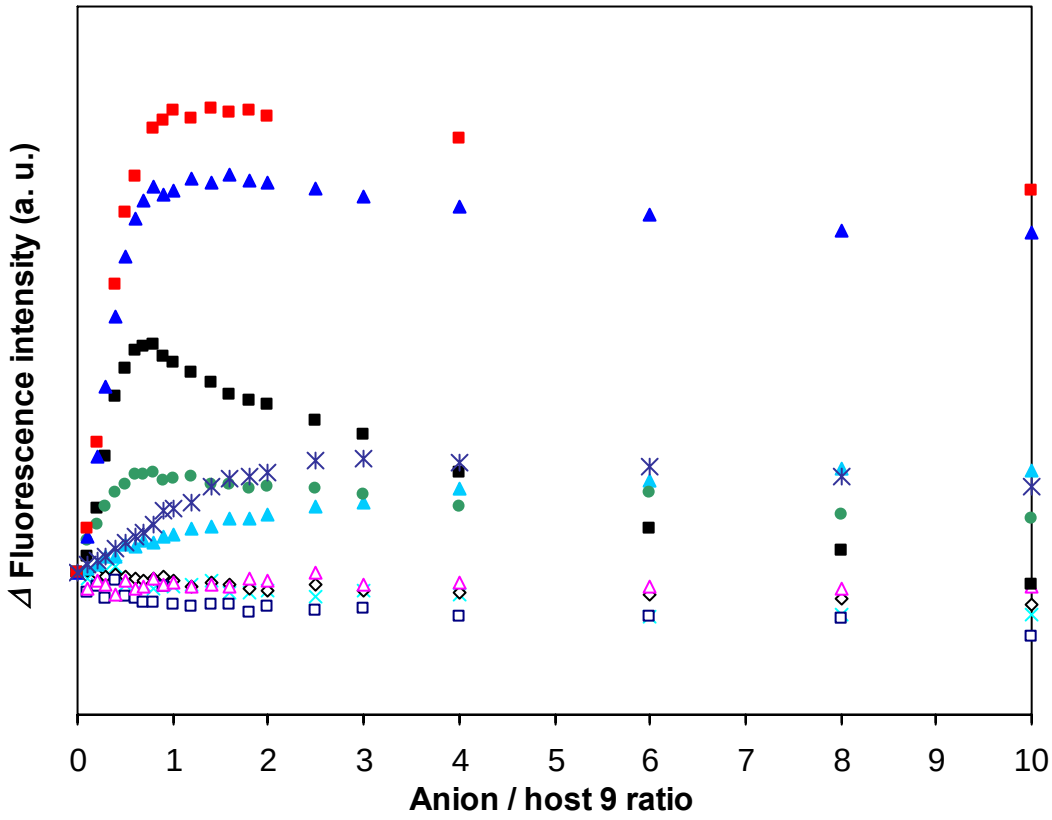

Figure 2-36. TICT intensity changes (491 nm) upon fluorescence titrations of host **9** with $(TBA)_2SO_4$ (■), $(TBA)_2HPO_4$ (▲), $(TBA)_2H_2P_2O_7$ (●), $(TBA)_2AMP$ (■), $(TBA)ClO_4$ (▲), $(TBA)NO_3$ (△), $(TBA)BF_4$ (□), $(TBA)HSO_4$ (◇), $(TBA)PF_6$ (×), and $(TBA)H_2PO_4$ (*) in CH_3CN. Excitation wavelength: 280 nm.

2-2-3-2 Conclusions

The DMAB group in host **9** as a signaling subunit successfully showed distinctive LE and TICT fluorescence responses on recognition of a variety of anions. Divalent anions (SO_4^{2-}, HPO_4^{2-}, $H_2P_2O_7^{2-}$, and AMP^{2-}) with tetrahedral geometries exhibited substantial decreases of LE emissions first up to a half amount addition of the anions and then gradual increases on further addition of the anions, while TICT emissions showed simple increases up to a half amount addition of the anions. However, the monovalent anions (ClO_4^-, NO_3^-, BF_4^-, HSO_4^-, PF_6^-, and $H_2PO_4^-$) with weak coordination ability, the corresponding LE emissions exhibited a simple increase on gradual addition of the anions, whereas almost no change was observed in TICT bands. Meanwhile, the fluorescence titration profiles allowed us to know that the binding stoichiometry of host **9** with the divalent anions would be successive 2:1 and 1:1 complexation but only week 1:1 complexation of host **9** toward the monovalent anions occurred, which are highly consonant with the conclusions obtained in ^{1}H NMR titrations. In addition, the countercation TBA strongly enhanced the LE intensity of the DMAB group via reducing the microenvironmental polarity around the signaling subunit. The large volume of quite hydrophilic residue in AMP strongly reduced the LE and TICT intensity of DMAB group via increasing the microenvironmental polarity around the signaling subunit.

2-3 Conclusions

The novel host **9** with a chiral bicyclic guanidinium ion moiety as a binding subunit linked to a DMAB group as a signaling subunit was applied for binding a variety of anions by means of ^{1}H NMR, CD, and fluorescence spectroscopy.

In ^{1}H NMR titrations, the DMAB signaling subunit provided quantitative information on complexation of host **9** with anions. The binding constants of host **9** toward the divalent anions were quite large (SO_4^{2-}: log $K_{1:1}$ = 6.2 and log $K_{2:1}$ = 4.7, HPO_4^{2-}: log $K_{1:1}$ = 6.2 and log $K_{2:1}$ = 4.9, $H_2P_2O_7^{2-}$: log $K_{1:1}$ = 4.4 and log $K_{2:1}$ = 1.8, AMP^{2-}: log $K_{1:1}$ > 7 and log $K_{2:1}$ > 5), whereas host **9** gave relatively small binding constants toward the monovalent anions (log $K_{1:1}$ < 2.0, exceptional case of $H_2PO_4^-$: log $K_{1:1}$ = 4.4). Host **9** gave successive 1:1 and 2:1 complexation stoichiometry with the divalent anions (SO_4^{2-}, HPO_4^{2-}, $H_2P_2O_7^{2-}$, and AMP^{2-}) and 1:1 complexation with the monovalent anions (ClO_4^-, NO_3^-, BF_4^-, HSO_4^-, PF_6^-, and $H_2PO_4^-$). Therefore, host **9** exhibited strong complexation ability and high selectivity toward SO_4^{2-}, HPO_4^{2-}, $H_2P_2O_7^{2-}$, and AMP^{2-} having a tetrahedral array of oxygen atoms with divalent negative charge as compared with those with monovalent anions, ClO_4^-, NO_3^-, BF_4^-, HSO_4^-, and PF_6^-, except for $H_2PO_4^-$.

In CD titrations, the DMAB signaling subunit successfully showed the complexation information for host **9** with divalent anions in terms of the exciton chirality method. Anions having strong affinity for host **9** such as SO_4^{2-}, HPO_4^{2-}, and AMP^{2-} gave bisignate Cotton effect peaks upon CD titrations, while $H_2P_2O_7^{2-}$ and $H_2PO_4^-$ having strong affinity for host **9** gave the simple intensity decreases in CD profiles during titrations. On the contrary, ClO_4^- with weak coordination ability for host **9** showed almost no CD intensity change. On the other hand, divalent anions, SO_4^{2-},

HPO_4^{2-}, and AMP^{2-}, exhibited weak but clear negative first positive second Cotton effect peaks in the 2:1 complexes, which indicates that the two DMAB groups in the corresponding 2:1 complexes are arranged with negative chirality (counterclockwise) rather than positive chirality (clockwise). Thus, the combination of the DMAB signaling subunit and the chiral guanidinium binding site made it possible to obtain detailed information on the complexation process of host **9** with the anions as well as on the absolute configuration of the 2:1 complexes of host **9** with the divalent anions using CD spectroscopy.

In fluorescence titrations, the DMAB group embedded in host **9** as a signaling subunit successfully exhibited clear fluorescence responses on LE and TICT emissions in accordance with the recognition of a variety of divalent and monovalent anions. The LE and TICT intensity changes of host **9** by the anions having strong binding affinities, such as SO_4^{2-}, HPO_4^{2-}, AMP^{2-}, and $H_2P_2O_7^{2-}$ were remarkably different from those by the monovalent anions having weak binding affinities. Host **9** showed the successive 2:1 and 1:1 complexation with the divalent anions as well as 1:1 complexation with the monovalent anions, which were highly consonant with the conclusions obtained in ^1H NMR titrations. In addition, the participation of the countercation TBA, or the large residue in AMP showed strong influences on increasing or decreasing the LE intensity of the DMAB group through decreasing or increasing the micro environmental polarity around the signaling subunit.

The rational design of the binding-signaling principle introduced in the thesis, therefore, provided not only quantitative information about binding constants but also detailed understanding of the complexation behavior such as stoichiometry of the complexes, chiral sense of the 2:1 complexes, and participation of a countercation or a

hydrophilic group in the coordination process. As conclusions, the investigation in the thesis allowed us to understand not only the scope and the limitations of the DMAB signaling subunit in host **9** on complexation with divalent and monovalent anions but also the versatility of the DMAB group as an excellent signaling subunit by means of ^{1}H NMR, CD, and fluorescence spectroscopic studies.

2-4 Experimental Section

2-4-1 General

^{1}H NMR spectra were obtained on a Varian UNITY INOVA 400 NMR spectrometer. CD spectra were obtained on a JASCO J-820 spectropolarimeter. Fluorescence spectra were recorded by a Fluorolog JOBIN YVON-SPEX spectrophotometer. Elemental analyses were performed on an Elementar Vario EL III. pH Measurements were done on a HORIBA F-22 pH meter. Spectroscopic grade acetonitrile from Dojindo Laboratories was used without further purification for all spectrophotometric measurements. Tetrabutylammonium nitrate, tetrabutylammonium dihydrogenphosphate, tetrabutylammonium tetrafluoroborate, tetrabutylammonium perchlorate, tetrabutylammonium hydrogensulfate, tetrabutylammonium hexan-fluorophosphate, and tetrabutylammonium hydroxide were purchased from Aldrich and used without further purification.

2-4-2 Preparation of bis(tetrabutylammonium) hydrogenphosphate, bis(tetrabutylammonium) dihydrogenpyrophosphate, and bis(tetra-butylammonium) adenosine 5'-monophosphate

2-4-2-1 Method

A potentiometric titration method in water was applied to prepare bis(tetrabutylammonium) hydrogenphosphate, bis(tetrabutylammonium) dihydrogen-pyrophosphate, and bis(tetrabutylammonium) adenosine 5'-monophosphate. An acid solution (0.1 mol/L solution of phosphoric acid, pyrophosphoric acid, or adenosine 5’-monophosphoric acid in water) was titrated by 0.1 mol/L water solution of tetrabutylammonium hydroxide. The endpoint of the titration was monitored by pH

meter. The resulting solution containing tetrabutylammonium salt was lyophilized to give pure salt.

2-4-2-2 ^{1}H NMR and elemental analysis

Bis(tetrabutylammonium) hydrogenphosphate•5H_2O (white solid, hygroscopic). ^{1}H NMR (400 MHz, CD_3CN): δ 3.16 -3.09 (m, 16H), 1.67 - 1.56 (m, 16H), 1.44 - 1.29 (m, 16H), 0.97 (t, J = 7.4 Hz, 24H). Anal. Calcd for $C_{32}H_{83}N_2O_9P$: C, 57.28; H, 12.47; N, 4.18. Found: C, 57.35; H, 12.65; N, 4.23.

Bis(tetrabutylammonium) pyrophosphate•3H_2O (white solid, hygroscopic). ^{1}H NMR (400 MHz, CD_3CN): δ 3.16 - 3.09 (m, 16H), 1.68 - 1.56 (m, 16H), 1.44 - 1.28 (m, 16H), 0.97 (t, J = 7.4 Hz, 24H). Anal. Calcd for $C_{32}H_{80}N_2O_{10}P_2$: C, 53.76; H, 11.28; N, 3.92. Found: C, 53.61; H, 11.41; N, 3.84.

Bis(tetrabutylammonium) 5'-adenosine monophosphate•3H_2O (white solid, hygroscopic). ^{1}H NMR (400 MHz, D_2O): δ 8.44 (s, 1H, adenine CH), 8.07 (s, 1H, adenine CH), 5.95 and 5.94 (d, J = 3.0 Hz, 1H, O-CH-N), 4.66 - 4.52 (m, 1H, C*H*-OH), 4.35 - 4.30 (dd, J = 4.2 Hz, 1H, O-C*H*-CH_2), 4.18 (br, 1H, C*H*-OH), 3.84 - 3.77 (t, J = 3.8 Hz, 2H, CH_2O), 3.08 - 2.92 (m, 16H), 1.52 - 1.40 (m, 16H), 1.24 - 1.10 (m, 16H), 0.76 (t, J = 7.2 Hz, 24H). Anal. Calcd for $C_{42}H_{90}N_7O_{10}P$: C, 57.05; H, 10.26; N, 11.09. Found: C, 57.39; H, 10.61; N, 10.76.

2-4-3 Spectral titrations of host 9 by anions

In ^{1}H NMR titrations, a 2.00×10^{-3} mol/L solution of host **9** and a 1.20×10^{-2} mol/L solution of anions as tetrabutylammonium salts were first prepared in CD_3CN separately. Next, 0.600 mL of host solution was transferred into an NMR tube. After the NMR spectrum of host itself was measured, an aliquot of the guest solution was added to the NMR tube, and the chemical shift changes of host molecule were monitored; this

procedure was repeated for each aliquot addition.

In CD titrations, the procedures were similar to above descriptions except for the concentration used in ^{1}H NMR titrations. For HPO_4^{2-}, $H_2PO_4^-$, and ClO_4^-: a 4.50×10^{-5} mol/L solution of host **9** and a 2.70×10^{-3} mol/L solution of the anions as tetrabutylammonium salts were used in CH_3CN. For $H_2P_2O_7^{2-}$ and AMP^{2-}: a 3.65×10^{-5} mol/L solution of host **9** and a 2.19×10^{-3} mol/L solution of the anions as tetrabutylammonium salts were used in CH_3CN. $(TBA)_2AMP$ itself has strong absorption around 270 nm in the CD spectra, which interferes with the signal of host **9** in CD titration. To cancel the influence of the AMP signal, the following procedures were performed. CD spectra of $(TBA)_2AMP$ were recorded, then the intensity of $(TBA)_2AMP$ was subtracted from each titration result in each experiment.

In fluorescence titrations, the procedures were similar to above described except for the concentration used in ^{1}H NMR titrations. A 4.05×10^{-5} mol/L solution of host **9** and a 2.43×10^{-3} mol/L solution of anions as tetrabutylammonium salts were used in CH_3CN.

2-4-4 Semiempirical molecular orbital calculation

AM1 semiempirical calculations were performed using CAChe WorkSystem Pro Version 6.01 software.

References and notes

1. (a) A. Bianchi, K. Bauman-James, and E. Garcia-España, Eds. *Supramolecular Chemistry of Anions*, WILEY-VHC: New York, 1997. (b) J. W. Steed and J. L. Atwood, *Supramolecular Chemistry*, John Wiley & Sons, Ltd.: West Sussex, 2000.
2. For reviews, see: (a) F. P. Schmidtchen and M. Berger, *Chem. Rev.* **1997**, 97, 1609. (b) P. A. Gale, *Coord. Chem. Rev.* **2000**, *199*, 181. (c) P. A. Gale, *Coord. Chem. Rev.* **2001**, *213*, 79.
3. K. Kobiro and Y. Inoue, *J. Am. Chem. Soc.* **2003**, *125*, 421.
4. (a) K. A. Connors, *Binding Constants, The Measurement of Molecular Complex Stability*, A Wiley-Interscience Publication: New York, 1987, pp 189-215. (b) C. S. Wilcox, *Frontiers in Supramolecular Organic Chemistry and Photochemistry*, H. -J. Schneider, H. Dürr, Eds; VCH: Weinheim, 1991, pp 123-143.
5. M. J. Hynes, *J. Chem. Soc., Dalton Trans.* **1993**, 311.
6. J. J. P. Stewart, *Comput. Chem.* **1989**, *10*, 209.
7. Low affinity of HSO_4^- as compared with $H_2PO_4^-$ toward anion receptors is also reported in (a) C. Lee, D. H. Lee, and J. I. Hong, *Tetrahedron Lett.* **2001**, *42*, 8665. (b) Z. R. Grabowski, K. Rotkiewicz, A. Siemiarczuk, D. J. Cowley, and W. Baumann, *Nouv. J. Chim.* **1979**, *3*, 443.
8. The UV-vis spectral titration method is a simple and convenient method to study interactions between hosts and guests. We applied UV-vis spectral titration technique to investigate complexation behavior of host **1** toward anions in CD_3CN, while the spectral change was too small to discuss in detail. Host **1** is instead CD active, because the DMAB group is connected to the chiral guanidinium ion

moiety. Thus, we utilized CD spectra instead of UV-vis spetra to get complexation information through the DMAB group.

9. (a) N. Berova, K. Nakanishi, and R. W. Woody, *Circular Dichromism, Principle and Applications* 2nd ed., Wiley-VCH: New York, 2000. (b) D. A. Lightner and J. E. Gurst, *Organic Conformational Analysis and Stereochemistry from Circular Dichromism Spectroscopy*, Wiley-VCH: New York, 2000.

10. E. V. Anslyn, *Curr. Opin. Chem. Biol.* **1999**, *3*, 740.

11. (a) D. J. Cowley and P. J. Healy, *Proc. R. Ir. Acad. Soc.*, **1977**, *B77B*, 397. (b) Z. R. Grabowski, K. Rotkiewicz, A. Siemiarczuk, D. J. Cowley, and W. Baumann, *Nouv. J. Chim.* **1979**, *3*, 443. (c) W. Rettig, *Angew. Chem., Int. Ed.*, **1986**, *25*, 971. (d) R. Hayashi, S. Tazuke, and C. W. Frank, *Macromolecules*, **1987**, *20*, 983. (e) S. Tazuke, R. K. Guo, and R. Hayashi, *Macromolecules*, **1989**, *22*, 729. (f) S. Tazuke, R. K. Guo, and T. Ikeda, *Macromolecules*, **1990**, *23*, 1208. (g) J. Paczkowski and D. C. Neckers, *Macromolecules*, **1991**, *24*, 3013-3016. (h) J. Paczkowshi1 and D. C. Neckers, *J. Polym. Sci., Polym. Chem.*, **1993**, *31*, 841. (i) W. Rettig, In *Topics in Current Chemistry*; J. Mattay, Ed.; Springer Verlag: Berlin, 1994; Vol. 169, pp 253-299.

12. F.-Y. Wu, and Y.-B. Jiang, *Chem. Phys. Lett.* **2002**, *355*, 438.

Chapter 3.

Simple 4-(*N*,*N*-Dimethylamino)benzoic Acid as a New Class of Chromogenic and Fluorogenic Host for Anion Recognition

3-1 Introduction

Many efforts have recently been contributed to the design and synthesis of anion receptors in the field of molecular recognition due to the importance of anions in the areas of chemistry, environment, and biology. However, these efforts resulted in not simple but quite massive and complicated molecular features of the hosts to accomplish such selective recognition and sensitive signaling on the specific anions.[1] Thus, the author has concentrated on developing simple, efficient, and, if possible, commercially available reagents for anion hosts. If such easily obtained host molecules could be successfully utilized, they would facilitate the process of design and synthesis of anion receptors. Some commercially available chromogenic and fluorogenic reagents, hence, are taken into account and expected to act as host molecules, for example, aromatic acid derivatives, sulfonic acid derivatives, and so on. The optical properties of some of the reagents such as UV-vis absorption and fluorescence emission are quite well-known. However, the complexation behavior of the reagents with anion guests is still unknown.

Based on the above considerations and the fact that 4-(*N*,*N*-dimethylamino) benzoate (DMAB) group was utilized as an excellent signaling subunit for anion recognition as introduced in Chapter 2, aromatic acid derivatives, for instance, 4-(*N*,*N*-dimethylamino)benzoic acid (**10**) would be one of the candidates suitable for the

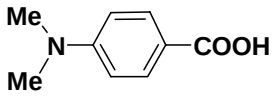

10

purpose to develop a new class of anion receptors. In addition, two characteristic properties of host **10** would be taken into account: 1) acid **10** and its conjugate base have large absorption coefficients (ε = 2.62 × 10^4 [L·mol^{-1}·cm^{-1}]),[2] which makes it possible to use host **10** at very low concentration such as 10^{-6} mol/L level, and 2) host **10** shows dual fluorescence feature originating from the simultaneous emissions of locally excited (LE) state and twisted intramolecular charge transfer (TICT) state,[3] which are quite sensitive to the microenvironment of the media surrounding **10**.[4] Simple and commercially available 4-(*N*,*N*-dimethylamino)benzoic acid (**10**), therefore, was directly utilized as an anion host in a preliminary investigation for developing the new signaling methodology for anion recognition.

Host **10** has an acidic hydrogen atom to be transferred to guest anions as well as an aromatic moiety to show spectral response upon complexation with guest anions. If the aromatic acid interacts with the guest anion whose conjugate acid is less acidic than the host acid (i.e. the basicity of the guest anion is stronger than that of the conjugate base of the host acid), the host acid would easily *transfer* a proton to the guest anion to give the corresponding carboxylate anion, which would cause notable spectral changes. In the case of the guest anion whose conjugate acid is more acidic than the host acid (i.e. the basicity of the guest anion is weaker than that of the conjugate base of the host acid), proton exchange between the host acid and the guest anion would be quite difficult. However, even in this case, if the structure of the guest anion is complementary to the

host acid, *complexation* between the host acid and the guest anion could occur to give a partially anionic species of the acid concomitant with spectral changes as reported by Wu et al.[5] Table 3-1 lists the acid dissociation constants (pK_a) of a variety of acids and base dissociation constants (pK_b) of their conjugate bases. As can be seen in Table 3-1, divalent anion HPO_4^{2-} has the highest basicity among typical inorganic anions which frequently appear in the environment. In addition, charge densities on guest anions would play a crucial role in effective interaction between the host acid and the guest anion.

In order to know the complexation behavior of host **10** with a variety of anions, the UV-vis and fluorescence titration experiments were carried out. Divalent anions, SO_4^{2-}, HPO_4^{2-}, and $H_2P_2O_7^{2-}$, and monovalent anions, $H_2PO_4^-$, HSO_4^-, ClO_4^-, BF_4^-, PF_6^-, and NO_3^- were selected, all of which were used as tetrabutylammonium (TBA) salts.

Table 3-1. Acid Dissociation Constants (pK_a) of a Variety of Acids and Base Dissociation Constants (pK_b) of Their Conjugate Bases

acid	pK_a	conjugate base	pK_b[a]
H_2SO_4	ca. -3[b]	HSO_4^-	ca. 17
HNO_3	-1.64[c]	NO_3^-	15.6
$HClO_4$	-1.6[d]	ClO_4^-	15.6
HBF_4	0.5[d]	BF_4^-	13.5
HSO_4^-	1.99[b]	SO_4^{2-}	12.0
$H_3P_2O_7^-$	2.10[d]	$H_2P_2O_7^{2-}$	11.9
H_3PO_4	2.16[d]	$H_2PO_4^-$	11.8
C_6H_5COOH	4.19[d]	$C_6H_5COO^-$	9.81
$H_2PO_4^-$	7.21[d]	HPO_4^{2-}	6.79

[a] Calculated by equation $K_b = K_w / K_{a.}$ [b] Ref. 7. [c] Ref. 8. [d] Ref. 6.

In this chapter, the availability of host **10** as a new class of anion receptors and the versatility of the DMAB group as an excellent signaling subunit are investigated to develop a new signaling methodology for anion recognition.

3-2 Results and Discussion

3-2-1 UV-vis spectral titrations

3-2-1-1 UV-vis spectral titrations

The UV-vis spectral titration method is a simple and convenient approach to study interactions between hosts and guests. Since acid **10** and its conjugate base has strong absorption, as introduced in former section, the UV-vis spectral titration technique was applied to investigate complexation behavior of host **10** toward a variety of anions in CH_3CN.

Host **10** showed maximum absorption at 309 nm in CH_3CN. The possibility of the dimerization of host **10** in CH_3CN was checked by monitoring the absorption changes of host **10** at different concentrations. No change was observed in the spectral shape of host **10** at the concentration ranging from 6.5×10^{-7} mol/L to 6.5×10^{-5} mol/L. The values of the maximal absorbance monitored at 309 nm against the concentration of host **10** exactly obeyed the Lambert-Beer equation with an excellent correlation coefficient ($r^2 = 0.9999$, n = 10). The results indicated that no substantial intermolecular interactions of **10** took place in acetonitrile at such concentration range. Meanwhile, the molar absorption coefficient of host **10** in CH_3CN was determined to be 2.8×10^4 [$L \cdot mol^{-1} \cdot cm^{-1}$].

Gradual addition of HPO_4^{2-}, whose basicity ($pK_b = 6.79$)[6] is stronger than that of the conjugate base of **10** (pK_b of benzoate itself = 9.81),[6] led to substantial decrease of the absorbance at 309 nm along with obvious increase of the absorbance of a new absorption at 275 nm, as shown in Figure 3-1. In a separate experiment, similar absorption around 275 nm appeared when equimolar amounts of host acid **10** and tetrabutylammonium hydroxide ((TBA)OH) were mixed together in CH_3CN. This result

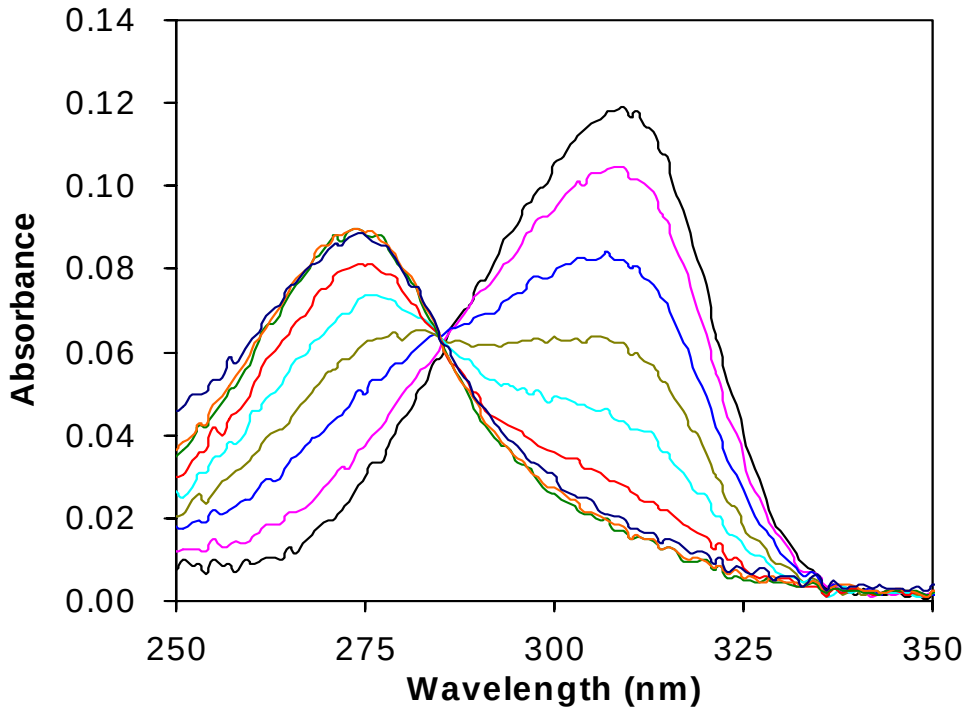

Figure 3-1. Absorption spectra of host **10** in CH_3CN (4.46×10^{-6} mol/L) in the absence (──) of and in the presence of 0.1 (──), 0.2 (──), 0.3 (──), 0.4 (──), 0.5 (──), 1.0 (──), 2.0 (──), and 10.0 (──) equivalent of $(TBA)_2HPO_4$, respectively.

clearly indicated that the new absorption at 275 nm should be ascribed to the absorption of the conjugate base (4-(*N*,*N*-dimethylamino)benzoate anion) of host acid **10** generated by simple proton exchange between acid **10** and base HPO_4^{2-}. In addition, the author supposes that the resulting host carboxylate and conjugate acid of anion would not be separated by the solvent fully to give complete ion species but would make a pair through hydrogen bonding in CH_3CN, because titrations of host **10** by the strongest base (OH^-), a strong base (HPO_4^{2-}), and a weak base (SO_4^{2-}) gave similar spectra finally. Moreover, a clear isosbestic point was observed at the position around 285 nm in the titration spectra of host **10** with HPO_4^{2-}, which indicated that only one complex was formed during the complexation process.

The Job's method was adopted to determine the binding stoichiometry of host **10**

with HPO_4^{2-}. As shown in Figure 3-2, a maximum absorption was clearly observed when the molar function of host **10** ([**10**]/([**10**] + [HPO_4^{2-}])) approached 0.65, which indicated that the complexation stoichiometry between host **10** and HPO_4^{2-} was 2:1 (host **10** : anion). The structure of the postulated 2:1 complex between host **10** and HPO_4^{2-} was shown in Figure 3-3.

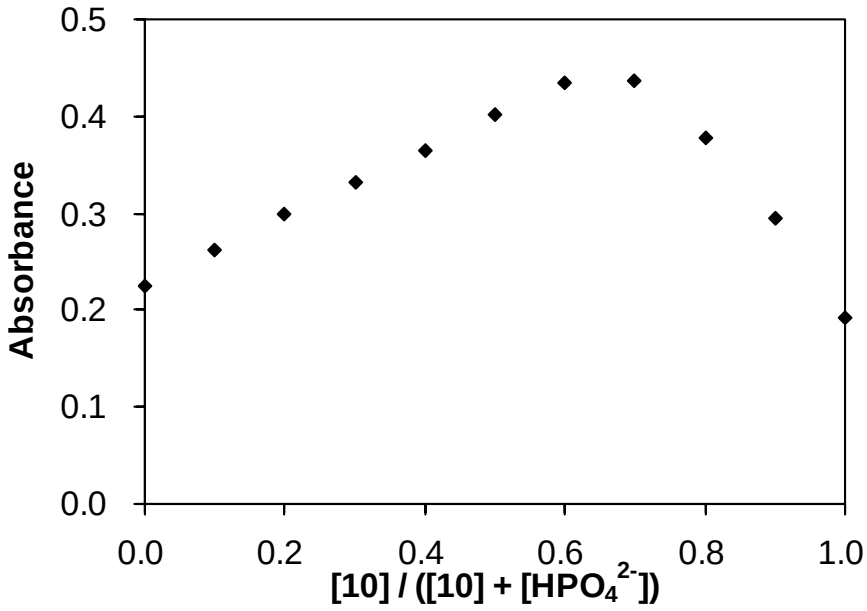

Figure 3-2. Job's plot for complexation of host **10** (3.00×10^{-5} mol/L) with $(TBA)_2HPO_4$ in CH_3CN monitored at 275 nm.

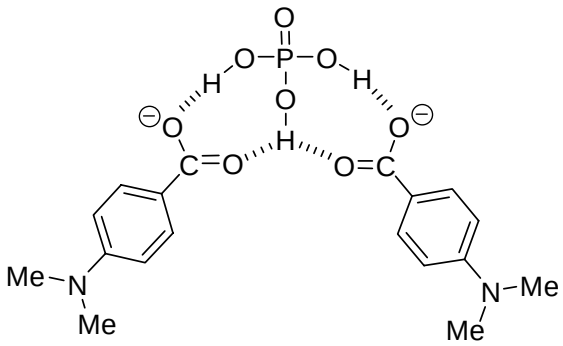

Figure 3-3. Postulated structure of 2:1 complex between host **10** and HPO_4^{2-}.

It is quite interesting that almost comparable changes such as large spectral changes both at 275 nm and 309 nm as well as rapid saturation of titration were obtained on the titration of host **10** by SO_4^{2-} (Figure 3-4) and were relatively close to those by HPO_4^{2-}, because judging from the weaker bacisity of SO_4^{2-} (pK_b = 12.0)[7] than that of the conjugate base of **10** (pK_b of benzoate itself = 9.81), almost no spectral changes of host **10** upon titration by SO_4^{2-} should be expected. In addition, a clear isosbestic point was also observed in the titration spectra around 285 nm upon SO_4^{2-} addition, which meant that only one complex was formed in the titration.

The titration curves of host **10** at higher concentration (3.10×10^{-5} mol/L) by SO_4^{2-} monitored both at 275 and 309 nm showed clear inflection points at SO_4^{2-}/**10** ratio equal to 1.0 (Figure 3-5). The observation ensured that the binding stoichiometry

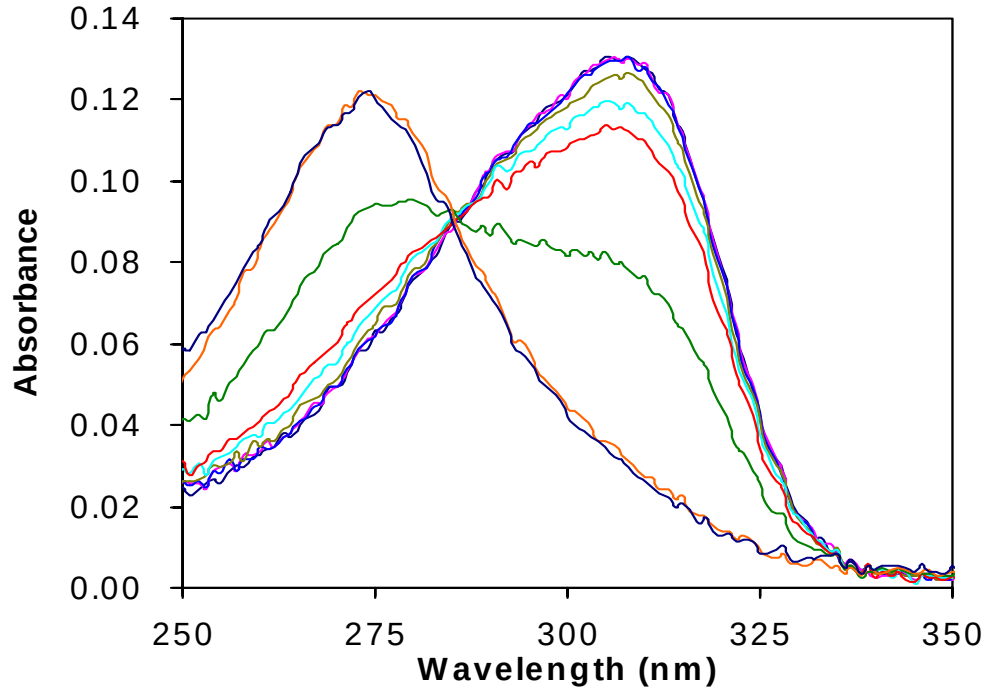

Figure 3-4. Absorption spectra of host **10** in CH_3CN (4.46×10^{-6} mol/L) in the absence (——) of and in the presence of 0.1 (——), 0.2 (——), 0.3 (——), 0.4 (——), 0.5 (——), 1.0 (——), 2.0 (——), and 10.0 (——) equivalent of $(TBA)_2SO_4$, respectively.

between host **10** and SO_4^{2-} is 1:1 in this concentration. Furthermore, the Job's method was adopted to determine the binding stoichiometry of host **10** with SO_4^{2-}. A maximum absorption was clearly observed in the Job's plot when [**10**]/([**10**] + [SO_4^{2-}]) equaled 0.5 (Figure 3-6), which also meant that the complexation stoichiometry between host **10** and SO_4^{2-} was 1:1 (host **10** : anion) in this concentration.

In the case of divalent anion $H_2P_2O_7^{2-}$, whose basicity is weaker (pK_b = 11.9)[6] than that of the conjugate base of **10** (pK_b of benzoate itself = 9.81), the absorption changes monitored at 275 nm and 309 nm (Figure 3-7) were relatively smaller as compared with those in the cases of divalent anions, HPO_4^{2-} and SO_4^{2-}. An isosbestic point was again observed around 285 nm upon addition of $H_2P_2O_7^{2-}$, which also indicated that one complex was formed in this case.

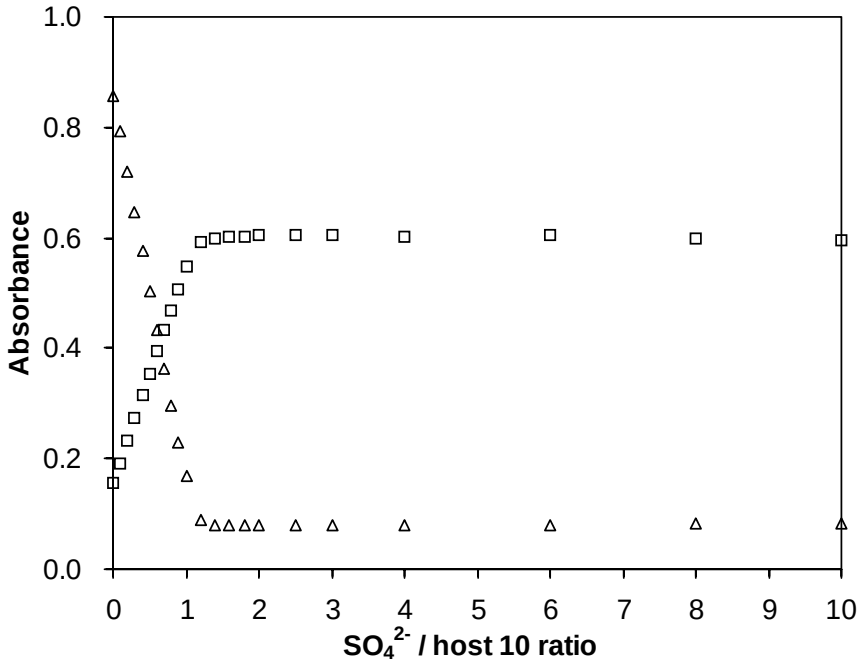

Figure 3-5. Absorption changes monitored at 275 nm (□) and 309 nm (△) upon titration of host **10** (3.10×10^{-5} mol/L) with of $(TBA)_2SO_4$ in CH_3CN.

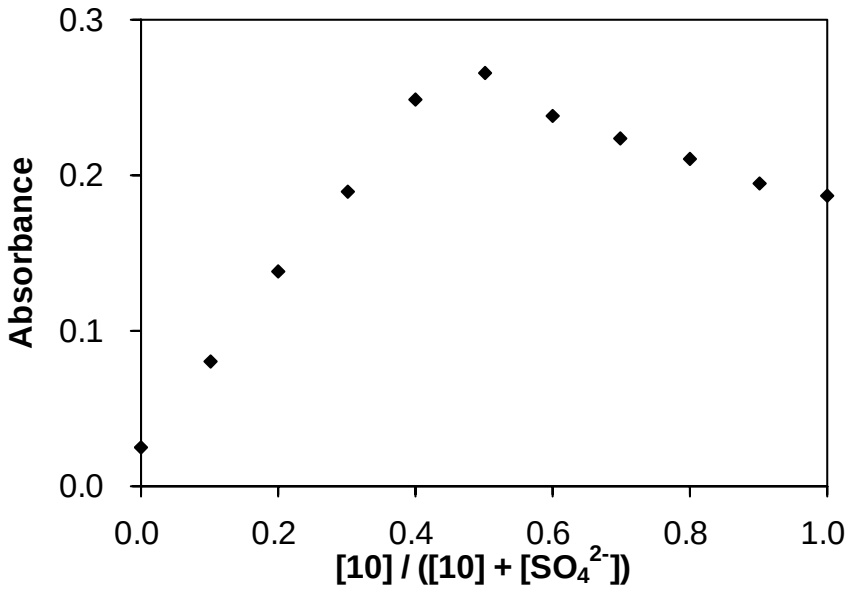

Figure 3-6. Job's plot for complexation of host **10** (3.00×10^{-5} M) with $(TBA)_2SO_4$ in CH_3CN monitored at 275 nm.

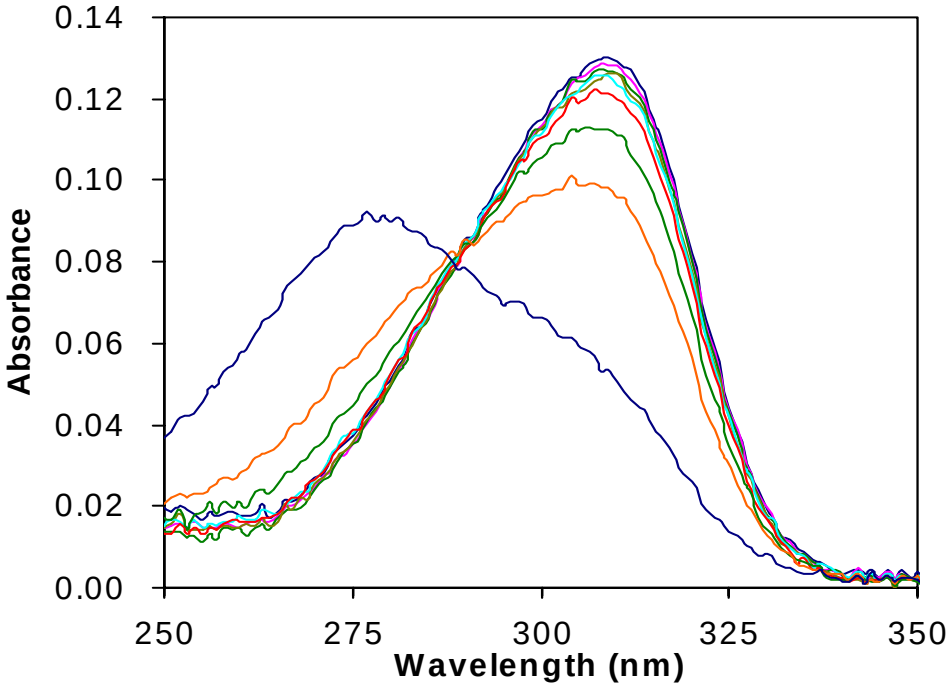

Figure 3-7. Absorption spectra of host **10** in CH_3CN (4.46×10^{-6} mol/L) in the absence (—) of and in the presence of 0.1 (—), 0.2 (—), 0.3 (—), 0.4 (—), 0.5 (—), 1.0 (—), 2.0 (—), and 10.0 (—) equivalent of $(TBA)_2H_2P_2O_7$, respectively.

On the other hand, monovalent anions, such as $H_2PO_4^-$, HSO_4^-, ClO_4^-, BF_4^-, PF_6^-, and NO_3^-, have very weak basicity ($pK_b > 11$)[6, 7, 8] as compared to the conjugate base of host **10** (pK_b of benzoate itself = 9.81). The UV-vis titration spectra of host **10** gave rise to quite limited absorption changes both observed at 275 and 309 nm upon gradual addition of the monovalent anions (Figure 3-8 for $H_2PO_4^-$, Figure 3-9 for HSO_4^-, Figure 3-10 for ClO_4^-, Figure 3-11 for BF_4^-, Figure 3-12 for PF_6^-, and Figure 3-13 for NO_3^-).

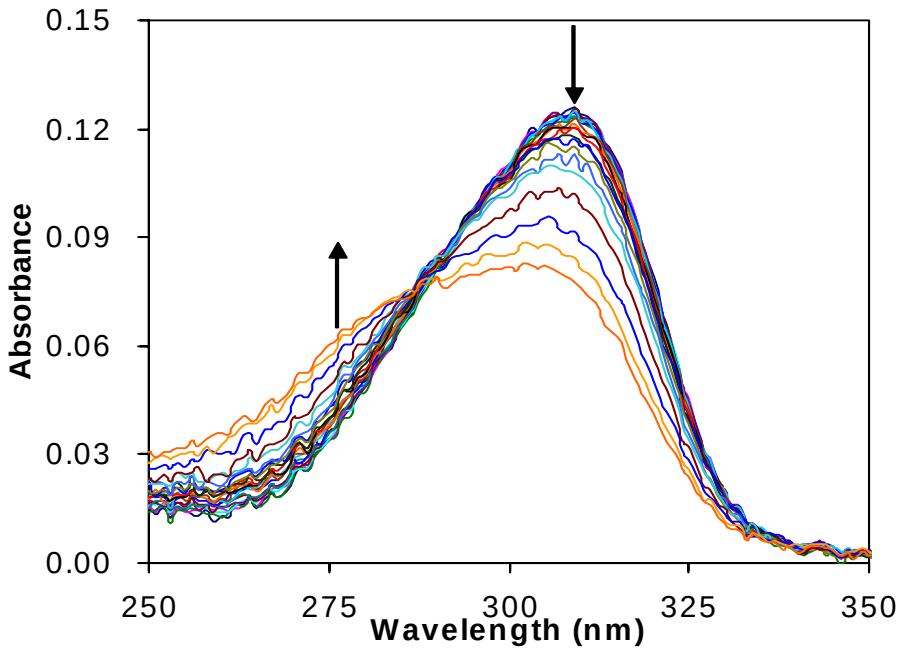

Figure 3-8. Absorption spectra of host **10** in CH_3CN (4.46×10^{-6} mol/L) upon addition with (TBA)H_2PO_4. The arrows denote the direction of absorption changes along with increasing the amounts of the anion.

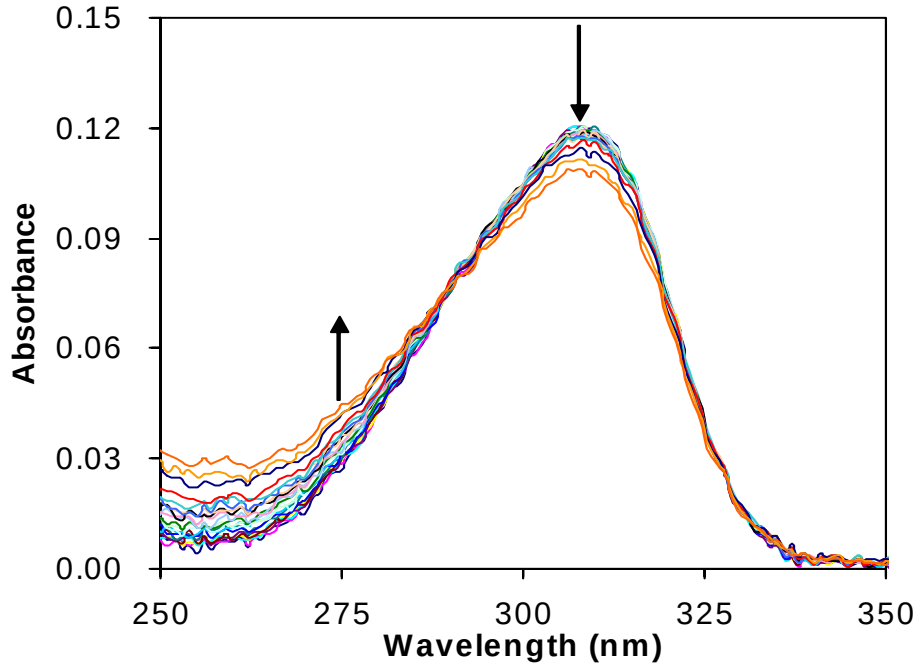

Figure 3-9. Absorption spectra of host **10** in CH_3CN (4.46×10^{-6} mol/L) upon addition with (TBA)HSO_4. The arrows denote the direction of absorption changes along with increasing the amounts of the anion.

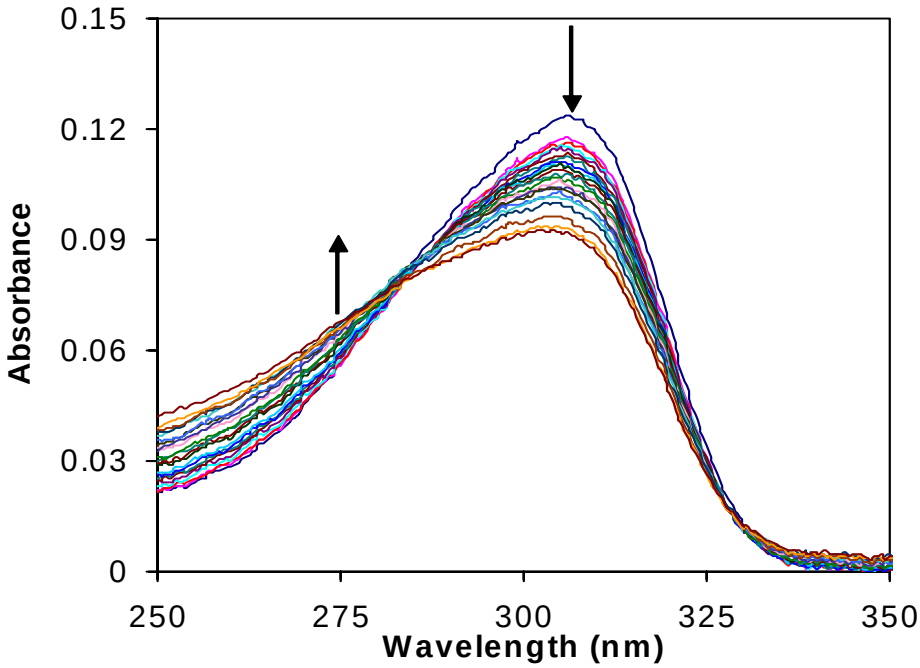

Figure 3-10. Absorption spectra of host **10** in CH_3CN (4.46×10^{-6} mol/L) upon addition with (TBA)ClO_4. The arrows denote the direction of absorption changes along with increasing the amounts of the anion.

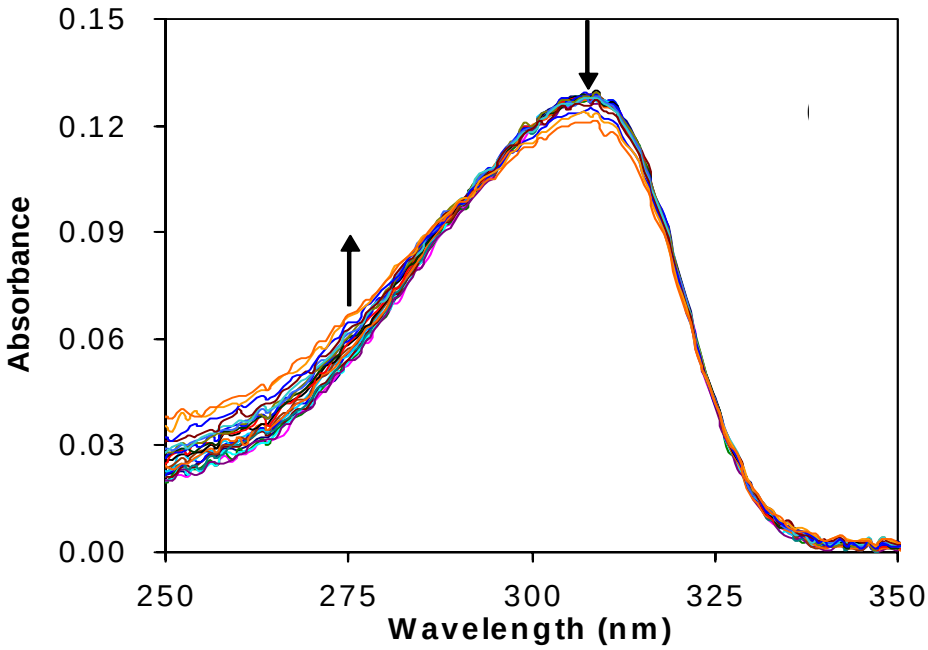

Figure 3-11. Absorption spectra of host **10** in CH_3CN (4.46×10^{-6} mol/L) upon addition with (TBA)BF_4. The arrows denote the direction of absorption changes along with increasing the amounts of the anion.

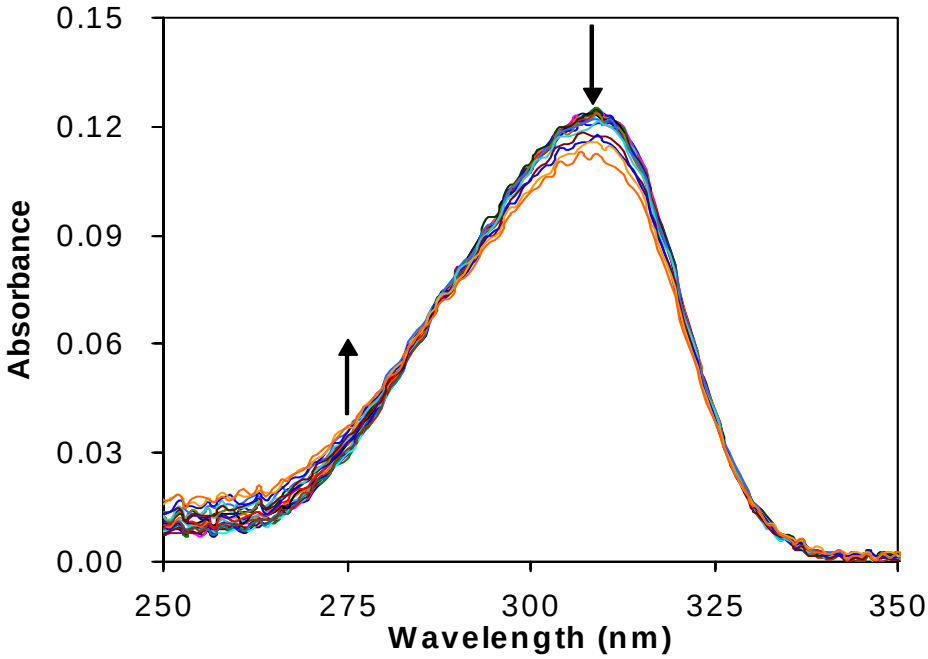

Figure 3-12. Absorption spectra of host **10** in CH_3CN (4.46×10^{-6} mol/L) upon addition with (TBA)PF_6. The arrows denote the direction of absorption changes along with increasing the amounts of the anion.

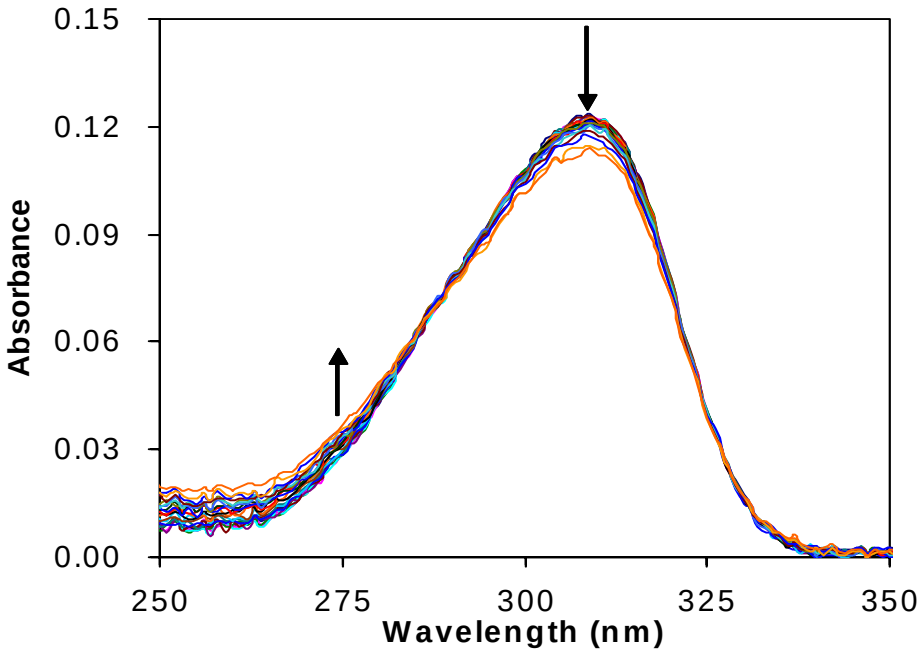

Figure 3-13. Absorption spectra of host **10** in CH_3CN (4.46×10^{-6} mol/L) upon addition with (TBA)NO_3. The arrows denote the direction of absorption changes along with increasing the amounts of the anion.

In order to easily compare the differences on the titration profiles of host **10** upon addition of divalent anions, HPO_4^{2-}, SO_4^{2-}, and $H_2P_2O_7^{2-}$, as well as monovalent anions, $H_2PO_4^-$, HSO_4^-, ClO_4^-, BF_4^-, PF_6^-, and NO_3^-, the absorbance monitored at maximal absorption wavelengths (275 nm and 309 nm) were selected to generate the titration curves, as shown in Figure 3-14 for 275 nm and Figure 3-15 for 309 nm, respectively. As can be seen in Figure 3-14, the absorbance at 275 nm increased almost linearly from the beginning to 0.5 equivalent amounts upon addition of HPO_4^{2-} and then maintained almost horizontal even in the presence of an excess amount of HPO_4^{2-}. In the case of SO_4^{2-}, the absorption changes were very small up to 0.3 equivalent amounts of addition of SO_4^{2-}, and then increased sharply till the ratio of SO_4^{2-}/**10** equaled 2, finally went flatly. In the cases of $H_2P_2O_7^{2-}$ and $H_2PO_4^-$, the absorptions were gradually enhanced along with increasing the amounts of the anions. The increasing tendency observed in

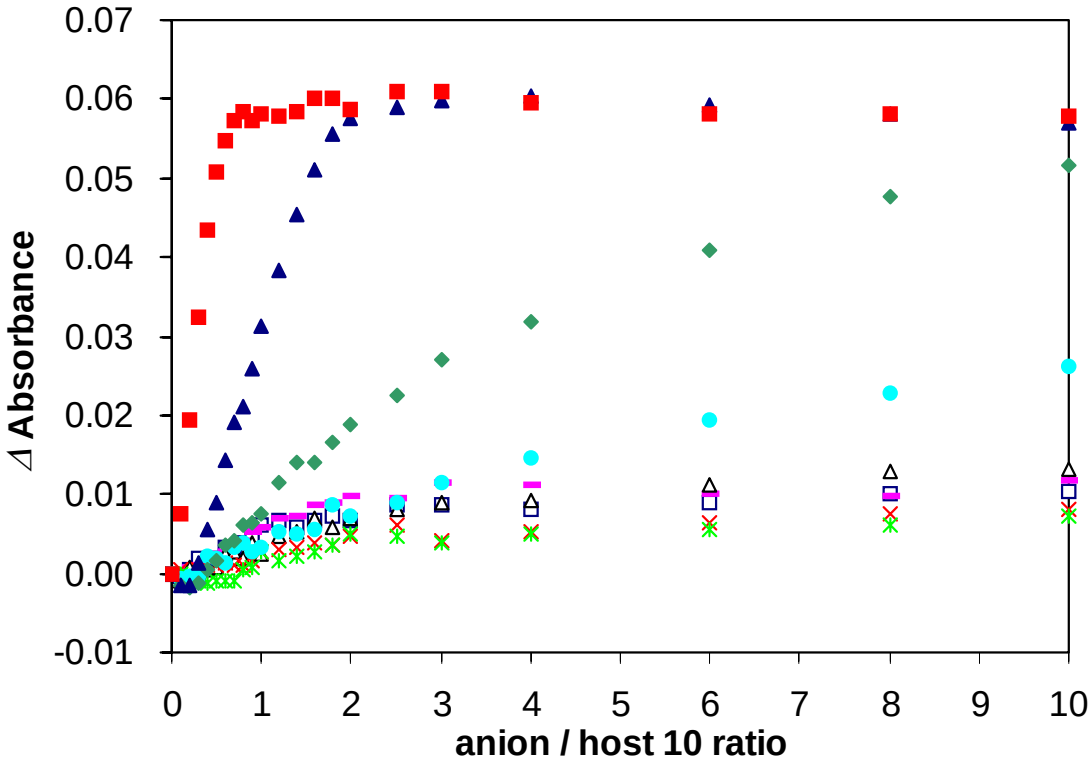

Figure 3-14. Absorbance changes monitored at 275 nm upon titrations of host **10** (4.46 × 10^{-6} M) with $(TBA)_2HPO_4$ (■), $(TBA)_2SO_4$ (▲), $(TBA)_2H_2P_2O_7$ (◆), $(TBA)H_2PO_4$ (●), $(TBA)HSO_4$ (□), $(TBA)ClO_4$ (—), $(TBA)BF_4$ (△), $(TBA)PF_6$ (×), and $(TBA)NO_3$ (*) in CH_3CN.

the case of $H_2P_2O_7^{2-}$ was stronger than that in the case of $H_2PO_4^-$. With respect to the monovalent anions, small absorption changes were observed during titrations.

By contrast with Figure 3-14, the absorption at 309 nm decreased rapidly from beginning to half amount of addition of HPO_4^{2-} and saturated thereafter (Figure 3-15). The titration profile of host **10** with SO_4^{2-} showed slightly sigmoidal decreasing up to twice amount addition of SO_4^{2-} and kept no absorption change till the end of the titrations. The absorption changes of host **10** upon addition of $H_2P_2O_7^{2-}$ as well as monovalent anions, such as $H_2PO_4^-$, HSO_4^-, ClO_4^-, BF_4^-, PF_6^-, and NO_3^- showed monotonic decreasing during titrations.

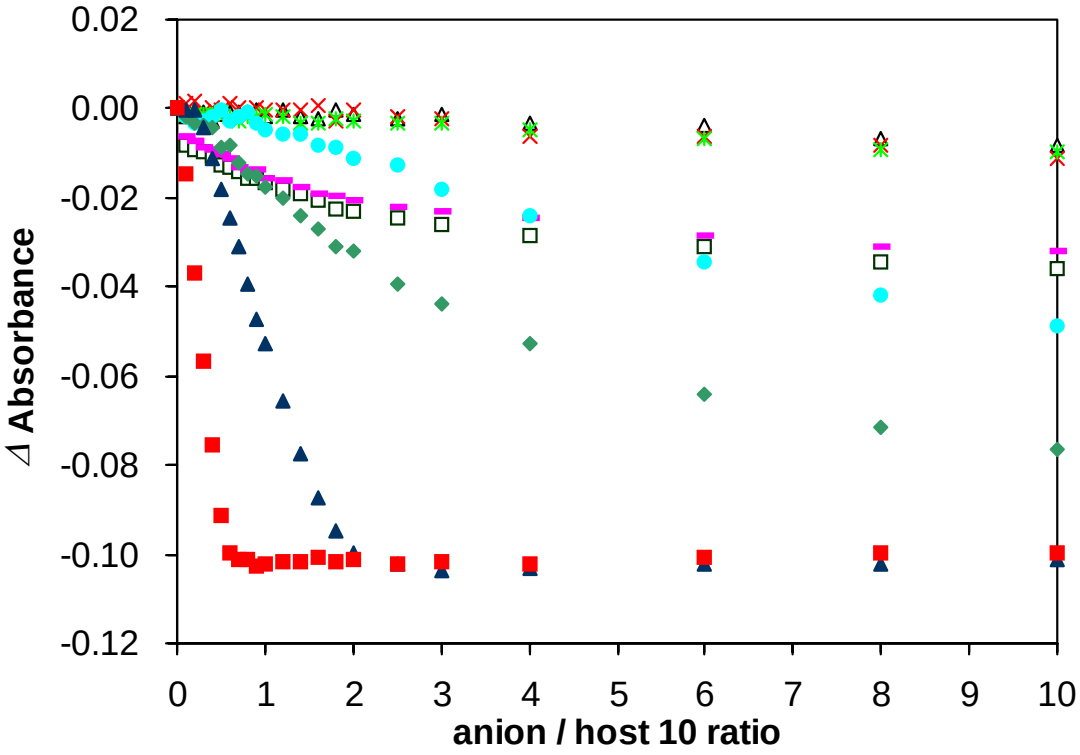

Figure 3-15. Absorbance changes monitored at 309 nm upon titrations of host **10** (4.46 × 10^{-6} M) with $(TBA)_2HPO_4$ (■), $(TBA)_2SO_4$ (▲), $(TBA)_2H_2P_2O_7$ (◆), $(TBA)H_2PO_4$ (●), $(TBA)HSO_4$ (□), $(TBA)ClO_4$ (—), $(TBA)BF_4$ (△), $(TBA)PF_6$ (×), and $(TBA)NO_3$ (*) in CH_3CN.

Thus, the observation of distinct titration profiles of host **10** upon titrations with a variety of divalent and monovalent anions allowed us to understand that different complexation behavior occurred. The DMAB signaling subunit successfully displayed the UV-vis spectral changes during the complexation processes.

3-2-1-2 Binding Constants

The UV-vis titration data monitored at 309 nm (Figure 3-15) were subjected to non-linear least square curve fitting to determine binding constants of host **10** with the anions.[9] The existence of clear inflection points around $[HPO_4^{2-}]/[\mathbf{10}] = 0.5$ in titration profiles (Figures 3-14 and 3-15) clearly demonstrated that the complexation stoichiometry of host **10** and HPO_4^{2-} would be 2:1. Monotonic changes were observed in the cases of divalent $H_2P_2O_7^{2-}$ as well as monovalent anions ($H_2PO_4^-$, HSO_4^-, ClO_4^-, BF_4^-, PF_6^-, and NO_3^-), whereas slightly sigmoidal change was observed in the case of divalent anion SO_4^{2-} (Figure 3-15). Taking into account of the charge balance between host acid **10** and guest anions as well as the above titration profiles, 1:1 (host **10**: anion) complexation model was applied for the binding constant calculations in the cases of $H_2P_2O_7^{2-}$ and the monovalent anions and 2:1 complexation models were applied for divalent anions HPO_4^{2-} and SO_4^{2-}. The postulated 2:1 complex structure of host **10** and SO_4^{2-} was shown in Figure 3-16. The binding constants K_1 for 1:1 complexation and K_2 for 2:1 complexation were, therefore, defined by equations (1) and (2), respectively,

$$\mathbf{10} + A^- \overset{K_1}{\rightleftharpoons} \mathbf{10}\bullet A^- \qquad K_1 = [\mathbf{10}\bullet A^-]/([\mathbf{10}][A^-]) \qquad (1)$$

$$\mathbf{10}_2 + A^{2-} \overset{K_2}{\rightleftharpoons} \mathbf{10}_2\bullet A^{2-} \qquad K_2 = [\mathbf{10}_2\bullet A^{2-}]/([\mathbf{10}]^2[A^{2-}]) \qquad (2)$$

where A^- and A^{2-} denote a monovalent anion and a divalent anion, respectively. Table 3-2 summarized the calculation results of binding constants of host **10** toward a variety of anions. In Table 3-2, K_1 denotes 1:1 complexation constants for $H_2P_2O_7^{2-}$ and the monovalent anions, and K_2 denotes 2:1 complexation constants for HPO_4^{2-} and SO_4^{2-}.

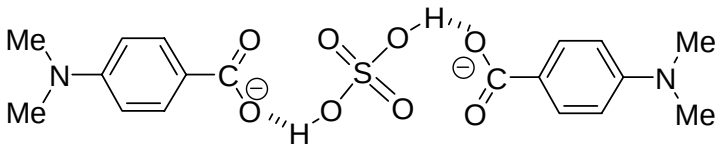

Figure 3-16. Postulated structure of 2:1 complex between host **10** and SO_4^{2-}.

Table 3-2. Binding Constants of Host **10** toward Anions

anion	binding constants	
	log K_1 (log M^{-1})	log K_2 (log M^{-2})
$H_2PO_4^-$	4.3	—
HSO_4^-	3.6	—
ClO_4^-	4.2	—
BF_4^-	3.4	—
PF_6^-	3.4	—
NO_3^-	3.5	—
$H_2P_2O_7^{2-}$	4.8	—
SO_4^{2-}	—	$> 10^a$
HPO_4^{2-}	—	$> 10^a$

[a] K_2 was too large to be accurately determined.

As results, monovalent anions ($H_2PO_4^-$, HSO_4^-, ClO_4^-, BF_4^-, PF_6^-, and NO_3^-) as well as divalent anion, $H_2P_2O_7^{2-}$ showed almost equal binding affinities to host **10** (log K_1 = 3.4 - 4.8), while divalent anions (HPO_4^{2-} and SO_4^{2-}) showed quite high binding affinities (log $K_2 > 10$). The binding constants K_2 for divalent anions (SO_4^{2-} and HPO_4^{2-}) are too large to be calculated accurately. Judging from the titration profiles as shown in Figure 3-15, however, the binding constant for HPO_4^{2-} would be larger than that for SO_4^{2-}. The strongest basicity of HPO_4^{2-} (pK_b = 6.79) among the anions also suggests

that the interaction between acid **10** and HPO_4^{2-} would be very strong**.** It is quite interesting that anions, $H_2PO_4^-$ and SO_4^{2-}, have almost the same basicity (pK_b = 11.8 and 12.0, respectively),[6] while the binding constant for SO_4^{2-} was much larger than that for $H_2PO_4^-$. This result turned out that the basicity of anions did not play an important role in the complexation between host **10** and the anions in these examples. Therefore, it would be concluded that the charge density on anion would be the most important factor influencing the complexation ability between host **10** and anions with weaker basicity than the conjugate base of host **10**. Thus, it is quite reasonable that monovalent anions ($H_2PO_4^-$, HSO_4^-, ClO_4^-, BF_4^-, PF_6^-, and NO_3^-) showed relatively weak binding ability to host **10**, since they have monovalent negative charge and the weaker basicity of the anions (pK_b > 11) than that of the conjugate base of host **10**. The observed weak binding affinity of host **10** toward $H_2P_2O_7^{2-}$ could be rationalized by its weaker basicity (pK_b > 10.9) as well as the "dual-$H_2PO_4^-$" structure, as introduced in Chapter 2.

3-2-1-3 Conclusions

Commercially available 4-(*N*,*N*-dimethylamino)benzoic acid (**10**) was directly used as an anion host molecule to investigate the complexation behavior toward a variety of anions in terms of UV-vis titrations. Host **10** exhibited strong affinities and high binding selectivity toward divalent anions (HPO_4^{2-} and SO_4^{2-}) over monovalent anions (NO_3^-, BF_4^-, ClO_4^-, HSO_4^-, PF_6^-, and $H_2PO_4^-$) as well as $H_2P_2O_7^{2-}$. The binding stoichiometry of host **10** with HPO_4^{2-} and SO_4^{2-} turned out to be 2:1 and that with $H_2PO_4^-$, HSO_4^-, ClO_4^-, BF_4^-, PF_6^-, NO_3^-, and $H_2P_2O_7^{2-}$ turned out to be 1:1. Host **10** in high concentration (3.10×10^{-5} mol/L) gave a 1:1 complex with SO_4^{2-}. The basicity and negatively charges of anions were the main factors to influence the selectivity of host **10** toward anions.

3-2-2 Fluorescence Titrations

3-2-2-1 Fluorescence titrations

Fluorescence titration method is a simple and sensitive technique to investigate the interactions between hosts and anions. Since acid **10** has unique dual fluorescence feature, as introduced in former section, the fluorescence technique was applied to investigate the complexation behavior of host **10** with a variety of anions in CH_3CN.

Host **10** in CH_3CN exhibited dual fluorescence emissions at 343 nm (LE) and 491 nm (TICT) by excitation at 300 nm. First, the fluorescence titrations of host **10** by divalent anions (HPO_4^{2-}, SO_4^{2-}, and $H_2P_2O_7^{2-}$) were performed and the titration spectra were shown in Figure 3-17 for HPO_4^{2-}, Figure 3-18 for SO_4^{2-}, and Figure 3-19 for $H_2P_2O_7^{2-}$. Stepwise addition of the divalent anions caused different fluorescence intensity changes of host **10** at LE and TICT states.

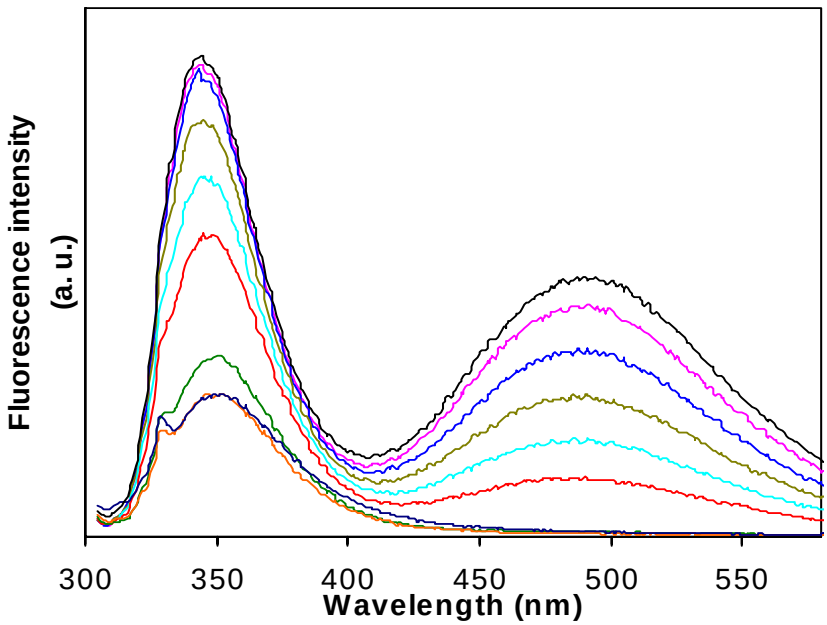

Figure 3-17. Fluorescence spectra of host **10** in CH_3CN (4.46×10^{-6} mol/L) in the absence (———) of and in the presence of 0.1 (———), 0.2 (———), 0.3 (———), 0.4 (———), 0.5 (———), 1.0 (———), 2.0 (———), and 10.0 (———) equivalent of $(TBA)_2HPO_4$, respectively. Excitation wavelength: 300 nm.

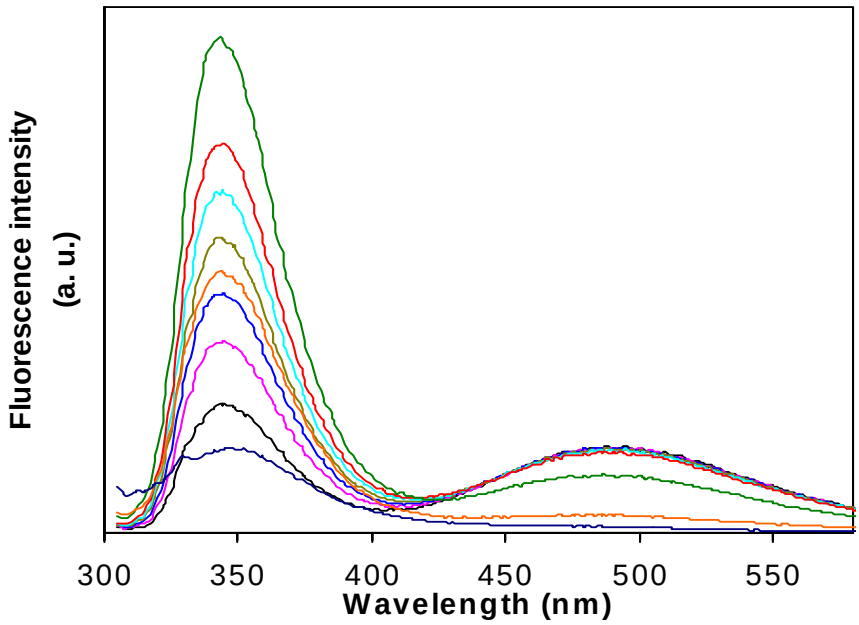

Figure 3-18. Fluorescence spectra of host **10** in CH_3CN (4.46×10^{-6} mol/L) in the absence (——) of and in the presence of 0.1 (——), 0.2 (——), 0.3 (——), 0.4 (——), 0.5 (——), 1.0 (——), 2.0 (——), and 10.0 (——) equivalent of $(TBA)_2SO_4$, respectively. Excitation wavelength: 300 nm.

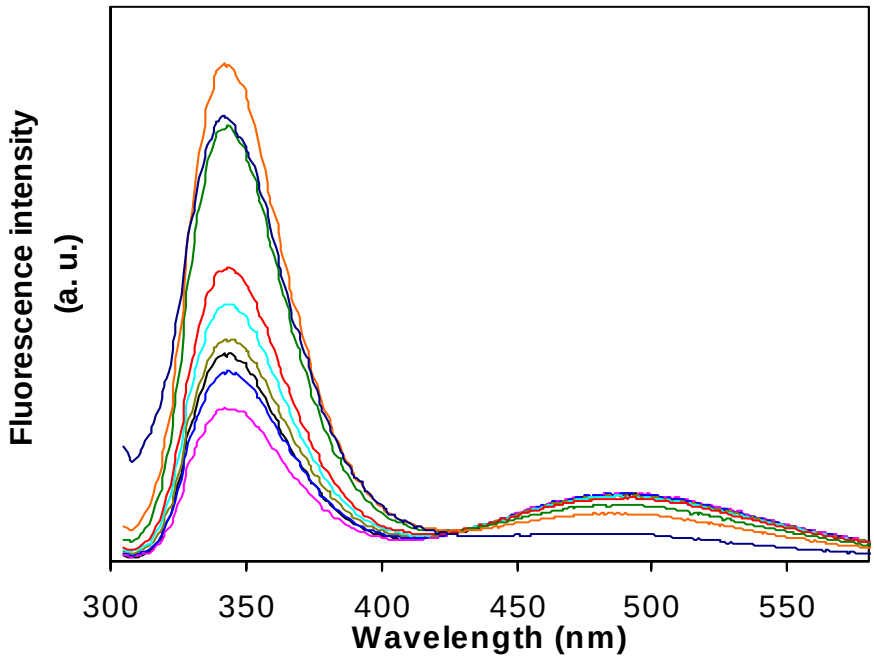

Figure 3-19. Fluorescence spectra of host **10** in CH_3CN (4.46×10^{-6} mol/L) in the absence (——) of and in the presence of 0.1 (——), 0.2 (——), 0.3 (——), 0.4 (——), 0.5 (——), 1.0 (——), 2.0 (——), and 10.0 (——) equivalent of $(TBA)_2H_2P_2O_7$, respectively. Excitation wavelength: 300 nm.

However, addition of monovalent anions, such as $H_2PO_4^-$, HSO_4^-, ClO_4^-, BF_4^-, PF_6^-, and NO_3^-, caused quite similar intensity changes both at LE and TICT bands, as shown in Figure 3-20 for $H_2PO_4^-$, Figure 3-21 for HSO_4^-, Figure 3-22 for ClO_4^-, Figure 3-23 for BF_4^-, Figure 3-24 for PF_6^-, and Figure 3-25 for NO_3^-.

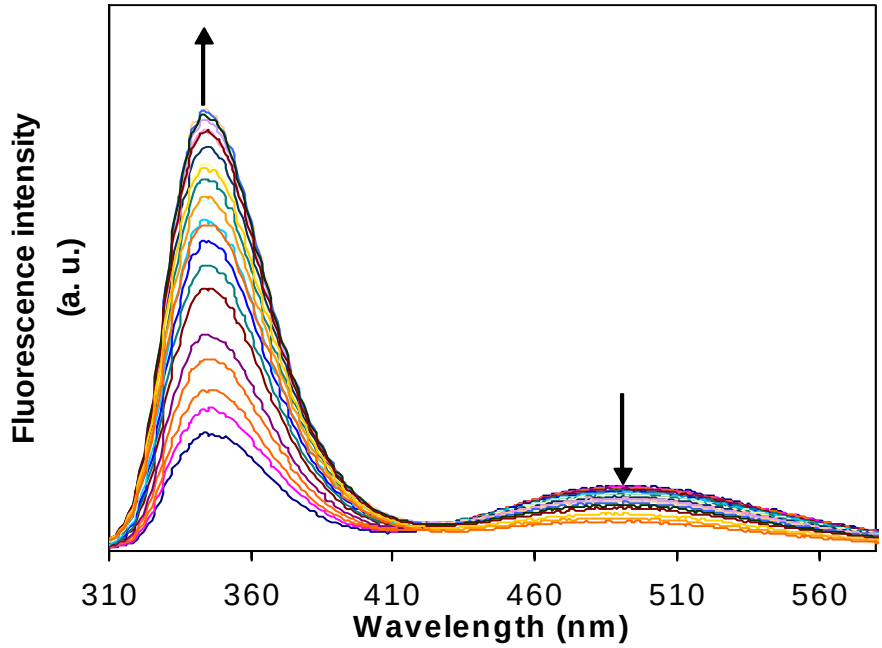

Figure 3-20. Fluorescence spectra of host **10** in CH_3CN (4.46×10^{-6} mol/L) upon addition with (TBA)H_2PO_4. Excitation wavelength: 300 nm. The arrows denote the direction of intensity changes along with increasing the amounts of the anion.

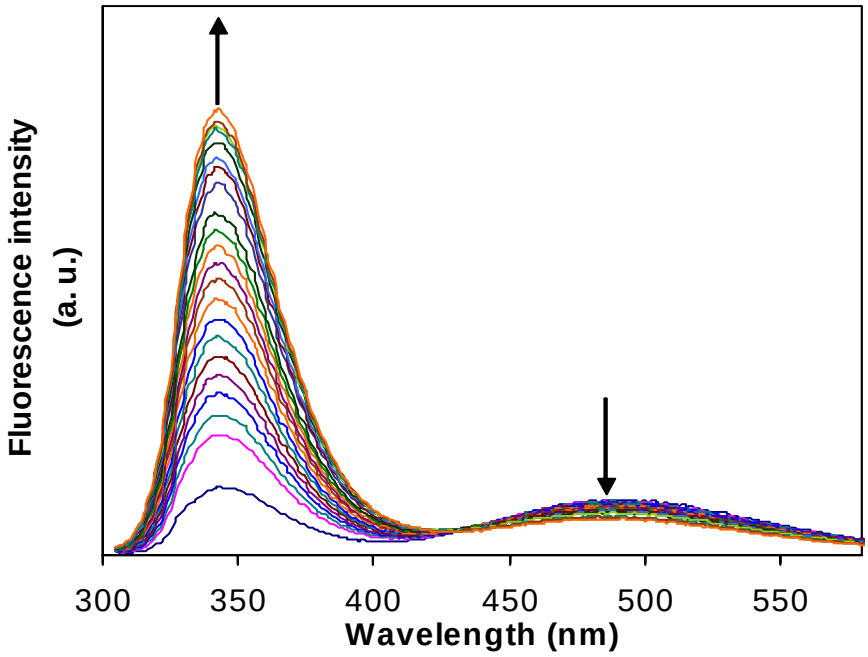

Figure 3-21. Fluorescence spectra of host **10** in CH_3CN (4.46×10^{-6} mol/L) upon addition with (TBA)HSO_4. Excitation wavelength: 300 nm. The arrows denote the direction of intensity changes along with increasing the amounts of the anion.

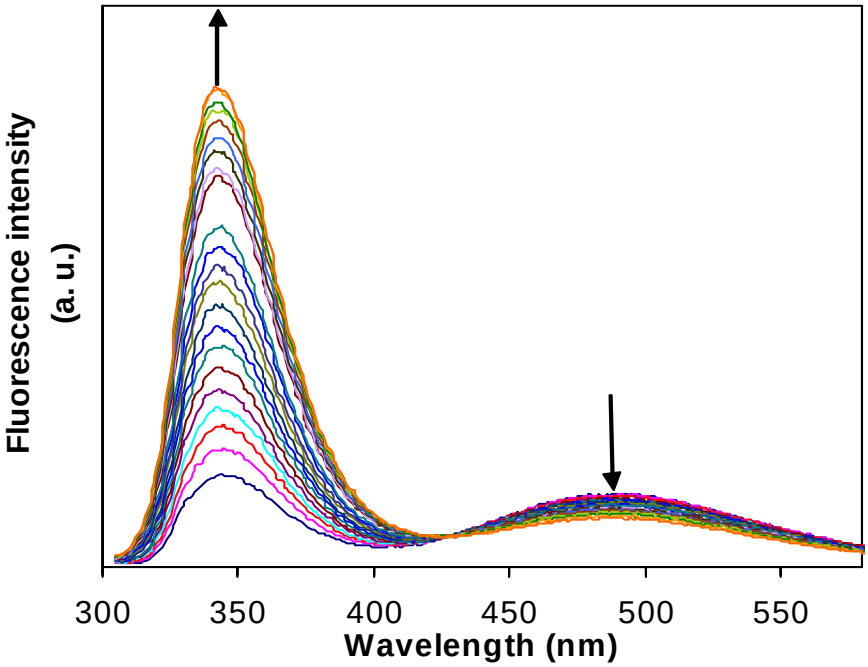

Figure 3-22. Fluorescence spectra of host **10** in CH_3CN (4.46×10^{-6} mol/L) upon addition with (TBA)ClO_4. Excitation wavelength: 300 nm. The arrows denote the direction of intensity changes along with increasing the amounts of the anion.

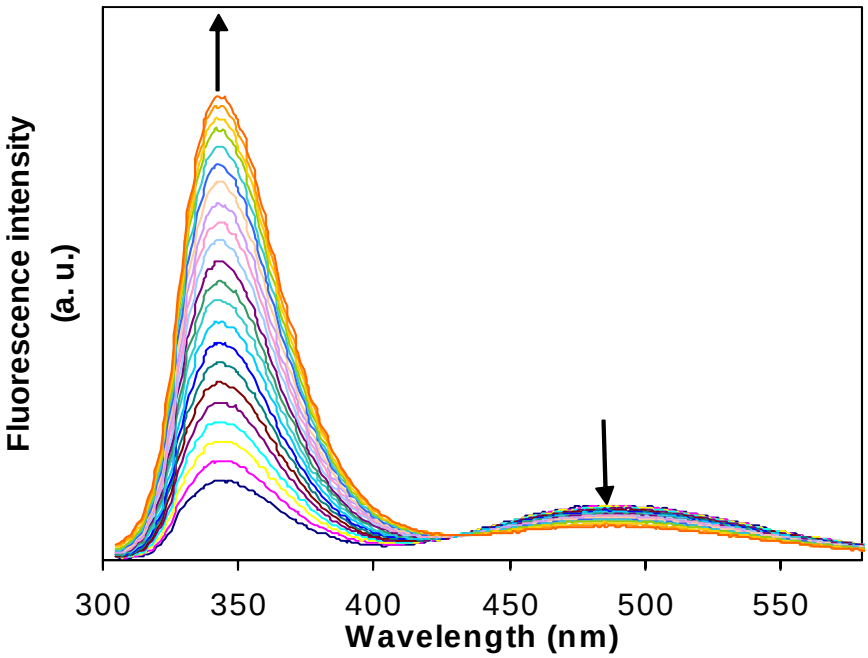

Figure 3-23. Fluorescence spectra of host **10** in CH_3CN (4.46×10^{-6} mol/L) upon addition with $(TBA)BF_4$. Excitation wavelength: 300 nm. The arrows denote the direction of intensity changes along with increasing the amounts of the anion.

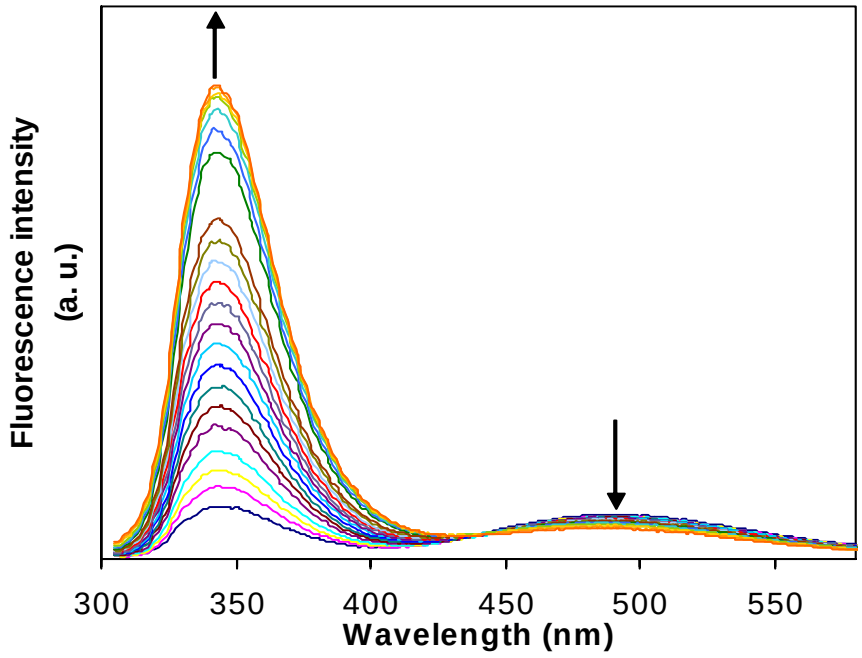

Figure 3-24. Fluorescence spectra of host **10** in CH_3CN (4.46×10^{-6} mol/L) upon addition with $(TBA)PF_6$. Excitation wavelength: 300 nm. The arrows denote the direction of intensity changes along with increasing the amounts of the anion.

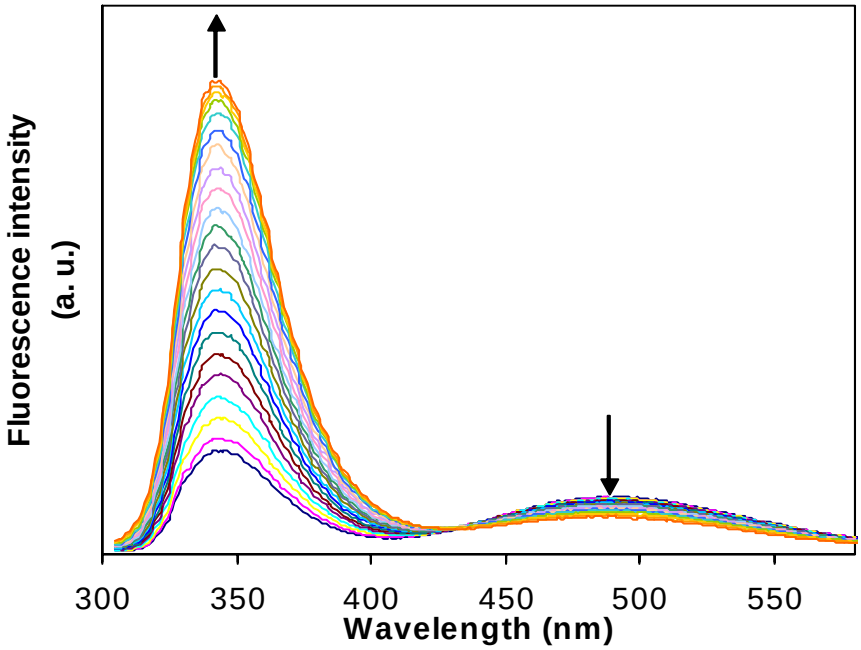

Figure 3-25. Fluorescence spectra of host **10** in CH_3CN (4.46×10^{-6} mol/L) upon addition with (TBA)NO_3. Excitation wavelength: 300 nm. The arrows denote the direction of intensity changes along with increasing the amounts of the anion.

For clear comparison of the LE and TICT intensity changes of host **10** upon titrations with divalent anions, HPO_4^{2-}, SO_4^{2-}, and $H_2P_2O_7^{2-}$, as well as monovalent anions, $H_2PO_4^-$, HSO_4^-, ClO_4^-, BF_4^-, PF_6^-, and NO_3^-, the intensity data monitored at LE state (343 nm) and TICT state (491 nm) were selected to generate the titration curves, as shown in Figure 3-26 for 343 nm and Figure 3-27 for 491 nm.

As can be seen, titration profiles of host **10** by divalent HPO_4^{2-} and SO_4^{2-} monitored at LE and TICT emission bands were remarkably different from those by $H_2P_2O_7^{2-}$ as well as monovalent anions ($H_2PO_4^-$, HSO_4^-, ClO_4^-, BF_4^-, PF_6^-, and NO_3^-). In Figure 3-26, stepwise addition of divalent HPO_4^{2-} caused gradual fluorescence quenching of host **10** at LE band till the concentration ratio of HPO_4^{2-}/**10** reached around 0.5 and, then, the LE intensity maintained almost no change even addition of an excess amount of HPO_4^{2-}. In the case of SO_4^{2-}, the LE intensity first increased sharply

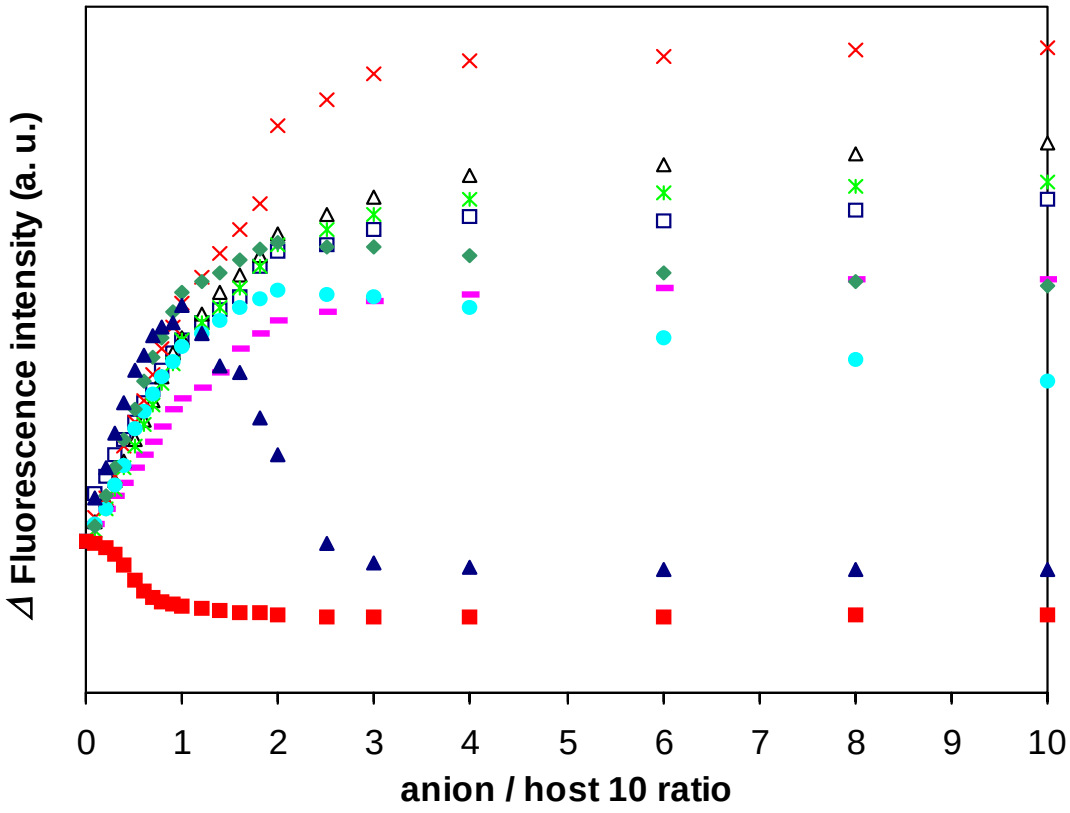

Figure 3-26. LE intensity changes monitored at 343 nm upon titrations of host **10** (4.46 × 10^{-6} mol/L) with $(TBA)_2HPO_4$ (■), $(TBA)_2SO_4$ (▲), $(TBA)_2H_2P_2O_7$ (◆), $(TBA)H_2PO_4$ (●), $(TBA)HSO_4$ (□), $(TBA)ClO_4$ (—), $(TBA)BF_4$ (△), $(TBA)PF_6$ (×), and $(TBA)NO_3$ (*) in CH_3CN. Excitation wavelength: 300 nm.

from the starting point to addition of 1.0 equivalent amounts of SO_4^{2-} and then oppositely decreased up to around 2.5 equivalent addition of SO_4^{2-}. Almost no change at LE state was observed even large amounts of SO_4^{2-} used. In contrast, the gradual increasing of LE intensity was observed in the cases of $H_2P_2O_7^{2-}$ and monovalent anions ($H_2PO_4^-$, HSO_4^-, ClO_4^-, BF_4^-, PF_6^-, and NO_3^-). Since the binding affinities of host **10** toward $H_2P_2O_7^{2-}$ and the monovalent anions were relatively weaker than those toward divalent HPO_4^{2-} and SO_4^{2-}, as discussed in Section 3-2-1, the observed LE intensity increases would not be caused by the complexation behavior between host **10** and these

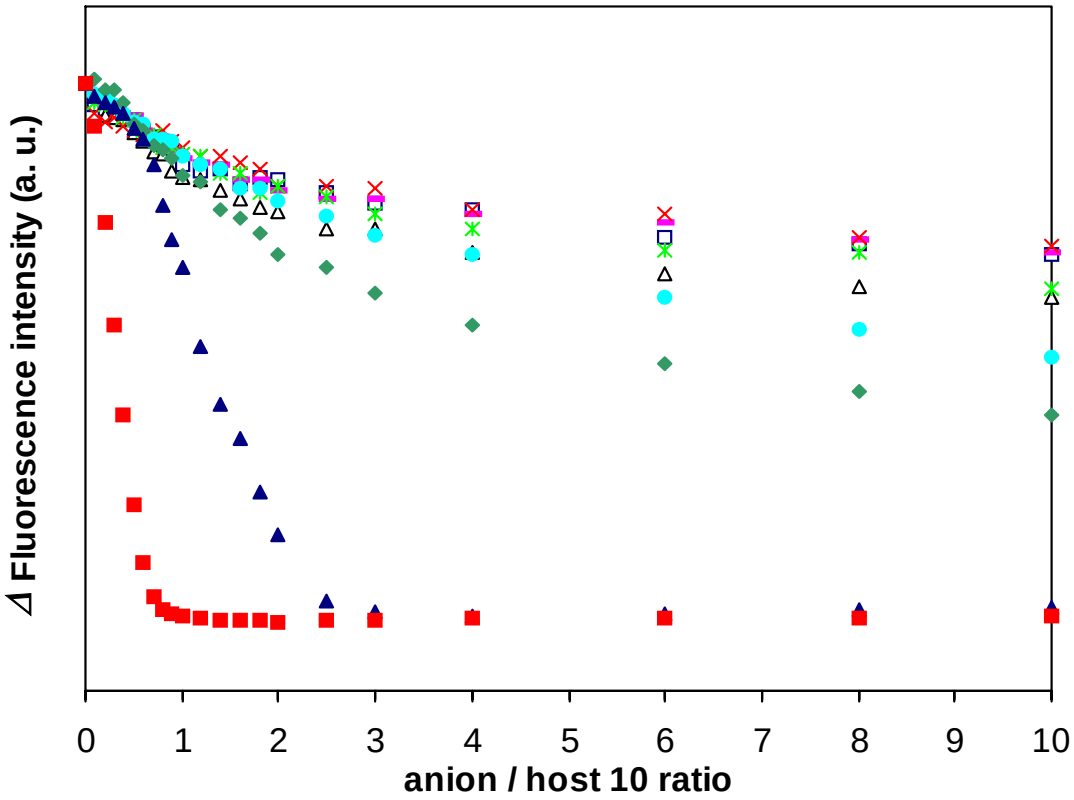

Figure 3-27. TICT intensity changes monitored at 491 nm upon titrations of host **10** (4.46×10^{-6} mol/L) with $(TBA)_2HPO_4$ (■), $(TBA)_2SO_4$ (▲), $(TBA)_2H_2P_2O_7$ (◆), $(TBA)H_2PO_4$ (●), $(TBA)HSO_4$ (□), $(TBA)ClO_4$ (━), $(TBA)BF_4$ (△), $(TBA)PF_6$ (×), and $(TBA)NO_3$ (*) in CH_3CN. Excitation wavelength: 300 nm.

anions, but would ascribe to the influence of the microenviorental polarity around host **10** by lipophilic counteraction TBA, as pointed out in Chapter 2.

In Figure 3-27, gradual addition of divalent HPO_4^{2-} caused rapid decrease at TICT band until the concentration ratio of HPO_4^{2-}/**10** reached around 0.5 and, then, the TICT intensity maintained almost no change even addition of an excess amount of HPO_4^{2-}. In the case SO_4^{2-}, the TICT intensity showed smooth decrease from beginning to around 0.4 equivalent amounts of SO_4^{2-} added, and then sharply decreased till the concentration ratio of SO_4^{2-}/**10** approached 2.5. Almost no change at the TICT state was observed even large amounts of SO_4^{2-} used. By contrast with HPO_4^{2-} and SO_4^{2-}, the additions of

$H_2P_2O_7^{2-}$ and monovalent anions ($H_2PO_4^-$, HSO_4^-, ClO_4^-, BF_4^-, PF_6^-, and NO_3^-) resulted in the monotonic decreasing of TICT intensity.

Titration profiles of host **10** monitored at TICT emission (491 nm, Figure 3-27) were quite similar to those observed in UV-vis titrations monitored at 309 nm as shown in Figure 3-15. The existence of clear inflection points around $[HPO_4^{2-}]/[\mathbf{10}] = 0.5$ in TICT emission (Figure 3-27) demonstrated that the binding stoichiometry of host **10** with HPO_4^{2-} would be 2:1. Consideration of the charge balance between host **10** and SO_4^{2-} and sigmoidal TICT changes turned out that the complexation stoichiometry of host **10** and SO_4^{2-} would likely be 2:1. In addition, monotonic decreasing of TICT emissions of host **10** was observed in the titrations by $H_2P_2O_7^{2-}$ as well as monovalent anions, $H_2PO_4^-$, HSO_4^-, ClO_4^-, BF_4^-, PF_6^-, and NO_3^-, which indicated that the binding stoichiometry of host **10** with $H_2P_2O_7^{2-}$ and the monovalent anions would be 1:1. The titration profiles of host **10** by divalent anions (HPO_4^{2-} and SO_4^{2-}) monitored at LE emission (343 nm, Figure 3-26) exhibited completely different features from those by $H_2P_2O_7^{2-}$ and the monovalent anions, which suggested the chemical species generated by interactions of host **10** with the divalent anions were quite different from those with the monovalent anions. Therefore, the results, such as selectivity and complexation stoichiometry of host **10** toward the anions obtained in fluorescence titrations, are highly consistent with those obtained in UV-vis titrations.

3-2-2-2 Stern-Volmer's Equation

The intensity data monitored at TICT state (491 nm) were applied to the Stern-Volmer equation in order to obtain more fluorescence binding information of host **10** toward a variety of anions. The fluorescence quenching of host **10** by $H_2P_2O_7^{2-}$ and monovalent anions ($H_2PO_4^-$, HSO_4^-, ClO_4^-, BF_4^-, PF_6^-, and NO_3^-) was found out to obey the Stern-Volmer equation, as shown in Figure 3-28, which indicated that the amounts of the non-fluorescent complexes generated by the interactions between the host and the anion in ground state would be limited as compared with the amounts of the fluorescent host itself in titration solution and that the binding affinities of the host with the anion in ground state would be relatively weak. Therefore, the observation of the almost linear Stern-Volmer plots ensured that the complexation ability of host **10** with $H_2P_2O_7^{2-}$ and monovalent anions ($H_2PO_4^-$, HSO_4^-, ClO_4^-, BF_4^-, PF_6^-, and NO_3^-) would be very weak, which sustained the accordance with the results obtained in UV-vis titrations as well as fluorescence titrations.

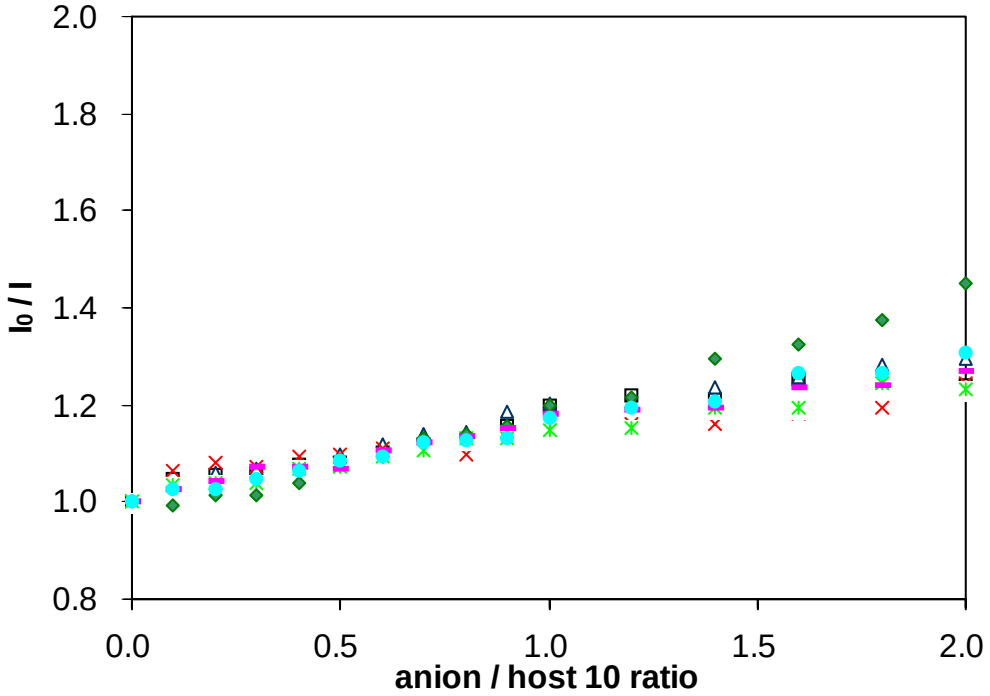

Figure 3-28. Stern-Volmer's plots of host **10** at TICT band upon addition of $(TBA)_2H_2P_2O_7$ (◆), $(TBA)H_2PO_4$ (●), $(TBA)HSO_4$ (□), $(TBA)ClO_4$ (─), $(TBA)BF_4$ (△), $(TBA)PF_6$ (×), and $(TBA)NO_3$ (*) in CH_3CN.

In contrast, the Stern-Volmer plots showed sigmoidal and monotonic increasing profiles for HPO_4^{2-} (Figure 3-29) and SO_4^{2-} (Figure 3-30), respectively, which meant that the interaction of host **10** with HPO_4^{2-} and SO_4^{2-} in ground state would be so strong that large amounts of complexes would be produced. The observation demonstrated that the binding affinities of host **10** with HPO_4^{2-} and SO_4^{2-} would be very high, especially in the case of HPO_4^{2-}. The results obtained from the Stern-Volmer plots also were consistent with those obtained in UV-vis titrations as well as fluorescence titrations.

In addition, the notably different fluorescence quenching behavior of host **10** in Stern-Volmer plots between the divalent anions (HPO_4^{2-} and SO_4^{2-}) and $H_2P_2O_7^{2-}$ and the monovalent anions also apparently indicated that host **10** had high selectivity to the divalent anions over $H_2P_2O_7^{2-}$ and the monovalent anions.

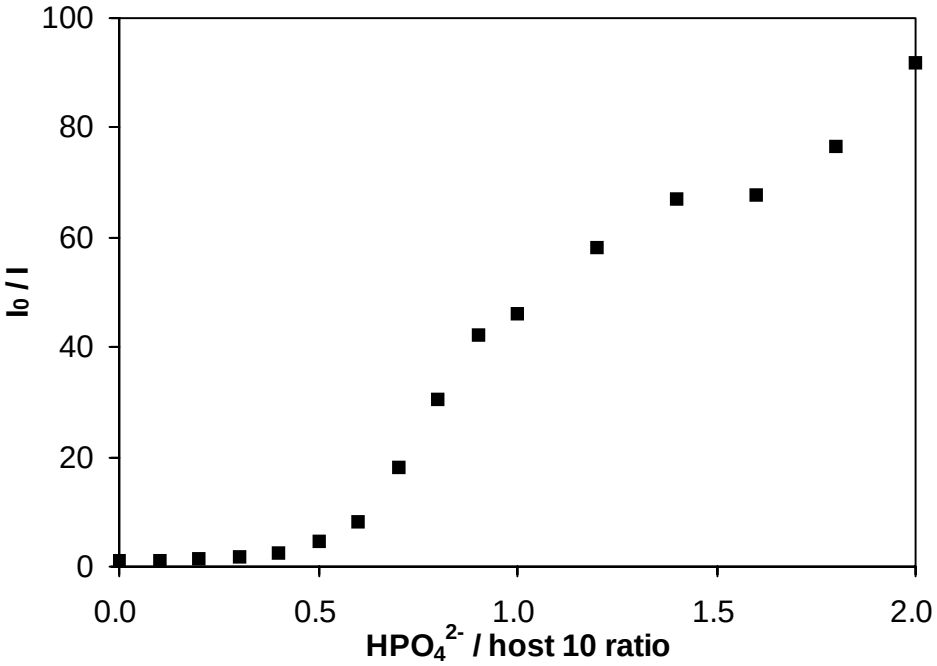

Figure 3-29. Stern-Volmer's plot of host **10** at TICT band upon addition of $(TBA)_2HPO_4$ in CH_3CN.

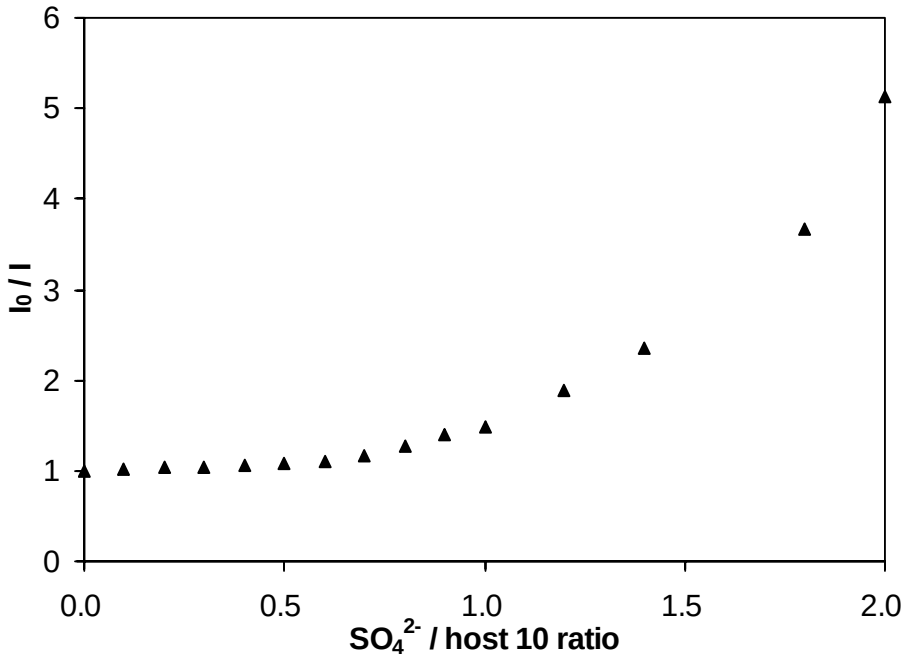

Figure 3-30. Stern-Volmer's plot of host **10** at TICT band upon addition of $(TBA)_2SO_4$ in CH_3CN.

3-2-2-3 Conclusions

Commercially available 4-(*N*,*N*-dimethylamino)benzoic acid (**10**) was directly used as an anion host to investigate the complexation behavior toward a variety of anions by means of fluorescence titrations. The observation on the titration profiles of the LE and TICT emissions as well as the Stern-Volmer's plots demonstrated that host **10** exhibited strong affinities and high binding selectivity toward divalent anions (HPO_4^{2-} and SO_4^{2-}) over monovalent anions ($H_2PO_4^-$, HSO_4^-, ClO_4^-, BF_4^-, PF_6^-, and NO_3^-) and $H_2P_2O_7^{2-}$. The complexation stoichiometry of host **10** with HPO_4^{2-} and SO_4^{2-} turned out to be 2:1, while host **10** showed 1:1 complexation with $H_2PO_4^-$, HSO_4^-, ClO_4^-, BF_4^-, PF_6^-, and NO_3^-, and $H_2P_2O_7^{2-}$. These results were in agreement with those obtained in UV-vis titrations.

3-3 Conclusions

Simple and commercially available 4-(*N*,*N*-dimethylammino)benzoic acid (**10**) was directly used as an anion host for anion recognition. The versatility of the DMAB signaling subunit was investigated in terms of UV-vis and fluorescence spectroscopy.

In UV-vis titrations, host **10** exhibited strong affinities and high binding selectivity toward divalent anions (HPO_4^{2-} and SO_4^{2-}) over monovalent anions ($H_2PO_4^-$, HSO_4^-, ClO_4^-, BF_4^-, PF_6^-, and NO_3^-) and $H_2P_2O_7^{2-}$. The binding constants of host **10** with HPO_4^{2-} and SO_4^{2-} (HPO_4^{2-} and SO_4^{2-}: log $K_2 > 10$) were quite larger than those with $H_2P_2O_7^{2-}$ and the monovalent anions (log K_1 = 3.4-4.8). Host **10** showed 2:1 binding stoichiometry with HPO_4^{2-} and SO_4^{2-} and 1:1 binding stoichiometry with the monovalent anions and $H_2P_2O_7^{2-}$. The combination of the basicity and negative charges of anions played a crucial role in influencing the selectivity of host **10** toward anions.

In fluorescence titrations, the titration profiles obtained both at LE and TICT states of host **10** exhibited remarkable differences upon addition of the divalent anions and the monovalent anions as well as $H_2P_2O_7^{2-}$. The binding stoichiometry of host **10** with HPO_4^{2-} and SO_4^{2-} also turned out to be 2:1, while in the cases of $H_2PO_4^-$, HSO_4^-, ClO_4^-, BF_4^-, PF_6^-, NO_3^-, and $H_2P_2O_7^{2-}$, host **10** showed 1:1 complexation. In addition, the Stern-volmer plots also revealed that host **10** had high selectivity with the divalent anions over the monovalent anions and $H_2P_2O_7^{2-}$. All of the results obtained from dual fluorescence titrations and Stern-Volmer plots were in agreement with those obtained in UV-vis titrations.

The research[10] presented in the thesis demonstrated that commercially available host **10** is capable of being a new class of anion receptor and the DMAB group is a versatile signaling subunit with UV-vis and fluorescence responses for anion

recognition. A promising signaling methodology by utilization of chromogenic and fluorogenic reagents as anion hosts has been developed. The author believes that the investigation would open a novel prospect in the field of anion recognition chemistry.

3-4 Experimental Section

3-4-1 General

UV-vis spectra were obtained on a Perkin Elmer UV-VIS/NIR Lamnda 19 spectropolarimeter. Fluorescence spectra were recorded by a Fluorolog JOBIN YVON-SPEX spectrophotometer. Spectroscopic grade acetonitrile from Dojindo Laboratories was used without further purification for all spectrophotometric measurements. Tetrabutylammonium nitrate, tetrabutylammonium dihydrogen-phosphate, tetrabutylammonium tetrafluoroborate, tetrabutylammonium perchlorate, tetrabutylammonium hydrogensulfate, tetrabutylammonium hexanfluorophosphate, and tetrabutylammonium hydroxide were purchased from Aldrich and used without further purification. Bis(tetrabutylammonium) hydrogenphosphate, bis(tetrabutylammonium) dihydrogenpyrophosphate were prepared in laboratory. The detailed preparation methods were described in Chapter 2.

3-4-2 Spectral titrations of host 10 by anions

In UV-vis and fluorescence titration experiments, a 4.46×10^{-6} mol/L solution of host **10** and a 2.68×10^{-4} mol/L solution of anions as tetrabutylammonium salts were first prepared in CH_3CN separately. Next, 3.0 mL of host solution was transferred into a quartz cell. After the UV-vis or fluorescence spectrum of host itself was measured, an aliquot of the guest solution was added to the quartz cell, and the absorption or intensity changes of host solution were monitored; this procedure was repeated for each aliquot addition. In the experiment to examine the possibility of the dimerization of host **10**, a 6.50×10^{-5} mol/L solution of host **10** was first prepared in CH_3CN. It was diluted to prepare different concentration solution of host **10** ranging from 6.5×10^{-7} mol/L to 6.5×10^{-5} mol/L. Then, the UV-vis spectrum of each solution was measured.

References

1. For reviews, see: (a) F. P. Schmidtchen and M. Berger, *Chem. Rev.* **1997**, *97*, 1609. (b) P. A. Gale, *Coord. Chem. Rev.* **2000**, *199*, 181. (c) P. A. Gale, *Coord. Chem. Rev.* **2001**, *213*, 79. (d) P. D. Beer and P. A. Gale, *Angew. Chem., Int. Ed.* **2001**, *40*, 486. (e) R. Martínez-Máñez and F. Sancenón, *Chem. Rev.* **2003**, *103*, 4419. (f) K. A. Schug and W. Lindner, *Chem. Rev.* **2005**, *105*, 67.
2. X. Zhang, C.-J. Wang, L.-H. Liu, and Y.-B. Jiang, *J. Phys. Chem. B*, **2002**, *106 (48)*, 12432.
3. W. Rettig, In *Topics in Current Chemistry*; J. Mattay, Ed.; Springer-Verlag: Berlin, 1994; Vol. 169, pp 253-299.
4. (a) W. Huang, X. Zhang, L.-H. Ma, C.-J. Wang, and Y.-B. Jiang, *Chem. Phys. Lett.* **2002**, *352(5, 6)*, 401. (b) C.-H. Zhang, Z.-B. Chen, and Y.-B. Jiang, *Spectrochim. Acta. A*, **2004**, *60A(12)*, 2729.
5. F.-Y. Wu and Y.-B. Jiang, *Chem. Phys. Lett.* **2002**, *355*, 438.
6. D. D. Perrin, *Ionization Constants of Inorganic Acids and Bases in Aqueous Solution, Second Editio*; Pergamon: Oxford, 1982. (7) Lange's Handbook of Chemistry, 13th Edition; McGraw-Hill: New York, 1985.
7. *Lange's Handbook of Chemistry*, 13th Edition; McGraw-Hill: New York, 1985.
8. A. J. Gordon and R. A. Ford, *The Chemist's Companion: A Handbook of Practical Data, Techniques, and References.* Wiley-Interscience: New York, 1972.
9. K. Kobiro and Y. Inoue, *J. Am. Chem. Soc.* **2003**, *125*, 421.
10. X.-H. Hou and K. Kobiro, *Chem. Lett.* **2006**, *35*, 116.

Chapter 4.
Conclusions

The thesis treats with the development of a new signaling methodology for anion recognition. The artificial anion receptor **9** and quite simple commercially available 4-(*N,N*-dimethylamino)benzoic acid (**10**), both of which possessing 4-(*N,N*-dimethylamino)benzoate (DMAB) group, have been applied to investigate the scope and limitations of the DMAB group upon complexation with a variety of anions and the versatility of the DMAB group as a signaling subunit by means of ^{1}H NMR, UV-vis, CD, and/or fluorescence spectroscopic studies. The results obtained through the research are summarized and concluded as follows:

The author has focused on the investigation of complexation behavior of host **9** with a variety of divalent and monovalent anions in terms of ^{1}H NMR, CD, and fluorescence spectroscopic studies. The artificial host **9** has a chiral bicyclic guanidinium ionic moiety as a binding subunit and DMAB group as a signaling subunit. Strong intramolecular hydrogen bonding is present between the carbonyl oxygen atom of the DMAB group and one of the N-H groups of the guanidinium ion moiety in the host **9**. Thus, it is rationally assumed that host **9** would show a "covered" structure first, in which the binding site would be covered with DMAB signaling subunit via the intramolecular hydrongen bonding. When anions, having stronger affinity to host **9** than the DMAB group, bind to the guanidinium ion moiety, the intramolecular hydrogen bonding would be cleaved and the DMAB group would be driven out. The host **9** would

show an "open" structure finally. The DMAB signaling subunit would lead to the complexation information via the spectral changes on ^{1}H NMR, CD, and fluorescence spectroscopy. All of the results obtained in ^{1}H NMR, CD, and fluorescence titrations are in agreement with the strategy.

In ^{1}H NMR titrations, the DMAB signaling subunit provided quantitative information upon complexation of host **9** with divalent and monovalent anions. Host **9** showed strong binding ability and high selectivity toward divalent anions (SO_4^{2-}, HPO_4^{2-}, $H_2P_2O_7^{2-}$, and AMP^{2-}) over monovalent anions (ClO_4^-, NO_3^-, BF_4^-, HSO_4^-, and PF_6^-). The binding constants of host **9** toward divalent anions (SO_4^{2-}: log $K_{1:1}$ = 6.2 and log $K_{2:1}$ = 4.7, HPO_4^{2-}: log $K_{1:1}$ = 6.2 and log $K_{2:1}$ = 4.9, $H_2P_2O_7^{2-}$: log $K_{1:1}$ =4.4 and log $K_{2:1}$ =1.8, AMP^{2-}: log $K_{1:1}$ > 7 and log $K_{2:1}$ > 5) were much larger than those toward the monovalent anions (log $K_{1:1}$ < 2.0), except for $H_2PO_4^-$ (log $K_{1:1}$ = 4.4). Host **9** exhibited successive 2:1 (host **9** : anion) and 1:1 complexation stoichiometry with the divalent anions and 1:1 complexation stoichiometry with the monovalent anions.

In CD titration experiments, the DMAB signaling subunit successfully exhibited the complexation information of host **9** with divalent anions in terms of the exciton chirality method. Anions, such as SO_4^{2-}, HPO_4^{2-} and AMP^{2-} as well as $H_2P_2O_7^{2-}$ and $H_2PO_4^-$, all of which have strong affinities to host **9**, gave negative first and positive second Cotton effect peaks for SO_4^{2-}, HPO_4^{2-}, and AMP^{2-}, while simple decreasing intensity for $H_2P_2O_7^{2-}$ and $H_2PO_4^-$ in CD titration profiles. In contrast, in the case of ClO_4^- having quite weak coordination affinity to host **9**, the CD titration profile hardly showed intensity changes. The observation of the negative first and positive second Cotton effect peaks in the 2:1 complexes clearly indicated that the two DMAB signaling subunits were arranged with negative chirality (counterclockwise) rather than positive chirality (clockwise) in the corresponding 2:1 complexes. Thus, the combination of the

DMAB signaling subunit and the chiral guanidinium binding subunit provides detailed complexation information on the titration profiles of host **9** with anions as well as on the absolute configuration of 2:1 complexes of host **9** with the divalent anions using CD spectroscopy.

In fluorescence titrations, the DMAB group in host **9** as a signaling subunit successfully showed distinctive LE and TICT fluorescence responses on recognizing a variety of divalent and monovalent anions. Anions, having strong binding affinities to host **9**, for instance, SO_4^{2-}, HPO_4^{2-}, AMP^{2-}, and $H_2P_2O_7^{2-}$, broke the present intramolecular hydrogen bonding in host **9** to make the rotation easy and hence gave a TICT state from the LE state, which caused the increasing intensity of TICT emission concomitant with the decreasing intensity of LE emission in the 2:1 complexation. Meanwhile, host **9** showed the successive 2:1 and 1:1 complexation stoichiometry with the divalent anions as well as 1:1 complexation stoichiometry with the monovalent anions, which are highly consonant with the conclusions obtained in ^{1}H NMR titrations. In addition, the active participation of lipophilic countercation tetrabutylammonium (TBA) ion and large residue in AMP strongly increased and decreases, respectively, the LE and TICT intensity changes in the 1:1 complexation via varying the microenvironmental polarity around the signaling subunit.

Therefore, the rational design of the signaling principle introduced in Chapter 2 provided not only quantitative information about binding constants but also detailed understanding of the complexation behavior such as stoichiometry of the complexation, chiral sense of the 2:1 complexes, and participation of a countercation and a hydrophilic group in the coordination process. Thus, the investigation presented in the thesis allows us to clearly understand the scope and the limitations of the DMAB signaling subunit on

recognizing a variety of anions. The DMAB group is proved to be a versatile signaling subunit by means of ^{1}H NMR, CD, and fluorescence spectral studies.

The author has also focused on the investigation of complexation behavior of 4-(*N,N*-dimethylammino)benzoic acid (**10**) with a variety of anions in terms of UV-vis and fluorescence spectroscopic studies. The availability of chromogenic and fluorogenic reagents applied as potential anion receptors and the versatility of the DMAB signaling subunit have been discussed. Host **10** has an acidic hydrogen atom as well as an aromatic moiety. Thus, it was rationally assumed that the acidic hydrogen atom would be transferred to guest anions to make complexes and the aromatic 4-(*N,N*-dimethylammino)benzoate (DMAB) as a signaling subunit would show spectral response upon complexation with guest anions. The basicity and the charge density of anions would be the main factors to influence the complexation behavior of host **10** toward anions. All of the results obtained in UV-vis and fluorescence titrations are consistent with the strategy.

In UV-vis titrations, host **10** exhibited strong affinities and high binding selectivity toward divalent anions (HPO_4^{2-} and SO_4^{2-}) over monovalent anions ($H_2PO_4^-$, HSO_4^-, ClO_4^-, BF_4^-, PF_6^-, and NO_3^-) and divalent anion, $H_2P_2O_7^{2-}$. The UV-vis titration profiles obviously distinguished the complexation behavior of host **10** with HPO_4^{2-} and SO_4^{2-} from that with the monovalent anions and $H_2P_2O_7^{2-}$. The binding constants of host **10** for HPO_4^{2-} and SO_4^{2-} (HPO_4^{2-} and SO_4^{2-}: log $K_2 > 10$) were quite larger than those for $H_2P_2O_7^{2-}$ as well as the monovalent anions (log $K_1 = 3.4$-4.8). The binding stoichiometry of host **10** with HPO_4^{2-} and SO_4^{2-} turned out to be 2:1, while those with $H_2PO_4^-$, HSO_4^-, ClO_4^-, BF_4^-, PF_6^-, and NO_3^-, and $H_2P_2O_7^{2-}$ turned out to be 1:1. The combination of the

basicity and negative charges of anions played a crucial role in influencing the selectivity of host **10** toward anions.

In fluorescence titrations, host **10** showed dual fluorescence emissions from LE and TICT states. Upon titrations, host **10** also exhibited strong affinities and high binding selectivity toward divalent anions (HPO_4^{2-} and SO_4^{2-}) over monovalent anions ($H_2PO_4^-$, HSO_4^-, ClO_4^-, BF_4^-, PF_6^-, and NO_3^-) and $H_2P_2O_7^{2-}$. Host **10** gave rise to 2:1 complexation stoichiometry with HPO_4^{2-} and SO_4^{2-} and 1:1 complexation stoichiometry with $H_2PO_4^-$, HSO_4^-, ClO_4^-, BF_4^-, PF_6^-, and NO_3^-, and $H_2P_2O_7^{2-}$. Meanwhile, the Stern-Volmer plots of TICT intensity also indicated that host **10** exhibited strong affinities and high binding selectivity toward divalent anions (HPO_4^{2-} and SO_4^{2-}) over the monovalent and divalent anion, $H_2P_2O_7^{2-}$, which was consistent with the results of LE and TICT titrations. Thus, all of results obtained from UV-vis, fluorescence, and Stern-Volmer showed good agreement about the complexation behavior of host **10** toward a variety of anions.

The designed new signaling methodology introduced in Chapter 3 indicates that the simple and commercially available 4-(*N,N*-dimethylammino)benzoic acid (**10**) is capable of being a new class of chromogenic and fluorogenic hosts and the DMAB group is versatile to be a signaling subunit for anion recognition.

In conclusion, the artificially synthesized host **9** and commercially available host **10**, both of which having 4-(*N,N*-dimethylamino)benzoate group as a signaling subunit, have been developed and applied for anion recognition. The 4-(*N,N*-dimethylamino)-benzoate group has been found out to be one of the versatile signaling subunits for anion sensing in terms of ^{1}H NMR, CD, UV-vis, and/or fluorescence spectroscopic studies. The promising signaling methodology would open a new prospect in the field of

anion recognition chemistry.

List of Publications and Presentations

Publications

1. **Versatility of an Intramolecularly Hydrogen-bonded 4-(*N,N*-Dimethylamino) benzoate Group as a Signaling Subunit for Anion Recognition**

   Xiaohong Hou and Kazuya Kobiro, *Tetrahedron*, **2005**, *61*, 5866-5875.

2. **4-(*N,N*-Dimethylamino)benzoic Acid as a New Class of Simple Chromogenic and Fluorogenic Anion Host Exhibiting High Selectivity to HPO_4^{2-} and SO_4^{2-}**

   Xiaohong Hou and Kazuya Kobiro, *Chem. Lett.* **2006**, *35*, 116-117.

Presentations

1. **Recognition of Anions by Guanidinium-*p*-dimethylaminobenzoate Derivative**

   Xiaohong Hou and Kazuya Kobiro, 第２０回機能性ホスト-ゲスト化学研究会, 豊中, **2004**, P11.

2. **Complexation Behavior of Guanidinium-*p*-dimethylaminobenzoate Derivative toward Anions**

   Xiaohong Hou and Kazuya Kobiro, 日本化学会第８４春季年会，西宮，**2004**, 3PA-098.

3. **A New Chiral Probe for Anions with Tetrahedral Structure**

   Kazuya Kobiro and Xiaohong Hou, Sixth International Symposium on Functional π- Electron Systems, Ithaca, New York, USA, **2004**, AP55.

4. **Versatility of 4-(*N,N*-Dimethylamino)benzoate Group as a New Class of Signaling Subunit for Anion Recognition**

Xiaohong Hou and Kazuya Kobiro, 2005 International Chemical Congress of Pacific Basin Societies, Honolulu, Hawaii, USA, **2005**, 1143.

Acknowledgement

The work presented in the thesis was completed under the guidance of my supervisor Dr. Kazuya Kobiro. I would like to express my sincerest gratitude to Dr. Kazuya Kobiro for his valuable guidance and continuous encouragement throughout the research.

I would also like to express my appreciations to vice supervisors, Professor Masaoki Furue, Professor Takahiro Hosokawa, Associate Professor Kastuhiro Sumi, and Professor Keiichi Enomoto, for their useful advices, comments, and hearty encouragement.

Sincere thanks are extended to Mr. Masahiko Mustura, Mr. Naohisa Okimoto, Ms. Sayaka Gion, Mr. Shinya Hosogi, Mr. Daigo Nishimura, and other members of our laboratory for their kind help, collaboration, and friendships.

I really appreciated Professor Yoshihisa Inoue, Associate Professor Takehiko Wada, and Mr. Masaki Nishijima of Osaka University for their guidance and assistance on the measurement of CD spectra.

I am deeply grateful to visiting Professor Yasuhiro Kawanishi, Shenyang Pharmaceutical University, for building a bridge linking Kochi University of Technology and Shenyang Pharmaceutical University. Further, I sincerely appreciate Professor Chunfu Wu, President of Shenyang Pharmaceutical University, for his recommendation and assignment to provide me the opportunity to study here.

Grateful acknowledgements are given to Professor Testuya Sakai, the former

director of the international relations center, and Ms. Mariko Kubo, Japanese teacher for international students, Kochi University of Technology, for their kindness and concerns, especially when I felt confused.

I would like to acknowledge the scholarship of GAKUSYU SYOREI-HI.

Many thanks are given to all people who ever assisted me directly or indirectly in my stay in Japan.

Finally, I wish to express my special thanks to my mother-in-law, my parents, especially to my husband, Mr. Daqing Zhou, and my son, Mr. Zibo Zhou, for their understanding, encouragement, and assistance during the course of study.